

LANDSLIDE MICROZONATION IN HIMALAYAN REGION USING GEOSPATIAL TOOLS

Submitted to

DELHI TECHNOLOGICAL UNIVERSITY

in partial fulfilment of the requirements for the award of the degree of

DOCTOR OF PHILOSOPHY

In

CIVIL ENGINEERING

By

SANDEEP PANCHAL
(Reg. No. 2K17/PhD/CE/17)

Under the supervision of

Prof. (Dr.) Amit Kr. Srivastava



DEPARTMENT OF CIVIL ENGINEERING

DELHI TECHNOLOGICAL UNIVERSITY

SHAHBAD, DAULATPUR, BAWANA ROAD, DELHI - 110042 (INDIA)

January 2023

Dedicated to my family



DELHI TECHNOLOGICAL UNIVERSITY

Shahabad Daulatpur, Main Bawana Road

Delhi-110042 (India)

DECLARATION

I hereby declare that the thesis entitled “**Landslide Microzonation in Himalayan Region using Geospatial Tools**” submitted by me for the award of the degree of *Doctor of Philosophy* to **Delhi Technological University (Formerly Delhi College of Engineering)** is a record of bonafide work carried out by me under the guidance of Prof. (Dr.) Amit Kr. Srivastava, Department of Civil Engineering, Delhi Technological University.

I further declare that the work reported in this thesis has not been submitted and will not be submitted, either in part or in full, for the award of any other degree or diploma in this Institute or any other Institute or University.

Sandeep Panchal

Reg No: 2K17/Ph.D/CE/17

Department of Civil Engineering

Place: New Delhi

Date:



DELHI TECHNOLOGICAL UNIVERSITY

Shahabad Daulatpur, Main Bawana Road

Delhi-110042 (India)

CERTIFICATE

This is to certify that the thesis entitled “**Landslide Microzonation in Himalayan Region using Geospatial Tools**” submitted by **Mr. Sandeep Panchal** to **Delhi Technological University (Formerly Delhi College of Engineering)**, for the award of the degree of “*Doctor of Philosophy*” in Civil Engineering is a record of bonafide work carried out by him. Sandeep Panchal has worked under my guidance and supervision and has fulfilled the requirements for the submission of this thesis, which to our knowledge has reached requisite standards.

The results contained in this thesis are original and have not been submitted to any other university or institute for an award of any degree or diploma.

Dr. Amit Kr. Srivastava

Professor

Department of Civil Engineering

Delhi Technological University (DTU)

Bawana, Delhi-110042

ACKNOWLEDGEMENTS

First and foremost, I would like to thank Lord Rama, the almighty who blessed me with the strength and patience during my PhD journey. I would like to express my gratitude and appreciation to my PhD supervisor Dr. Amit Kr. Srivastava, Professor, Department of Civil Engineering, Delhi Technological University. He has guided me throughout this journey as a tremendous mentor. The lines are dedicated to my guide:

“सब धरती कागज करूँ, लेखनी सब बनराय/

सात समुंदर की मसि करूँ, गुरु गुण लिखा न जाय॥”

His guidance and advice helped me during every stage of this research work. He will always remain a source of inspiration for me throughout my life.

I would like to sincerely thank the staff members of Delhi Technological University for their cooperation at every stage. I am also thankful to Dr. Raman Parti and Dr. Chander Prakash from Department of Civil Engineering, NIT Hamirpur. I am indebted to my parents Mr. Chander Pal and Mrs. Sheela Devi for believing in me. I am thankful to

my younger brother Alaxender Panchal for motivating me as a researcher.

It is my pleasure to thank my wife Mrs. Anjali Panchal for her mental and moral support during my doctoral work. Some words goes to my son 'Shivansh' whose smile is always a motivation for me. I am also thankful to my sisters Kiran, Kareena and Shivani for abiding by my ignorance and showing the patience during my Ph.D. work.

My sincere thanks to my batch-mates and friends Mr. Parves, Mr. Yogesh Rajput, Mr. Abhishek Paswan, Mrs. Archita Bansal, Mr. Deepak and Mr. Rajat for their co-operation during this work.

I would like to appreciate the efforts of the anonymous reviewers for reviewing our research papers and giving constructive feedback which ultimately improved the quality of our research publications over the course of time.

Finally, I would like to thank all the people who have contributed directly or indirectly to achieving this goal.

Sandeep Panchal

ABSTRACT

Hilly regions are highly prone to natural disasters. Natural disasters like floods, forest fires, slope failures, erosion, and landslides are common phenomena in hilly terrains. Landslide is a disastrous phenomenon that is responsible for economic losses and loss of lives. Landslides are responsible for huge economic loss which makes them 3rd largest natural disaster after floods and earthquakes. The planners and engineers require information about the possibility of the occurrence of landslides in working regions. So, the landslide hazards must be planned carefully to avoid losses. Microzonation of landslides or slopes which are susceptible to failure is an important task for understanding and planning the mitigation measures for landslides. Microzonation of landslides is the identification of the potential occurrence of landslides in different areas. The microzonation maps of landslides represent the landslide susceptibility and distribution of previously occurred landslides.

The main objective of the thesis is to implement and compare the mixed methods and quantitative techniques of landslide susceptibility mapping. Due to the high subjectivity of the opinion of the experts, the qualitative techniques give lesser accuracy as compared to the statistical method. So, it is also attempted to propose a hybrid technique for enhancing the accuracy of expert-based methods. In this thesis, causative factors of landslides are identified using historical landslide data. The causative factors of landslides considered in this study are slope gradient, slope aspect, relative relief, topographic wetness index (TWI), lithology, drainage density, proximity to the road, proximity to faults/lineament and land use of the study area. The causative factors of the landslides are divided into simpler sub-categories. For example, the slope is divided into sub-categories like 0° to 15°, 15° to 30°, etc. Slope, aspect, relative relief and TWI are extracted by processing the

CARTOSAT DEM. The parameters that are not extracted from the digital elevation model (DEM) are converted into the digital format using the geographic information system (GIS). The impact of these causative factors on the occurrence of landslides is evaluated using an expert-based approach and mathematical approach.

In this study, four models are implemented for the microzonation of landslides in the study area. A landslide inventory containing more than 1500 landslide events is prepared using previous literature, news reports, Geological Survey of India (GSI) practical sheets, google imagery and field survey. Analytic hierarchy process (AHP), frequency ratio (FR) and Shannon's entropy models are used for landslide susceptibility mapping and a new technique by hybridization of Shannon's entropy and AHP model is proposed taking a case study of Shimla region in Himachal Pradesh (H.P). However, the analytic hierarchy process (AHP) is a semi-qualitative model and an improvement over expert-based techniques, the rest three models are mathematical models. The weightage of causative factors and sub-factors are determined based on expert opinion and are checked for consistency in AHP. The weightage of causative factors and sub-factors in the other three models is obtained using mathematical relationships. Four landslide susceptibility maps for the study area are prepared and the performance of each method is evaluated using the receiver operation characteristics (ROC) curve.

It can be observed that the frequency ratio (FR) model is the most effective approach in predicting the landslide susceptibility while the analytic hierarchy process (AHP) remained the least productive. The hybrid model i.e. SE-AHP model performed better as compared to the analytic hierarchy process (AHP) model. Shannon's entropy model assigns weightage to the causative

factors and sub-factors both, but still, the model's accuracy is lesser compared to the frequency ratio (FR) model. The mathematical models require a well-distributed landslide inventory while it is not essential for the expert-based models. It is observed that the accuracy of the results in mathematical methods depends upon the distribution and accuracy of the landslide inventory while the accuracy depends upon the expert's judgment in the case of expert-based methods. Some work has been reported related to mathematical and expert-based models but Shannon's entropy has been used very rarely. The performance of the AHP model is improved significantly by the hybridization of AHP with Shannon's entropy. The results of the study revealed that realistic weightage can be obtained only from an accurate and well-distributed inventory.

Finally, the thesis presents a comparison of expert-based methods and mathematical methods for landslide susceptibility mapping. The study helps in identifying the contribution of causative factors in the occurrence of landslides. The output of the study helps in the demarcation of the zones of high landslide potential. This study also provides information that can be used by the researchers in understanding and choosing the suitable method for landslide susceptibility mapping. The newly proposed mixed technique in this study can reduce the subjectivity in the expert-based methods and improve the accuracy of the AHP model. The results of the study will also help the planners and risk managers for understanding the landslide potential in the study area.

Keywords: landslide microzonation, GIS, remote sensing, AHP, Shannon's entropy, frequency ratio (FR), SE-AHP, weighted linear combination (WLC), landslide susceptibility

Table of Contents

Topics	Page No.
Candidate Declaration	i
Certificate	ii
Acknowledgment	iii
Abstract	v
Table of Contents	viii
List of Figures	xiii
List of Tables	xiv
Chapter 1: Introduction	01-15
1.1. Background	01
1.2. Classification and Types of Landslide	02
1.3. Causes of Landslides	05
1.4. Economic Aspects of Landslide	08
1.5. Mechanism of Failure	08
1.6. Microzonation of Landslide Susceptibility	10
1.7. Research Problem	10
1.8. Aim and Objectives of the Study	11
1.9. Research Questions	11
1.10 Organization of Thesis	12

Chapter 2: Literature Review	15-43
2.1. Introduction	15
2.2. Types of Landslide Studies	16
2.2.1. Landslide Inventory	17
2.2.2. Landslide Susceptibility Maps	18
2.2.3. Landslide Hazard Maps	19
2.2.4. Landslide Risk Maps	21
2.3 Role of Scale in Landslide Mapping	22
2.4. Landslide Susceptibility Mapping Techniques	22
2.4.1. Qualitative Approach	23
2.4.2. Quantitative Approach	25
2.4.3. Semi-qualitative/ Semi-Quantitative Techniques	33
2.4.4. Black Box Models	36
2.4. Discussion about Models in Landslide Susceptibility Mapping	38
2.5. Findings from the Literature Review	40
2.6. Research Gaps	42
2.7. Concluding Remarks	43
Chapter 3: Conceptual Framework	44-52
3.1. Introduction	44
3.2 Study Area	47
3.2.1. Climate Characteristics	48
3.2.2. Vegetation Characteristics	48
3.2.3 Geology and Seismology	49

3.3	Landslide Inventory	49
3.4	Accuracy Assessment of DEM	50
3.5	Mathematical Modelling	51
3.6	Processing of Data	51
3.7	Concluding Remarks	52

Chapter 4: Causative Factors of Landslides **53-67**

4.1	Introduction	53
4.2	Topographic Causative Factors	53
	4.2.1. Slope Gradient	54
	4.2.2. Slope Aspect	55
	4.2.3. Relative Relief	56
	4.2.4. Topographic Wetness Index (TWI)	58
4.3	Geological Causative Factors	59
	4.3.1. Lithology	59
	4.3.2. Distance from Faults	61
4.4	Hydrological Causative Factors	62
4.5	Anthropogenic Causative Factor	64
4.6	Land-use/ Land-cover	65
4.7	Discussion on Causative Factors	66
4.8	Concluding Remarks	66

Chapter 5: Mathematical Modelling	68-82
5.1 Introduction	68
5.2 Analytic Hierarchy Process (AHP)	69
5.3 Frequency Ratio (FR)	72
5.4 Shannon's Entropy	77
5.5 Hybridization of Models	81
5.6 Concluding Remarks	82
Chapter 6: Results and Discussion	83-102
6.1 Overview	83
6.2 Analysis of Landslide Susceptibility by Analytic Hierarchy Process (AHP)	83
6.2.1. Analysis of Sub-factors of Landslides	84
6.2.2. Analysis of Causative Factors of Landslides	86
6.2.3. Landslide Susceptibility Mapping using AHP	86
6.3 Analysis of Landslide Susceptibility by Frequency Ratio (FR)	87
6.3.1. Analysis of Sub-factors of Landslides	89
6.2.2. Landslide Susceptibility Mapping using Frequency Ratio (FR)	93
6.4 Analysis of Landslide Susceptibility by Shannon's Entropy	96
6.4.1. Landslide Susceptibility Map by Shannon's Entropy	98
6.5 Hybrid Map by SE-AHP Technique	98
6.6 Discussion, Comparisons and Validation of Results	100
6.7 Concluding Remarks	102

Chapter 7: Conclusions and Recommendations	103-109
7.1. Conclusions	103
7.2. Recommendations based on Landslide Potential of Study Area	104
7.3. Recommendations for Preparation of Landslide Susceptibility Maps	105
7.3.1. Selection of Causative Factors	106
7.3.2. Selection of Methods for Landslide Susceptibility Mapping	107
7.4. Future Scope	109
References	110
List of Publications/Proceedings	128
Appendix	130

List of Figures

Figure 1.1 a	Rotational Landslide	04
Figure 1.1 b	Translational Landslide	05
Figure 1.2	Modified Classification of Landslides	06
Figure 2.1	Approaches in Landslide Susceptibility Mapping	23
Figure 3.1	Flow Chart of the Study	45
Figure 3.2	Study Area	47
Figure 3.3	Landslide Inventory	50
Figure 4.1	Slope in Degrees	54
Figure 4.2	Slope Aspect	55
Figure 4.3	Relative Relief	57
Figure 4.4	Topographic Wetness Index (TWI)	58
Figure 4.5	Lithology	61
Figure 4.6	Distance from Faults	62
Figure 4.7	Distance from Roads	63
Figure 4.8	Drainage Density	64
Figure 4.9	Landuse/Landcover	65
Figure 6.1	Landslide Susceptibility Map by AHP	88
Figure 6.2	Landslide Susceptibility Map by Frequency Ratio	94
Figure 6.3	Landslide Susceptibility Map by Shannon's Entropy	95
Figure 6.4	Landslide Susceptibility Map by SE-AHP Approach	99
Figure 6.5	ROC Curve	101
Appendix B	Some Photographs of Landslides from the Study Area	158

List of Tables

Table 3.1	Source of Data	46
Table 3.2	DEM Error Analysis	51
Table 4.1	Lithology of the Area	60
Table 5.1	Saaty's Scale of Pairwise Comparison	69
Table 5.2	Randomness Index	71
Table 5.3	Pairwise Comparison of Causative Factors	73
Table 5.4	AHP Pairwise Comparison Matrix	74
Table 5.5	Calculation of Weightage using Frequency Ratio and Shannon's Entropy	78
Appendix	Landslide Inventory Data of 500 Landslides in the Study Area	128

List of Abbreviations

GIS	:	Geographic Information System
DEM	:	Digital Elevation Model
MSK Scale	:	Medvedev–Sponheuer–Karnik Scale
FIR	:	First Investigation Report
IV	:	Info Value
WOE	:	Weight of Evidence
ANN	:	Artificial Neural Network
ROC Curve	:	Receiver Operation Characteristics Curve
FS	:	Factor of Safety
AHP	:	Analytic Hierarchy Process
ANP	:	Analytic Network Process
FR	:	Frequency Ratio
SE	:	Shannon’s Entropy
LSI	:	Landslide Susceptibility Index
GSI	:	Geological Survey of India
WoS	:	Web of Science
AUC	:	Area under Curve
NRSC	:	National Remote Sensing Centre
CI	:	Consistency Index
RI	:	Randomness Index
TWI	:	Topographic Wetness Index

Chapter 1

Introduction

1.1. Background

Landslides are considered one of the most disastrous natural phenomena resulting in the loss of property and life. The development and environment are interrelated. The hilly regions are developing at a rapid rate [1]. The anthropogenic human activities like construction, mining, cutting and filling of slopes, etc. have made the natural slopes prone to failure. Failure of slopes is a big problem in hilly regions [1]. Many researchers have defined landslides in many ways. A landslide is a downward movement of material under the effect of gravity [2]. Landslides are a type of "mass wasting," which denotes any down-slope movement of soil and rock under the direct influence of gravity [3]. A landslide can be broadly defined as a sudden mass movement that occurs on sloping terrain under the impact of gravity. It is clear from the definition that the failed material and its movement define a landslide. Landslides are a serious geological threat in mountainous terrains. Research on landslides is conducted majorly since the 20th century. The triggering factors like earthquakes and rainfall can increase the cost of damaged infrastructure. Asia is the most affected continent by landslide activities. Around 75% of the total landslides in the world occur in Asia [4]. The construction-induced landslides in India occur on a very large scale. India lies in the top 5 countries that are affected by natural disasters [4].

The Himalayan region in India faces a number of landslide events throughout the year. The landslides cause traffic jams and land degradation in the region. Shimla region in Himachal Pradesh (H.P) has faced some of the most destructive landslides in history. The state gazetteer

provides details of numerous disastrous landslides that occurred during the earthquake of 1803 [5]. The landslides in the region are frequently reported by the newspapers. In 1989, a disastrous landslide at Matiana in Shimla killed around 40 people and injured many [6]. Shimla Kalka road is jammed multiple times every year due to the debris caused by landslides [6]. The disastrous impact of landslides in the Himalayan region poses a major geological threat. So, it is necessary to plan, manage, and mitigate the landslide hazard. Landslide susceptibility maps are an efficient tool for planning and management of landslide disasters.

1.2. Classification and Types of Landslides

A landslide can be of two types i.e. rotational and translational. Rotational and translational landslides are the movements of one or more failure surfaces [7]. Rotational landslides are the movement of mass over a concave surface which will be downward and in an outward direction. The translational landslides are the movement of mass on the planar surface [7]. Varnes (1978) classified the landslides based upon the failed mass and its movement [8]. The classifications were based upon the failed mass and its movement. The various kind of materials that can fail are defined as follows:

a). Rock: Rock may be defined as an intact hard mass that is firm in nature. According to Varnes [8], it should be at its natural place before failure.

b). Soil: Soil is created by the minerals and fragments of rock. It may be transported from other parts or may be formed due to weathering of rock. The soils which are transported from one place

to other may show different characteristics than the surface on which it is lying. The gases and air in the soil pores form a part of the soil itself.

c). **Earth:** The material which contains 80% of its particles with dimensions less than 2 mm is defined as earth. The upper limit of sand-sized particles is 2 mm.

d). **Mud:** Mud is defined as a material that has 80% of the particles less than that of the upper limit of silt-sized particles. It means the material which has 80% of particles less than the size of 0.06 mm.

e). **Debris:** Debris represents coarse material. It contains a 20% to 80% proportion of particles with a diameter of more than 2 mm.

The second parameter for defining the landslides is the movement of the failed mass. The movement of the failed mass is classified by Varnes [8] in the following categories:

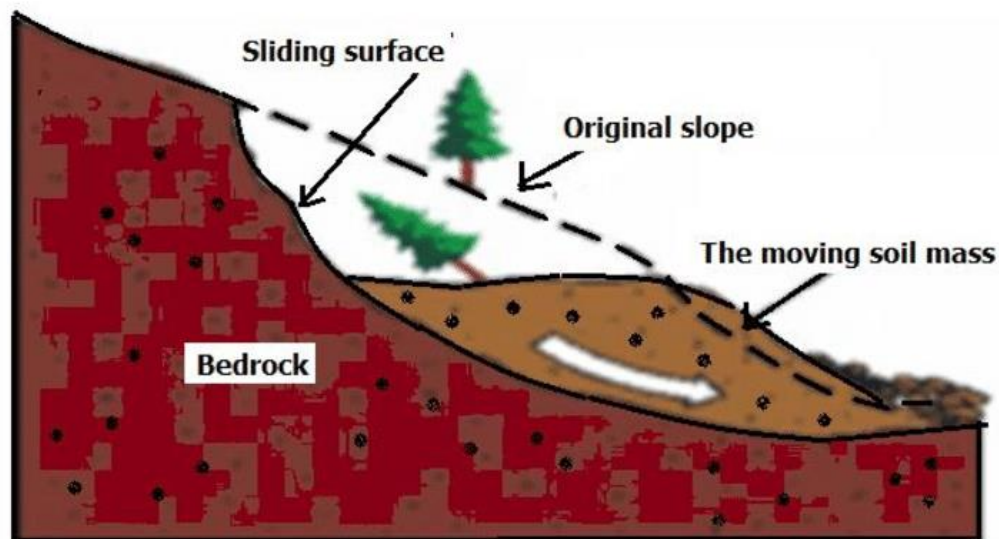
a). **Falls:** Falls are the sudden movement of rock or soil mass. The masses can get detached from the cracks and discontinuities. These occur normally on steep slopes or cliffs. Falls usually involve a mixture of free fall through the air, bouncing or rolling. The factors which affect the occurrence of falls are gravity, weathering of material and the presence of pore water.

b). **Topple:** Movement of rock, earth or debris in the forward rotation is termed as 'topple'. Topples occur due to an imbalance of forces and material fails along any axis near the base of rock or block. The failed material falls at the base of the block.

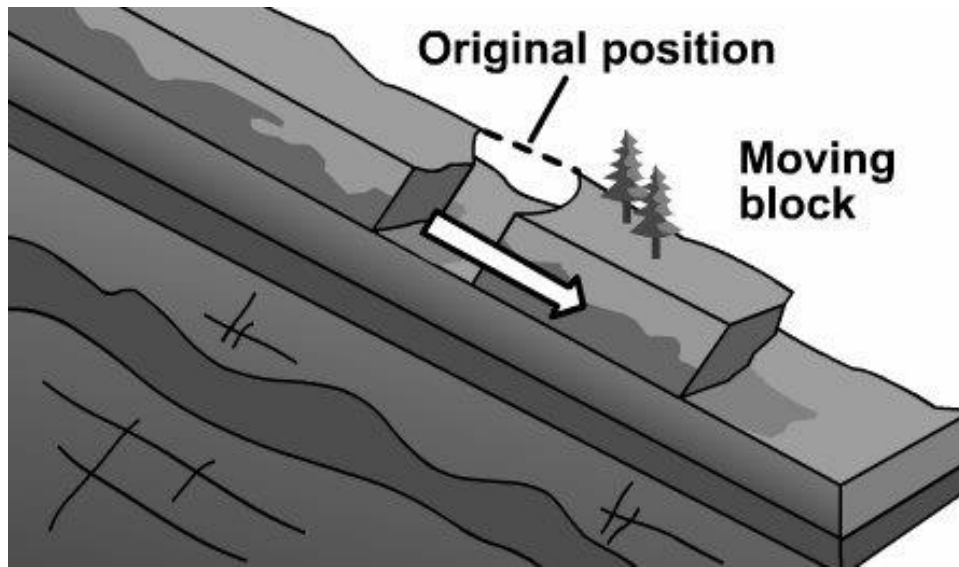
c). **Slide:** Slides are the movement of mass along distinct weakness zone. The underlying material is more stable and the weak zones fail along the cracks. Figures 1.1 a and 1.1 b show the rotational and translational slides.

d). **Lateral Spread:** Lateral spread takes place at a flat place. The failed mass spreads in the lateral direction with shear and tensile fractures. It takes place in loose, saturated, and cohesionless soil. Earthquakes generally trigger the process of failure.

e). **Flows:** The failed material behaves like liquid and flows. The speed of the movement may vary from rapid to extremely rapid. These may prove very disastrous. The combination of any two or more movements described above shows the complex nature of the mass failure.



(a)



(b)

Figure 1.1. (a) Rotational Landslide [9] (b) Translational Landslide [10]

These two terms can be combined to get the type of landslide. For example, rockfall, rock topple, debris slide, debris flow, earth slide, earth spread, earth flow, etc. Figure 1.2 shows the modified classification of landslides [11].

1.3. Causes of Landslides

Landslides occur when the shear stress in the soil or rock mass exceeds the shear strength of the material. There are numerous causes of landslides. The materials or masses which have lower shear strength can fail in shear resulting in landslides [12-13]. The materials can be sensitive to moisture and weather. The change in temperature and moisture conditions can change the mass's characteristics, which can result in slope failures [14]. The occurrence of landslides also depends upon the fissures and cracks found in the mass. The sheared and jointed material can fail along the weaker zones [15]. The discontinuities in the masses can induce instability and result in the failure

of slopes. The permeability characteristics of the soil or rock mass also affect the occurrence of landslides. Permeability impact the pore water pressure in the soil or rock mass.

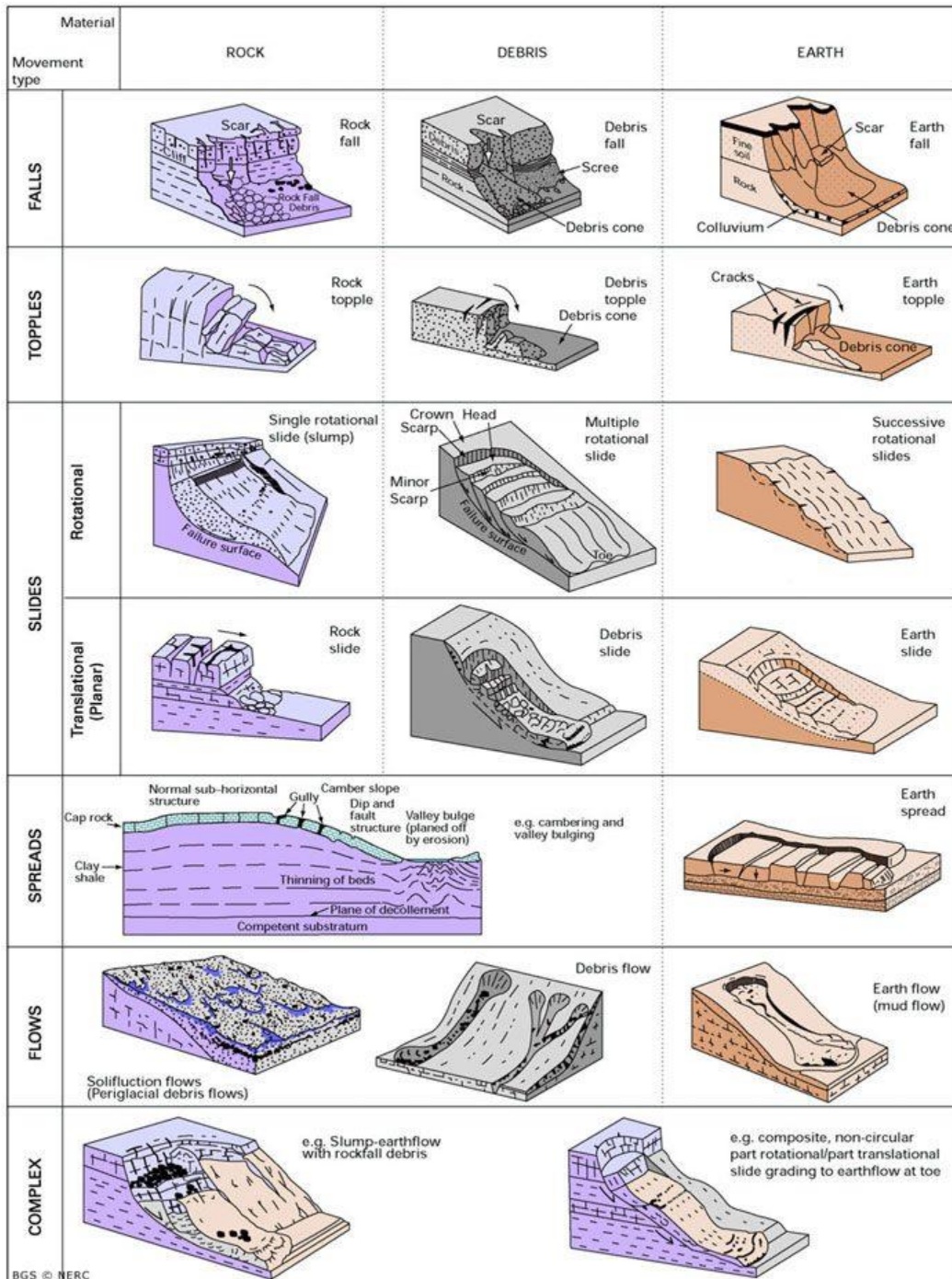


Figure 1.2. Modified Classification of Landslides [11]

Erosion is another important parameter that is responsible for the occurrence of landslides [15]. The erosion can be due to the water, wind, sunlight, and human activities. The erosion characteristics also depend upon the type of material. The banks of rivers are more prone to landslides as erosion takes place due to the excessive speed of river flow. The erosion along streams makes the toe of the soil or rock mass weak and hence results in the failure of slopes. The increased pore pressure due to moisture in mass can also cause slope failure [16]. The erosion can cause the loss of vegetation on the surface of the slopes which can make the slopes unstable. The vegetation has a two-way impact on the occurrence of landslides. The roots can bind the soil mass and make them stronger. Few studies show that the roots in the rock can pierce and make the cracks wider and hence resulting in poor slope stability [17].

There are many physical causes of landslides that act as triggering factors of the landslides. Intense rainfall is a major cause of landslides. The excess amount of precipitation increases the pore water pressure in the soil/rock masses and also makes the material weaker. The precipitation also increases the erosion of the mass which results in the instability of slopes. The number of landslides increases during the monsoon season in hilly regions. The earthquake is another major triggering factor of landslides [18]. High-intensity earthquake results in the liquefaction of the soil/rock masses. The vibration caused by an earthquake can induce instability in the soil or rock masses. The vibrations produced during earthquakes also impact the pore water pressure. Floods, tides and volcanic eruptions can also trigger landslide activities.

Many anthropogenic activities can trigger the movement of slopes. Rapid deforestation activities can change the pattern of vegetation which can increase the erosion in the study area increasing

landslide activities [19]. The mining activities can also trigger landslide activities. The vibrations from the mining activities and traffic increase the instability in the soil mass.

1.4. Economic Aspects of Landslide

The landslides are responsible for the huge economic losses which can be counted in monetary form [20-21]. The losses due to landslides also include traffic jams, delays in journeys, minor injuries and deaths. The economic impact of landslides can be direct and indirect [20]. The direct impact can be calculated easily. The debris and the failed material can come to the road. The direct cost of cleaning and the maintenance of roads can be calculated. The cost of damaged vehicles and the accident cost can also be calculated. The landslides can cut off the mode of communication in the areas which are situated remotely. The houses which are situated in landslide-prone areas can be damaged partially or fully. The differential settlement of the foundations can take place in landslide-prone areas. The cost of damage and the cost of maintenance of affected infrastructure can be calculated and may be borne by government agencies, insurance companies, or the victims [20-21].

1.5. Mechanism of Landslides

The material in slopes can move at a slow speed and can take years to fail. The speed of movement can be rapid also. The slope material moves under the effect of gravity. The stability of a slope depends upon the driving forces and the resisting forces. The driving forces are responsible for the downslope movement of the mass while the resisting forces resist the downslope movement of the mass. If the driving forces exceed the resisting forces, the slope is considered as unstable slope. If the resisting force of the material is more than the driving forces, then the slope is considered to

be a stable slope. The resisting force is the shear strength of the slope material while the driving force is the gravity. The driving force can be increased due to triggering factors like earthquakes and moisture. Moisture in the soils is an important factor that is responsible for the failure of slopes. The moisture increases the shear stress in the soil or rock mass. The increased shear stress results in slope failure. A majority of landslides take place in the rainy seasons. So, moisture is to be considered carefully in the slope studies. The factor of safety (F.S) is defined as the ratio of resisting forces in the soil or rock mass to the driving forces. The higher values of the factor of safety show stable slopes. The formula for the factor of safety is given as follows:

$$\text{Factor of Safety (F.S)} = \frac{\text{Resisting Forces}}{\text{Driving Forces}} \quad (1.1)$$

If the factor of safety is less than 1 then the slopes are unstable. If the factor of safety is more than 1, then the slopes are stable in nature. The simplest case is the failure of infinite slopes. The factor of safety is determined by the following formula:

$$\text{Factor of Safety (F.S)} = \frac{\text{Shear Strength}}{\text{Mobilized Shear Stress}} \quad (1.2)$$

If the factor of safety is more than unity, the slope is considered safe while the slope is considered unsafe or prone to failure if the factor of safety is less than 1.

Figure 1.1 shows the mechanism of the landslide. The slip surface formed in the soil mass or rock mass causes the failure of the slope. Due to the penetration of the water, the slopes may fail. The water increases the pore water pressure in the slopes which can break the connection between the soil particles resulting into the failure of the slopes. Slopes may fail due to the saturation caused

by the seepage of the water. Excess rainfall can cause the soil flow like a liquid which results into the debris flow or mud flow.

1.6. Micro-zonation of Landslide Susceptibility

In simple words, a landslide micro-zonation map is prepared by dividing a study area into three or four zones according to its susceptibility to the occurrence of landslides. A landslide susceptibility map identifies areas that are subject to landslides and is measured from low to high [3]. Micro-zonation of landslide susceptibility takes into account where the landslides occur and what causes them. According to USGS, these maps describe the relative likelihood of future landslides based solely on the properties of a site [3]. In simple words, landslide susceptibility maps show the possibility of the occurrence of landslides on a map with the help of some color combination.

1.7. Research Problem

Landslides are the third largest disaster in the world. Microzonation of landslide susceptibility can provide useful information for the planning and management of landslides. The failure of natural slopes is a complex phenomenon and the identification of the factors that are responsible for the occurrence of landslides is very important [5-6]. The causative factors act cumulatively resulting in the occurrence of landslides. Quantitative techniques and mixed methods can provide accurate information about the landslide potential of the region [14-15].

There is a need for a comparison of the expert-based techniques and statistical techniques to understand the suitability of these techniques in the study area. The statistical techniques depend on the available historical landslide data while the expert-based techniques consider the opinion

of experts for understanding the contribution of the causative factors of the landslides. There is a need to learn more about mixed methods of landslide susceptibility mapping.

1.8. Aim and Objectives of the Study

Qualitative and quantitative techniques are used for landslide susceptibility mapping in the GIS environment. The qualitative techniques use expert opinion for landslide susceptibility mapping while the quantitative techniques establish the mathematical relationship between the causative factors and the occurrence of the landslides. The different objectives of the study are given as follows:

- (1) To study the different causative factors of landslides from existing literature using the historical data and explore its impact on the occurrence of the landslides.
- (2) To prepare the landslide inventories for Shimla district in Himachal Pradesh (H.P.).
- (3) To study the different methods for landslide susceptibility mapping
- (4) To compare different available methods and suggest the most suitable method for landslide susceptibility mapping of the Shimla region.
- (5) To propose a hybrid method to reduce the subjectivity of expert opinion in the Analytic Hierarchy Process (AHP).

1.9. Research Questions

The following research questions arise after analyzing the available literature:

- (1) What is the type of landslides in the study area?
- (2) What are the different factors that are responsible for the occurrence of landslides?

(3) What is the suitability of the different statistical and mixed methods for microzonation of landslide susceptibility?

(4) How can we reduce the subjectivity in expert-based techniques?

1.10. Organization of Thesis

The thesis is organized into seven chapters. The details of each chapter are given as follows:

Chapter 1 describes the background and the motivation of the study. The problem of landslides and their economic aspects are discussed in this chapter. The problem statement, research problem, objectives of the study, and research questions are discussed in this chapter.

Chapter 2 describes the available literature in the field of landslide susceptibility mapping using geographic information system (GIS). The techniques for landslide susceptibility mapping are divided into three categories. The different categories of landslide susceptibility techniques are elaborated and the advantages and limitations of these approaches are discussed in detail. The techniques of landslide susceptibility mapping are evaluated based on the need for data, suitability and accuracy. The findings from the literature review are enlisted separately for better understanding. The research gaps from the literature are identified in this chapter.

Chapter 3 provides a conceptual framework for the study. The sources of different data sets are explained. A detailed discussion about the characteristics of the study area is included in this chapter. A brief description of the landslide inventory of the study area is also discussed. The photographs of the landslides that occurred in the study area are included. A flow chart explaining the procedure adopted for achieving the objectives is also included in this chapter. Chapter 3 provides a framework for the implementation of techniques discussed in Chapter 4 and Chapter 5.

Chapter 4 describes the different causative factors of landslides. The causative factors of landslides are classified into five categories i.e. topographic factors, geological factors, hydrological factors, anthropogenic factors and land-use factors. These factors are extracted from the different sources and processed in geographic information system (GIS) environment. The role of the causative factors and their processing is discussed according to the chapter 3.

Chapter 5 describes the mathematical modeling adopted in the study. The methods like analytic hierarchy process (AHP), frequency ratio (FR) and Shannon's entropy (SE) are explained. The weightage for sub-factors and causative factors are calculated using semi-qualitative and quantitative techniques. The equations for landslide susceptibility mapping based on the landslide susceptibility index are developed using different approaches in this chapter. The process of calculation of weightage is explained as needed in chapter 3 for the preparation of landslide susceptibility maps.

Chapter 6 describes the results of the study. The landslide susceptibility maps developed by different techniques are discussed in this chapter. The distribution of landslides in different susceptibility zones is also described. The impact of different causative factors and sub-factors is explained according to the different models. The outputs of the study are validated using the receiver operation characteristics (ROC) curve. The mathematical models used in this study are compared for their accuracy and their suitability. The distribution of landslide susceptibility zones and the occurrence of landslides in these zones are also discussed in this chapter.

Chapter 7 concludes the thesis and provides some recommendations based on the results of the study. The chapter discusses the sensitivity of the various landslide susceptibility zones. The achievement of the objectives is also discussed in this chapter. The conclusion is based on the previous chapters. Some recommendations and suggestions are given based on the landslide potential of the study area. The recommendations for the selection of causative factors for landslide susceptibility mapping are also given. The possible extension of the study and its applications are described in this chapter.

1.11. Concluding Remarks

As discussed in the background section, landslides are a crucial problem and it is important to develop landslide susceptibility maps for the planning of landslide hazards. The mechanism of slope failure and its economic aspects are studied in the previous sections. The microzonation of landslide susceptibility is performed using qualitative, quantitative, and mixed models. It is essential to understand the different techniques of landslide susceptibility mapping which requires an extensive review of the existing literature.

Literature Review

2.1. Introduction

In this chapter, a review of previously published literature in the field of landslide susceptibility mapping is performed. A literature database of more than 120 research items is created. The research items include journal articles, book chapters, conference articles and handbooks. Most of the literature is reviewed from the journal articles while a small number of book chapters and conference articles are also included. The research items are searched with the keywords such as landslide susceptibility, landslide mapping, landslide susceptibility using frequency ratio, AHP and statistical methods of landslide susceptibility mapping. The literature is searched and downloaded from the database of SCOPUS, DOAJ and Web of Science (WoS), journals from the library. The research items are shortlisted for review based on indexing and the quality of the articles.

Landslide susceptibility maps are very important and efficient tools in the planning and management of landslide hazards [22-25]. A geographic information system (GIS) is a tool that is used for storing, creating, managing and manipulating spatial data [26]. In landslide susceptibility mapping a large amount of spatial data is to be handled. So, GIS proves to be a good tool in landslide susceptibility mapping due to its ability to handle a large amount of spatial data [27-29]. The factors responsible for the occurrence of landslides can be identified on the maps and processed on a computer to create the landslide susceptibility map.

Several techniques for the evaluation of landslide susceptibility are available in the GIS environment. The different mathematical and non-mathematical models can be applied according to the suitability of available field data. In some methods, the field visits for assessing the information about landslides can be reduced as most of the work can be done in GIS environment and the field data is required for the validation purpose only [30]. It is also possible to improve the models by varying the inputs. Users can achieve better results by trial and error process in a single model.

The availability of satellite data like the digital elevation model (DEM) reduces the fieldwork to a minimum level [31]. There are some disadvantages of GIS also. The cost of required software and input data is high. Some open-access software are available but these software are not much user-friendly. The huge data is to be handled which requires high-class skill and a highly efficient computer system. It is necessary to understand the different ways to perform the landslide studies. The landslides are studied at different levels. The landslides can be mapped in the form of a simple landslide inventory to a complex risk assessment map. The different types of the landslide studies are discussed in the next section.

2.2. Types of Landslide Studies

Remote sensing is the science of obtaining information about a phenomenon or an object using satellites. The satellite data can be processed to obtain useful information. Satellite imagery is of high use in the geographic information system (GIS) environment. Remote sensing and GIS has found applications in monitoring, planning, and management of different natural disasters like

floods, landslide, wildfire, glacier failures, etc. Satellite imagery and GIS are used at various levels in landslide studies.

2.2.1. Landslide Inventory

The landslide events can be monitored using satellite imagery and the Google Earth platform. The landslide inventories are prepared from the satellite imagery, field surveys or previous literature. A landslide inventory is the first stage of landslide study which give details about the historical data of landslides [32-33]. The seasonal landslide inventories can be prepared using remotely sensed data. It shows the distribution of landslides and their characteristics. Landslide inventory maps investigate the types of landslides, their classification, date of occurrence, location of landslides and their distribution [33]. These can be used to understand the pattern of landslide occurrence and are also used to prepare the landslide susceptibility and hazard maps. The landslide inventories can be prepared using satellite imagery, drones and low-level flying aircraft or field surveys.

The landslide data collection formats are prepared according to the requirement of the user. Geological Survey of India (GSI) proposes a 41-point format for landslide data collection which consists of details about the location, date of occurrence, the activity of the landslide, material of landslide, type of landslide, area of landslide etc. [34]. The formats can be simplified depending on the needs of the user. According to the Geological Survey of India (GSI), a landslide inventory is a useful tool for the conversion of the susceptibility maps to the hazard or risk maps [34]. The landslide inventories have two parts- graphical and tabular. The graphical portion shows the spatial distribution of the landslides. The landslides can be shown by the polygons according to their

extent. The small landslides can also be shown in the form of points. The table consists of the attributes of the landslides. A simple inventory consists of the following information:

- Location of the landslide in the form of longitude and the latitude
- Area of the landslide
- The volume of the failed mass
- Type of failed material
- Type of movement
- Rate of movement
- Activity of landslide
- Date of survey
- Date of occurrence

The first investigation report (FIR) is a format for the collection of data related to the landslides. It is a 20-point report which is filled by the surveyor [34]. The format of FIR is suggested by the Survey of India and it is the simplest format for recording the data related to landslides. The format for the collection of the data can also be simplified to 12 points which are used to collect the data from the eyewitnesses. The format for the landslide data collection is modified making it more convenient for unskilled labour.

2.2.2. Landslide Susceptibility Maps

In simple words, a landslide map is prepared by dividing a study area into three or four zones according to its susceptibility toward land-sliding. The following definitions are given by the different agencies:

- According to the Geological Survey of Ireland, a landslide susceptibility map identifies the area that is subject to landslides and is measured from low to high [35]. The landslide susceptibility map takes into account where the landslides occur and what causes them.
- According to USGS, Landslide susceptibility maps describe the relative likelihood of future land-sliding based solely on the properties of a site. Landslide susceptibility may be defined as the likelihood of a landslide occurring in an area based on local terrain conditions [36].
- The spatial probability of the occurrence of the landslide event is known as the landslide susceptibility [37].

Landslide susceptibility maps are used widely for assessment of the landslides worldwide. Landslide susceptibility maps show the cumulative effect of different factors. Once the cumulative effect of different causative factors of landslides is evaluated, a landslide susceptibility map can be prepared. The landslide susceptibility maps consider the variation of possible landslide events according to the area. These maps forecast the location where the landslides can take place. This kind of map does not consider the temporal variation of landslide events [37]. The landslide susceptibility maps deal with the spatial probability of occurrence of landslides.

2.2.3. Landslide Hazard Maps

Landslide hazard maps are the advanced version of the landslide susceptibility maps. These maps provide more information about the landslides in a deep context. A landslide is considered a hazard if it has damaging effects on the infrastructure or the population [38]. If a disaster occurs in a

region of zero inhabitants, then it can't be called a hazard. A landslide hazard may be defined as the probability of occurrence of a damaging phenomenon within a specified time and region [38]. Landslide hazard maps give the probability of occurrence of potentially damaging landslides with some magnitude within a region at a specified time. Landslide hazard maps provide information about the temporal and spatial variation of landslide potential with the magnitude of the landslides [39]. So, landslide susceptibility is a part of landslide hazard zonation maps. Landslide hazards can be represented with the following formula:

$$\text{Landslide Hazard} = \text{Spatial Probabilitiy} * \text{Temporal Probability} \quad (2.1)$$

Landslide hazard zonation maps consider the two aspects:

- The spatial variability of the occurrence of landslide events in a specific area is considered as one part [39-40]. Factors like terrain characteristics, drainage characteristics and geological characteristics of the area are responsible for the spatial variability of the landslide events. The landslide susceptibility maps show the spatial variability of the landslide events. So, the landslide susceptibility map of the area becomes the first part of the landslide hazard maps.
- The second aspect is the probability of occurrence of triggering events like excessive rainfall or earthquake. The rainfall patterns can be forecasted according to the historical weather data. The combination of both aspects results in the landslide hazard maps.

2.2.4. Landslide Risk Maps

Landslide risk maps show the potential loss or the effect of the landslide on the property. It can be converted into monetary form also. The landslide risk maps provide information about the likelihood and extent to which the future failure of a slope can affect the society, people or infrastructure in an adverse manner [40]. The landslide risk maps help the planner to assess the risk of the landslide events. The risk assessment of the landslide events gives an idea if the risk due to failure of slopes in the future is tolerable or not. The risk of landslides can be predicted for the population, loss of life or loss of property [41-43]. The following terms are to be kept in mind while studying the risk of landslides.

- The elements of risk are the elements that can face the potential hazard from the landslide event. A house, property, human, infrastructure or environmental feature in the landslide risk zone is known as the element of risk [44]. The value of elements of risk is represented as E.
- The degree of loss to the particular element of risk is known as the vulnerability of the element towards risk. The degree of loss varies from 0 to 1 [44-45]. If there is no loss, the degree of loss is zero and if the loss is extreme then the degree of loss is considered as 1. The intermediate values can be considered also.

The risk of a landslide event is a function of landslide hazard (H), vulnerability (V) and the value of risk elements. The risk (R) is given as follows:

$$R = H * V * E \quad (2.2)$$

2.3. Role of Scale in Landslide Mapping

The scale for the mapping of the landslides varies according to the policies of the nation. According to the Geological Survey of India (GSI), the national scale lies from 1:100000 to 1:1000000 [46]. This is also known as the regional scale. Macro scales lie from 1:25000 to 1:50000 while the mesoscales are from 1:5000 to 1:10000 [46]. The scales larger than the mesoscales can be used for site-specific mapping. The regional or national scales are widely used for landslide susceptibility mapping using statistical and semi-qualitative techniques.

The gaps in the Indian system of scales are filled by Cees van Westen. The regional scale proposed by Westen is the same as that of the Indian code. However, a medium scale varying from 1:25000 to 1:100000 is introduced [47]. The landslide susceptibility maps can be prepared on the national scale and medium scales. However, the medium scales are very suitable for landslide hazard studies. Large scales are from 1:2000 to 1:25000 which are suitable for landslide risk assessment [47]. The site-specific scale is from 1:200 to 1:2000 which can't be used for the purpose of landslide susceptibility mapping.

2.4. Landslide Susceptibility Mapping Techniques

There are various techniques available in the literature for landslide susceptibility mapping. These techniques can be divided into four categories i.e. qualitative techniques, quantitative techniques, semi-qualitative/semi-quantitative techniques and black box models [37, 48-49]. The techniques have their own suitability and limitations based on the study area and availability of historical landslide data. Figure 2.1 shows the different approaches for landslide susceptibility mapping.

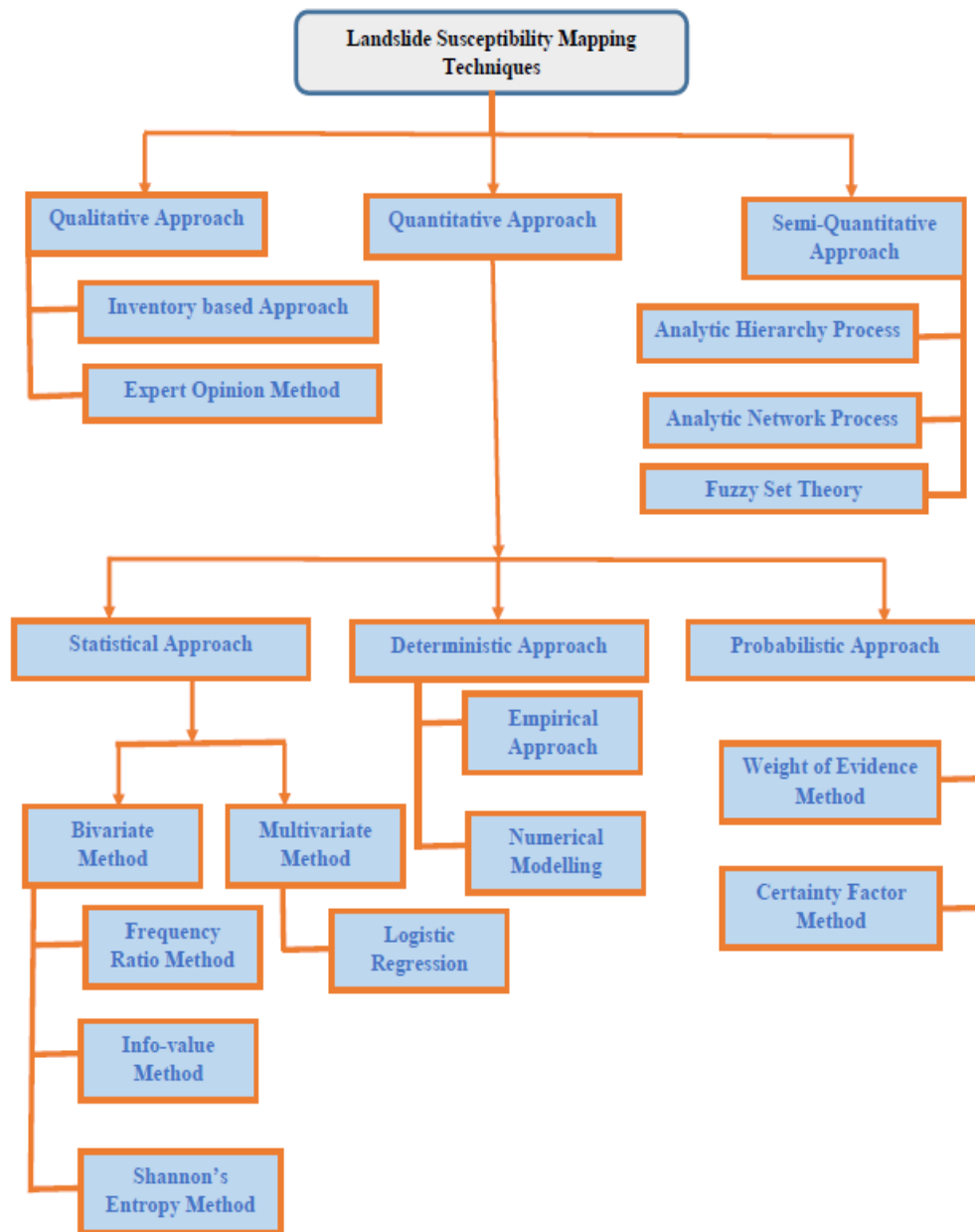


Figure 2.1. Approaches to landslide susceptibility mapping

2.4.1. Qualitative Approach

The qualitative approach to landslide susceptibility mapping depends upon the expert rating system [50]. The perception of experts can be used to evaluate the relative importance of the

causative factors of the landslides [51-52]. The expert can assign the weightage to the causative factors based on their experience and judgment. The multi-criteria decision-based methods can be included in this category. The experts may visit the site and the slopes are studied for the parameters like type of soil, erosion, moisture etc. [53]. The experts are selected based on their qualifications and working background. The engineers and researchers working in the field of slope stability of natural slopes and who have vast experience in the planning and management of landslides can be selected as experts. The policy makers and risk managers working in the hilly regions can also be selected as experts based on their work profile.

The qualitative landslide susceptibility mapping is based upon the pieces of evidence of mass movements, location of scraps, fractures, their age etc. [54]. The qualitative approaches are easy to implement. The field experience and expert perception are helpful in considering the unseen causative factors of landslides [55-57]. If a landslide inventory is not available, expert-based techniques are the only option for the preparation of landslide susceptibility maps. The accuracy of the qualitative method is very less as compared to the other techniques. The weightage assigned to the causative factors and sub-factors depends upon the subjective judgment of the expert [57-59]. The expert rating may vary from expert to expert.

The qualitative approach can be improved if data-driven perception is used. The historical data on landslides can be used by the experts as a reference. The expert-based inputs can be checked for consistency and can be validated using semi-qualitative techniques [55]. Expert weightage techniques and weighted linear combinations are examples of qualitative approaches. Purely expert-based outputs are voided as the results may be biased and accuracy remains very less.

2.4.2. Quantitative Approach

In the quantitative approach, a mathematical relationship is established between landslide occurrence and its causative factors [53]. The qualitative approach is biased based on the expert's perception while the quantitative approach is purely based on the available historical data and its mathematical relationship with the occurrence of landslides. A well-distributed landslide inventory is required for the preparation of landslide susceptibility maps using quantitative approaches [60-61]. The major advantage of quantitative approaches is that it gives higher accuracy as compared to the qualitative methods. These methods are relatively more reliable as they are based on historical pieces of evidence. The accuracy and results of these methods depend upon the landslide inventory. If the historical landslide data is not available, the methods can't be implemented. Moreover, if the landslide inventory is not well distributed, the accuracy is reduced [29]. These methods can be divided into three categories:

- Deterministic Models
- Statistical Models
- Probabilistic Models

- **Deterministic Models**

The simplest technique for landslide susceptibility mapping is based on the study of the landslide inventories [27]. The geomorphological approach is guided by the principle that 'past is the key of future' [3-4]. This means the study of the spatial locations of the past landslides is important to assess the possibility of the occurrence of landslides in the future. The distribution of the landslides in a region is shown in the landslide inventory map. The landslide inventories can be prepared from the archives or literature [27, 61].

A geomorphological approach is a heuristic approach that considers the opinion of the expert. The ability to understand the geomorphological condition and their impact on the stability of slope affects the results of the landslide susceptibility map [27, 61]. The landslide inventories are studied by the experts and the geomorphological characteristics of the area are considered for predicting the susceptibility of landslides. The landslide inventories give an idea to the expert about the correlation between the failure of slopes and the causative factors of landslides.

The deterministic models are site-specific models. The physical parameters of the region are considered for the development of landslide susceptibility maps [31-32, 62]. The factor of safety of different slopes is calculated experimentally in the study area and based on the factor of safety, the proneness of the region towards landslides is evaluated. The deterministic approach can be applied in the regions where the physical characteristics of the study area are homogenous and uniform. The site-specific maps of physical factors like hydrological characteristics, soil water distribution, factor of safety etc. can be prepared and a landslide susceptibility map is prepared by the combination of physical characteristics of the region [31, 60]. These models are not used in large areas as these are only suitable for site-specific landslide susceptibility mapping.

- **Statistical Models**

The statistical models establish the statistical relationship between causative factors and the occurrence of landslides. These methods can be further categorized into bivariate

statistical models and multivariate statistical models [34]. The bivariate techniques represent the relationship between causative factors of landslides and the distribution of historical landslides. The bivariate statistical models include the frequency ratio (FR) method, information value (IV) technique, and Shannon's entropy (SE) method [35-39]. In bivariate statistical analysis, the causative factors are considered individually and independent of each other [36-37].

The frequency ratio models are based upon the relationship between the occurrence of landslide events and the causative factors. The prediction of landslide susceptibility in this method is determined by analyzing the landslide distribution in the study area. The frequency ratio for each influencing factor is calculated using the landslide distribution data. The frequency ratio is the ratio between the percent areas where the landslide occurred in a class to the percent area of the influencing class relative to the whole study area. Demir et al used frequency ratio for the landslide susceptibility mapping of Tokat region, Turkey [23]. The causative factors elevation, slope gradient, slope aspect, distance to streams, roads, and faults, drainage density, and fault density are used in the analysis. The factors like geology and lithology are not considered in this study which led to the less accuracy of the model which is around 70%.

Khan et al used frequency ratio for the assessment of landslide susceptibility in Northern Pakistan [29]. The SPOT- 5 satellite imagery is used to prepare the landslide inventory. The inventory is verified by the field survey. The spatial resolution of the digital elevation model used in this study was 30 m. The factors such as Slope, aspect, geology, lithology,

fault distance, distance from the road, land cover and drainage distance are considered for the prediction of landslide susceptibility. The accuracy of the model is found to be nearly 70%.

Park et al prepared a landslide susceptibility map of Inje area in Korea using the frequency ratio (FR) approach [63]. Topographic factors considered in this study are elevation, slope and aspect. Curvature is not considered in this study. As the curvature indirectly shows the effect of water, so stream power index is considered with distance from drainage. Forest characteristics of the area are given importance [63]. The type, diameter and age of timber are considered. The type of soil is replaced with texture and effective thickness. The texture and effective thickness can represent the soil characteristics in a better manner. The accuracy of the model is found to be around 80%. If the effect of lithology would have been considered, it could have led to better accuracy of the model.

The multivariate models establish the relationship among multiple variables at the same time. In this technique, the relationship between the causative factors of landslides and landslide occurrence is established with the interrelationship among the causative factors [64-66]. The logistic regression technique is an example of a multivariate approach [67-68]. The multivariate models should have little or no multi-collinearity among the independent variables [66-68]. It means that the independent variables must not be highly correlated to each other as the output is affected by the correlation of the independent variable and errors are induced.

A landslide susceptibility map for the Chun'an County region in China using a logistic regression model is prepared in 2006 [69]. Most of the landslides have a length and breadth of less than 30m. The resolution of the DEM-based layers used is 30 m. The factors considered are elevation, slope, aspect, profile curvature, plan-curvature, distance to the river, fault, drainage line, residential area, road and digging, land use type, soil type, engineering and geological conditions [69]. The geological conditions are studied during the field visits also. The accuracy of the study was found to be 80%.

Mathew et al predicted the landslide susceptibility of the lower Garhwal Himalaya region in India [70]. The study area consists of lime, shale, quartzite, slate and phyllites. The resolution of the layer used in this study was 25 m. The LISS data is used to extract the slope, aspect, curvature and elevation layer. A higher density of geological structures shows a higher value of coefficient which means that the susceptibility of landslides increases with the density of geological structures [70]. The high value of slope angle and proximity of geological structure increases instability in the phyllite and slate rocks. Talei prepared a landslide susceptibility map using logistic regression for Hashtchin region in Iran in 2014 [71]. The resolution of satellite imagery was 50 m x 50 m. The rocks are classified into calcareous, plutonic, volcanic, and pyroclastic categories. Relative permeability of the formation is a new factor that is considered in this study [71]. The major landslides took place in the region of low permeability. The accuracy of the landslide susceptibility map was found to be 84.1%. Logistic regression models are very sensitive to the regression parameters. A small error in the input regression parameter results leads to erroneous output [72-75]. The causative factors must be selected carefully in multivariate

techniques. The impact of repetition of weights for the same effect induces error in the output. For example, some researchers consider the drainage density and distance from streams as two different factors while their impact is the same. So, the weightage given to the impact of streams on landslides becomes relatively high which affects the accuracy of the results.

- **Probabilistic Models**

In this technique, the probabilistic approach is used to determine the possibility of the occurrence of landslides in a region based on the causative factors. The contribution of the causative factors to the landslide probability is evaluated. Weight of evidence (WoE) and certainty factor (CF) are examples of the probabilistic approach [76-80]. Weight of evidence is a statistical method based on the Bayesian bivariate technique. It is a data-driven approach. The relationship between the spatial distribution of landslide-affected areas and the causative factors is assessed in this method using Baye's concept of prior and posterior probability [76]. The effect of various causative factors on landslides is analyzed and the susceptibility of the study area toward landslides is predicted. The weights that are calculated in this method are positive and negative [77]. The positive and negative weights show a positive and negative correlation [78].

The weight of Evidence (WoE) model is applied in the different parts of the world by various researchers [79-84]. Lee and Choi prepared a landslide susceptibility map for Boun area in Korea [79]. The map is prepared after the occurrence of frequent landslides in the study area in the years 1996, 1998, 1999 and 2002. Soil texture, type of soil and the

drainage characteristics of soil classes are considered separate factors. The other factors which are different from the normal studies are the forest density, age of trees and diameter of trees. The best combination of the causative factors is found which gives the best results. From 43 combinations of these factors, the dataset of factors slope, timber diameter, curvature, topography, geology and lineament gives the best results.

Kumar and Anbalagan published their work related to landslide susceptibility mapping of Tehri reservoir in India in Journal of Earth System Sciences [83]. The study concluded that the low relief area, lower values of slopes, northeast northwest aspect and forest soil don't contribute much to the landslide susceptibility of the area. Alluvium soil, south aspect, high relative relief, high slope, proximity to drainage and proximity to the reservoir are the main factors that are responsible for the occurrence of landslides in the study area. The accuracy of the output in this study was around 80%.

Pradhan et al performed landslide susceptibility mapping in Cameron Highlands area in Malaysia [85]. The landslide susceptibility map is prepared after the heavy rainfall of 2008, 2009 and 2010. The areas where the rainfall amount is more than 100mm, the landslide occurred in the area. Rainfall is considered as a triggering factor in the study area. Factors considered responsible for the occurrence of landslides are slope, aspect, curvature, distance from drainage, lineament distance, vegetation index, lithology and land cover. The combination of factors plan curvature, distance from drainage and lineament, lithology and land cover showed the best results. The accuracy of this model was 97% on the area of the curve method.

The certainty factor method is also a statistical approach that can give moderately accurate results in landslide mapping. Certainty factor is a way of combining the belief and disbelief in a numerical value. Certainty factor (CF) is a function of probability [86]. This method is used for managing uncertainty in a rule-based system. The values of the certainty factor can vary from -1 to 1. Positive values near 1 show the higher certainty of occurrence of landslide events while the negative values near -1 show the lesser certainty of occurrence of landslides [87]. The value 1 of the CF indicates that the evidence considered in the study is reliable to give the probability of occurrence of landslide 100% [86-87]. If CF is found to be near 0, the conditional probability will be equal to the prior probability. It means that the evidence for the occurrence or non-occurrence of landslides is not available and in this case the prediction can't be done [88].

Wang et al used the certainty factor method to prepare a landslide susceptibility map of Quianyang country in China [88]. The landslide inventory is prepared using the aerial survey photographs and the records of the historical landslide events. General curvature, profile curvature and plan curvature are considered as causative factor which shows the multiple effects of curvature. Stream power index, sediment transport index, distance from rivers and topographic wetness index are considered the factors which show the effect of rivers and water channels [88]. The accuracy of the study is around 84%. The multiple effects of factors like river and curvature may have affected the accuracy of the output. Devkota et al prepared a landslide susceptibility map along Mugling–Narayanghat road section in Nepal [89]. A landslide inventory of 341 landslides was prepared. The causative

factors considered in this study were slope gradient; slope aspect; altitude; plan curvature; lithology; land use; distance from faults, rivers and roads; topographic wetness index; stream power index; and sediment transport index [89]. The multiple effects of streams were considered but the curvature is considered only once. The accuracy of the model was found to be 87%.

The probabilistic models are based on the assumption of conditional independence [87-89]. So, the interrelation among the causative factors disturbs the accuracy of the results. The conditional independence is to be tested for the probabilistic models. The results in the probabilistic models depend upon the available pieces of evidence of the landslides in the field. So, an accurate landslide inventory is required for obtaining the accurate results.

2.4.3. Semi-quantitative/Semi-qualitative Approach

The qualitative approach of landslide susceptibility mapping considers the human perception only while the quantitative approach only deals with the establishment of a mathematical relationship between the occurrence of landslides and its causative factors. The accuracy of the qualitative techniques is found to be lower due to the subjective perception of the expert but at the same time the opinion of an expert is very important as there may be a shortage of the landslide evidence data. So, a combination of qualitative and quantitative methods is proposed for improving the accuracy of the qualitative techniques [61-62]. In the semi-qualitative techniques the relative importance of the causative factors of the landslides is evaluated by the opinion of the expert but the possible biasness of the expert weightage is checked by some mathematical solution.

Analytic hierarchy process (AHP) and analytic network process (ANP) are examples of the semi-quantitative/ semi-qualitative approach [26, 28, 50, 52, 90-95]. The analytic hierarchy process (AHP) is based upon three principles i.e. decomposition of the problem, comparative judgment and synthesis of relative importance or rankings [96-97]. In AHP, the problem is broken into hierarchical criteria. These criteria are compared to each other. This process of relative comparison is called pair-wise comparison. The Eigenvector method is used to calculate the rankings and after that consistency of the solution is also checked by calculating the consistency ratio [96-97]. If the consistency ratio lies below 10%, the solution is considered reliable. The pair-wise comparison is considered right in this condition. If the consistency ratio is found to be more than 10%, the solution is considered inconsistent and the values in the pair-wise comparison are varied to get a consistent solution. AHP is widely used in landslide susceptibility mapping at the regional level [28].

The analytic hierarchy process (AHP) is used widely for the assessment of landslide susceptibility [26, 28, 40, 52, 90-103]. Achour et al used AHP along the highway road section in Algeria [92]. The influencing factors of landslides considered in the study were slope, aspect, lithology, geology, distance from faults, drainage characteristics and land use of the area [92]. The characteristics of terrain are understood from the landslide inventory which is prepared by the field visits. The number of landslides in the inventory were 29 which were used for the evaluation of the accuracy of the final output. The accuracy of the landslide susceptibility map along the highway is found to be around 66%. The effect of rainfall and seismicity is not considered in this study.

Ali et al prepared a landslide susceptibility map along Karakoram highway [98]. Seismicity and rainfall intensity is considered in this study for the preparation of a landslide susceptibility map along the highway [98]. The characteristics of the terrain are evaluated by the field visits and the landslide inventory. The historical data on landslides is collected from the previous reports and also from the field visits [98]. The accuracy of the landslide susceptibility map is found to be 72%.

There are numerous studies conducted for the assessment of landslide susceptibility of the river basins [90-100]. Kayastha et al prepared a landslide susceptibility map of Tinau watershed in the West Nepal [99]. The study area was around 562 km². The accuracy was found to be around 78% in this study [99]. Mandal and Mandal prepared a landslide susceptibility map for the Lish river basin in India [100]. The factors considered in this study are slope angle, slope aspect, slope curvature, altitude, relative relief, geomorphology, geology, distance to lineaments, lineament density, soil, land use & land cover, NDVI, drainage density, distance of drainage, stream power index, topographic wetness index, and rainfall. The authors achieved the highest accuracy in the AHP technique [100]. The model shows an accuracy of around 90% which is exceptional in the case of the Analytic Hierarchy Process.

The fuzzy logic system is invented by L.A Zadeh in 1965. The practical application of fuzzy logic is given by Dr. E.H Mamdani in 1974. The different operators are available in fuzzy logic. AND and OR operators are commonly known but these are not used in the case of landslide studies [104]. In the case of AND operator minimum of all values of landslide susceptibility index gives output while in the case of the OR operator maximum of all gives the output value [105]. So, these operators fail to act on every layer of factors that affect landslides. The operators like weighted

sum, fuzzy product or gamma function can be used for landslide mapping [104]. The operators weighted sum and fuzzy product give either very low susceptibility or very high susceptibility, so these are also considered reliable [106]. Hence gamma function operator is found to be the most suitable [104].

Lee published his work on the application of various fuzzy operators such as OR, AND, GAMMA, SUM and MULTIPLY for the assessment of landslide susceptibility in Gangneung area, Korea [107]. The accuracy was found to be least in the case of the OR operator and highest in the case of the GAMMA operator. The GAMMA operator gave 97% accuracy of the AUC method. Pradhan applied the same operators on Penang Island, Malaysia [108]. The conclusion was the same as that of Lee. The OR operator gave the least accuracy while the GAMMA operator was the most accurate. Other operators like sum and multiply don't give satisfactory results [109]. The values of the GAMMA operator can be varied from 0.1 to 1.0 and the best-suited results can be used as the final output [109]. The semi-quantitative models are more accurate compared to the qualitative models. The models like AHP are rule-based models which can be designed based on the perception of the experts. So, there is no need for historical data for these models too.

2.3.4. Artificial Neural Networks

A black box model may be defined as a computer program into which users enter information and the system utilizes pre-programmed logic to return output to the user [110]. The black box models like neural networks are used for landslide susceptibility mapping. These models can give highly accurate results [111].

Artificial Neural Network (ANN) is relatively a new technique. The various causative factors are considered as processing units that are in connection with each other. In general, an ANN system can be divided into three layers i.e. input layer, an output layer and intermediate or hidden layers. The input layer is responsible for taking the input in the form of features, numerical values, information or signal [112]. The intermediate or hidden layers process the input data. The output layer represents the output after the processing. All the layers are made of neurons or processing units. The ANN models allow communication among the layers and the output layer is produced [113]. The susceptibility of an area to landslide is a classification problem. In this way, the ANN outputs can be considered as a sort of membership of each terrain unit to the class “landslide”.

Zeng-Wang proposed artificial neural network (ANN) as a tool for landslide susceptibility mapping [110]. The method is applied to Lantau Island in Hong Kong. Elevation, slope, aspect, curvature, vegetation, drainage and lithology are considered as causative factors. A relationship between terrain variables and the landslide distribution is created by the ANN model. It was one of the first applications of ANN in landslide susceptibility mapping. So, the accuracy of the model is not evaluated. The author concluded that the selection of a suitable algorithm is subjective, and the accuracy of the result is poor. The ANN models are modified and with the help of different algorithms the accuracy of the models is improved. The ANN models showed accuracies even more than 90% in many cases. The consideration of realistic factors and huge historical data increases the accuracy of the ANN models [111-114].

Black box models do not consider the landslide distribution. So, the models can be implemented in the absence of shreds of landslide evidence. The high accuracy of the black box models is an

advantage. In fuzzy logic, the operators can be varied to get a better output. ANNs can handle complicated nonlinear data efficiently [115]. ANN models can comprehensively deal with the data. The models are not sensitive to uncertain data and measurements of error [116]. The computational overburden in the black box models like ANN is a big disadvantage [117]. The data in ANN models are to be converted into ASCII codes which is a complicated and time-consuming process [115-117].

2.4. Discussion about Models in Landslide Susceptibility Mapping

Every model has its own advantages and limitations. Qualitative methods like fuzzy logic and AHP rely on the accuracy of input weightage given by experts. The accuracy observed by the area under cover (AUC) method for the landslide susceptibility maps prepared by using the analytic hierarchy process is found to be moderately accurate [26, 28, 50, 52]. The accuracy is more than 75% in the case of rockfall susceptibility mapping [118]. Human perception is included in the analytic hierarchy process. The pair-wise comparison of the causative factors depends upon the perception of the researcher [119]. It is simple to use in a spatial environment and the tools required for AHP calculations are easily available. AHP is suitable for regional-level mapping [120-121]. The accuracy of this method is less compared to the other methods [122]. The output of the study depends upon the expertise of the researcher. The perception of the expert is not always right [122]. The accuracy of the results also depends upon the values assigned in the pair-wise comparison.

Most of the landslide susceptibility maps produced by the fuzzy logic approach showed an accuracy of more than 80% to 85% [104-106]. In some cases, the accuracy of the fuzzy logic technique is found to be more than 90% [108]. Fuzzy logic models can give high accuracy as

compared to other models. It is a knowledge-driven model, so the need for past landslide data is reduced [104-108].

Statistical methods are very reliable as expert-driven approaches yield less accuracy. The accuracy of landslide susceptibility maps prepared using the weight of evidence (WOE) methods varies from 72% to 90% [82-83]. The weight of evidence (WoE) models work on the assumption of conditional independence. Ideally the causative factors should be independent of each other but practically it is not possible [13]. The output depends upon the conditional independence of the causative factors. The causative factors are to be considered carefully in this case. The factors which are independent of each other are selected. So, the weight of the evidence model is to be tested for conditional independence. The accuracy achieved by regression techniques is more than 80% in most of the studies [63-64, 68-69].

Logistic regression models require a big sample of data for successful implementation. If a study has 5 independent variables, the probability of a least frequent outcome is 0.05, a sample size of 1000 will be required. So, the fewer field data don't give an accurate picture of the effects of causative factors on the occurrence of landslides. The LR models should have little or no multicollinearity among the independent variables. It means that the independent variables must not be highly correlated to each other [123]. The output is affected by the correlation of the independent variable and errors are induced. The accuracy obtained by the certainty factor method varies from around 75% to 88% [124]. Most studies conducted using this method give more than 75% accuracy which is sufficient for regional level mapping [124]. The certainty factor of the existing knowledge can be changed by the new knowledge. In some cases, the certainty factor becomes the

opposite of conditional probability [77]. The results in a combination of dependent evidence are not satisfactory.

The accuracy of the frequency ratio techniques varies from 70% to 75% which is moderately accurate [13, 23, 29]. The frequency ratio method gives a correlation of landslide events with the causative factor which is not possible in the bi-variate method. The ANN models may have accuracy from 75% to 90% [63, 111-112]. The computational overburden in the black box models like ANN is a big disadvantage.

2.5. Findings from the Literature Review

The techniques used for landslide susceptibility mapping are classified into four categories i.e. qualitative, quantitative, semi-qualitative/semi-quantitative and black-box models. Every technique has its own suitability and limitations. The selection of the most suitable technique for a particular study area depends upon the availability of the data, required accuracy, size of the area and simplicity of the models during implementation. The following conclusions can be drawn based on the available literature:

- The qualitative methods are based on the expert opinion. So, the biasness in the results reduces the accuracy of the output. It has rich data in the case of different opinions of the experts.
- Qualitative techniques are the simplest to implement. There is no requirement for historical data if we are working on the opinion of the expert. So, the technique is suitable for the

regions where landslide inventory is not available or the places are inaccessible for field visits. The criteria for the selection of the experts should be well-defined.

- The qualitative models can be used for small sites. For large study areas, these techniques are not sufficiently accurate. Semi-qualitative/semi-quantitative techniques are an improvement over qualitative techniques.
- The semi-quantitative techniques consider the expert perception with some mathematical application. So, the biasness in the input can be reduced. The accuracy of the semi-quantitative techniques is significantly more as compared to purely expert-based solutions.
- The quantitative techniques are based on the mathematical relationship between the occurrence of landslide events and its causative factors. The quantitative techniques require a well-distributed landslide inventory for the implementation and preparation of landslide susceptibility maps. So, the techniques can be implemented only in the regions where landslide inventories are available or the region is accessible for field visits.
- The black box models use the instruction of the user and process them through some mathematical instructions and get the output. The accuracy is high for the black box models but the data needs to be converted into ASCII codes which is a cumbersome process [63, 111, 113].

- The output in the landslide susceptibility mapping depends upon the causative factors and the weightage given to these factors. If the realistic weightages are given to the causative factors, the accuracy can be increased significantly.
- As we have selected Shimla district as our study area, the statistical models and semi-quantitative models are not implemented for landslide susceptibility mapping in this region.

2.6. Research Gaps

The different research gaps observed from the literature in landslide susceptibility mapping are as follows:

- The analytic Hierarchy Process (AHP), Frequency Ratio (FR) and Shannon's Entropy (SE) models are not implemented for landslide susceptibility mapping in Shimla region till now.
- Some studies considered the effect of a single factor multiple times. Drainage density and distance from the stream both are considered in some studies. The drainage effect may be overrated in such studies. Similarly, curvature and topographic wetness index (TWI) both show the effect of rainfall. So, the multiple effects of a single factor can be removed for better results.
- The semi-qualitative and expert-based methods show less accuracy as compared to the statistical methods and ANN models.
- The analytic hierarchy process (AHP) shows the biasness of an expert. The subjectivity of expert opinion should be reduced.

2.7. Concluding Remarks

In this chapter, a detailed literature review is performed to understand the different techniques of the microzonation of the landslide susceptibility. It is observed that there are four categories of landslide susceptibility assessment techniques. The statistical techniques and ANN-based techniques give more accurate results than the expert-based techniques. However, the output of the each technique depends on the quality of the input data. After getting an idea about the research gaps from the literature review, there is need of developing a conceptual framework for achieving the objectives of the thesis.

Conceptual Framework

3.1. Introduction

In chapter 1, the objectives of the thesis are set. To achieve these objectives, a deep understanding of the modeling techniques of landslide susceptibility mapping was required. An extensive literature review is performed in Chapter 2 for understanding the recent developments in the field of landslide susceptibility mapping. In this chapter, a conceptual framework is developed that describes the procedures and steps adopted for achieving the objectives. The sources of the input data, landslide inventory, data processing, and mathematical modeling are discussed. A brief description of the study area and its characteristics is also included in this chapter. However, the mathematical modelling and a brief discussion on causative factors is discussed in the upcoming chapters.

The occurrence of landslides depends upon the various causative factors. The geological character, lithology, drainage characteristics and land use of a region can affect the occurrence of landslides. The first step to prepare a landslide susceptibility map is to collect satellite data and data from the maps of agencies. The field visits published reports, Google Earth imagery, etc. can be used for the preparation of landslide inventories. Mathematical modelling is the next step to achieve the relative importance of the causative factors and sub-factors. The input data is processed in a GIS environment to get the output and the final map is validated statistically. The complete flow chart of the work is discussed in the upcoming sections. Figure 3.1 shows the flow chart of the study and stepwise procedure.

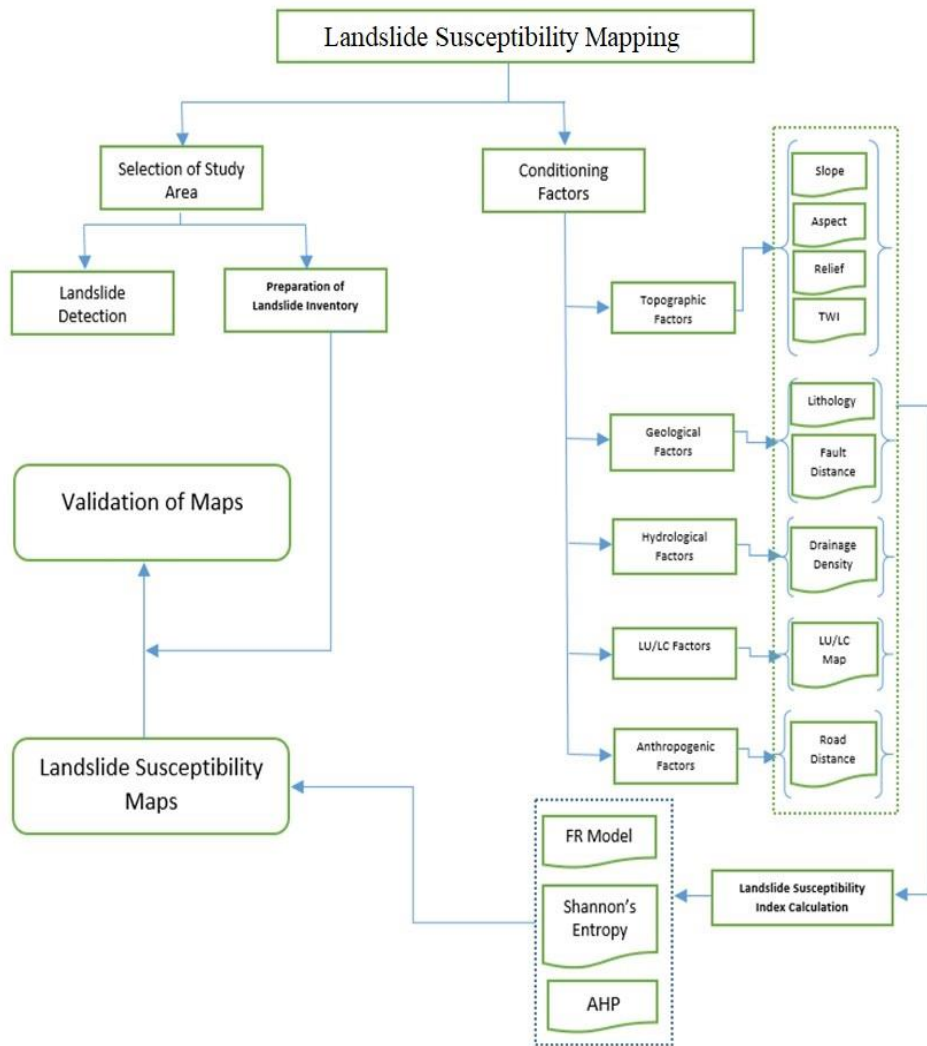


Figure 3.1. Flow Chart of the Study

Slope, aspect, curvature, relative relief etc. are the primary derivative from the digital elevation model while drainage density is the second derivative from the DEM. The DEM-based factors are extracted using geospatial analyst in ArcGIS. The lithology map of the study area is digitized in vector format which is converted into raster format. Roads are digitized from U.S. Army Corps of Engineers Map. Faults in the study area are obtained from the Groundwater Prospects Map of

Himachal Pradesh (H.P.). Land-use/land-cover map is extracted from the Landsat imagery. A landslide inventory is prepared from various sources like previous literature, field survey and majorly from Bhukosh portal [125]. Table 3.1 shows the details of the data obtained, the source of the data and their scales.

Table 3.1. Source of Data

Extracted Data	Scale	Source
Landslide Points		Literature, Field Survey, Google Earth, Bhukosh Portal
Slope		Derivative of DEM
Aspect		Derivative of DEM
Relative relief		Derivative of DEM
Topographic Wetness Index		Derivative of Landsat 8
Drainage density	1:50000	Derivative of DEM
Distance from Faults	1:50000	Ground Water Prospects Map
Lithology	1:50000	Bhukosh Portal
Drainage density	1:50000	Survey of India (SOI) Toposheet
Distance from the roads	1:250000	U.S. Army Corps of Engineers
Landuse/Landcover		Landsat 8 imagery

3.2. Study Area

The study area selected in this research work is Shimla district in Himachal Pradesh (H.P.) province in Northwestern India. Shimla was the former summer capital of British India. The study area lies between the longitudes 77°0' E and 78°19' E and latitudes 30°45' N and 31°44' N. Figure 1.3 shows the details of the study area. It is surrounded by Mandi and Kullu districts in the North, Kinnaur in the East and Sirmour in the West direction [126]. The southern part of the study area touches the boundaries of Uttarakhand province. The elevation of the study area varies from 300 m to 6000 m [126]. Figure 3.2 shows the study area.

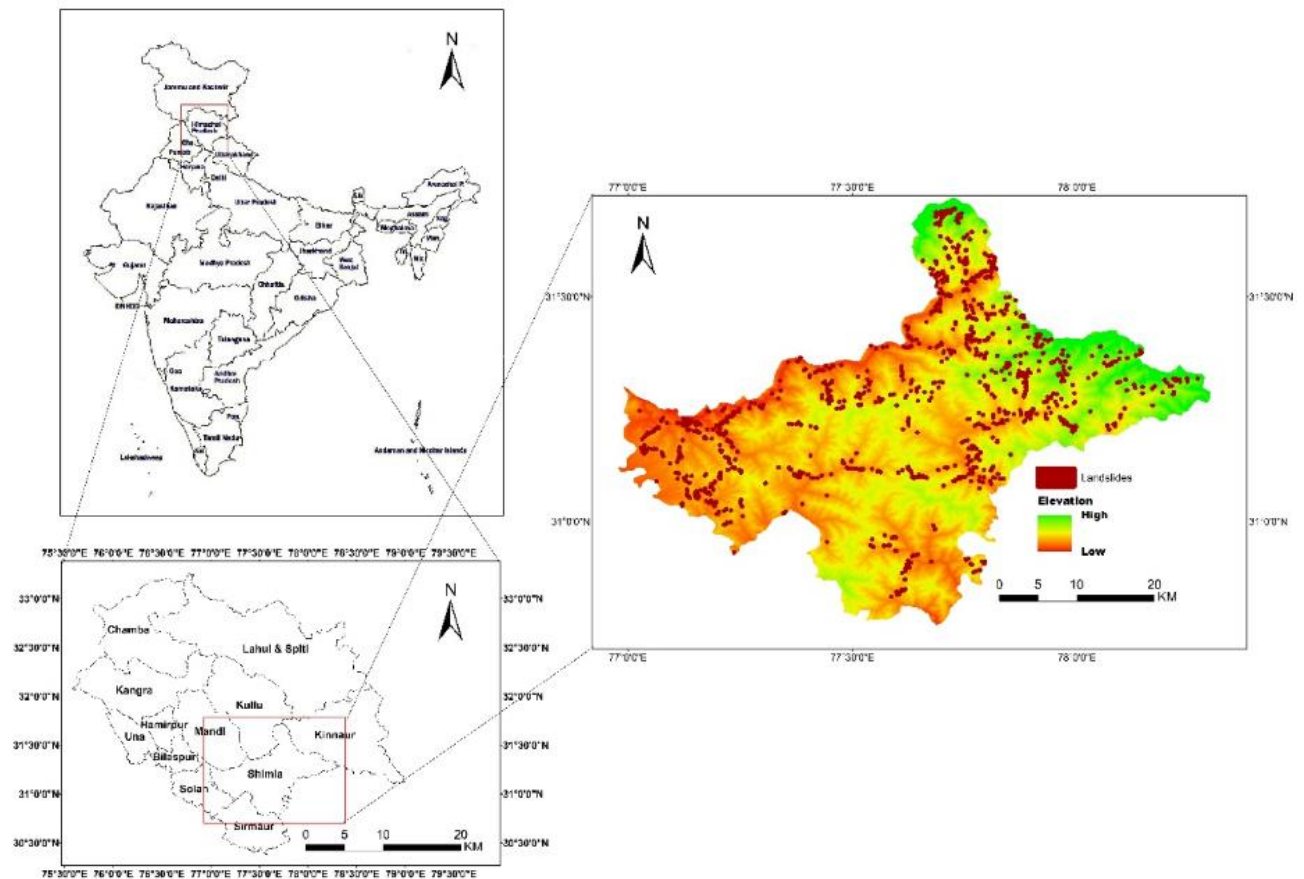


Figure 3.2. Details of the Study Area

3.2.1. Climate Characteristics

The climate of the study area remains cool in winter and moderately warm during the summer season. Currently, the temperature ranges from -4° C to 31°C typically throughout the year [126]. The average temperature during summer is 19.28° C and 1.10 °C in the winter. The precipitation pattern in the region shows high variability during different months and seasons. The average total precipitation in a year is 1575 ml [126]. The monsoon period remains from July to September. The snowfall in the study area takes place from December to February. The snowfall takes place in regions of higher elevation. The snowfall has been shifted from December to late January and early February months due to climate change.

3.2.2. Vegetation Characteristics

The study area has varying elevations forming the valleys and high hills. The cultivation activities are spread majorly in deep valleys and small parts of higher elevations. The region is covered with dense forests containing the trees of Chir and Pine up to the altitude of 1500 meters [127]. The higher altitude areas are covered with Kail, Deodar, Kanor, Rai, Ban etc. Higher altitude regions with steep slopes are suitable for horticultural activities. The apples, walnuts and almonds are grown in the upper region.

The forests create the major part of the land use with a variety of trees like Deodar, Chir, Pine etc [127]. Areas of lower elevations are suitable for growing cereal crops, stone and citrus fruits while places with higher altitudes are more suitable for the growing of seed potatoes off-season vegetables and temperate fruits especially apples.

3.2.3. Geology and Seismology of Area

Shimla district lies in a high damage risk zone in the case of seismic activity (MSK VIII). Major earthquakes that have occurred in Himachal Pradesh (H.P.) are the Kangra earthquake 1905 (M = 8), the Chamba earthquake 1945 (M = 6.5), the Kinnaur earthquake (M = 6.8), etc [126]. The study area is predominantly covered by the rocks from the Jutogh, Shali, Simla and Rampur groups. The study area consists of lithological units of shale, siltstones, quartzite, dolomites, phyllite, schist, conglomerate, etc [126-127]. The region is predominantly covered by the Proterozoic age group, Paleo-proterozoic age group and Neo-proterozoic age group.

3.3. Landslide Inventory

A landslide inventory provides information about the historical landslides in the study area. The landslide inventories can be very simple to very complex based on the requirements of the users. The landslide data is collected from the published reports, practical sheets of Geological Survey of India (GSI), Google Earth imagery and the Bhukosh portal [125]. Figure 3.3 shows the landslide inventory of the study area. The landslide inventory consists of the following data:

- Location of Landslide
- Types and Classification of Landslides
- Date of Occurrence and Date of Survey
- Material of landslides
- Activity of Landslide
- State of Moisture Content
- The remark about Landslide Event

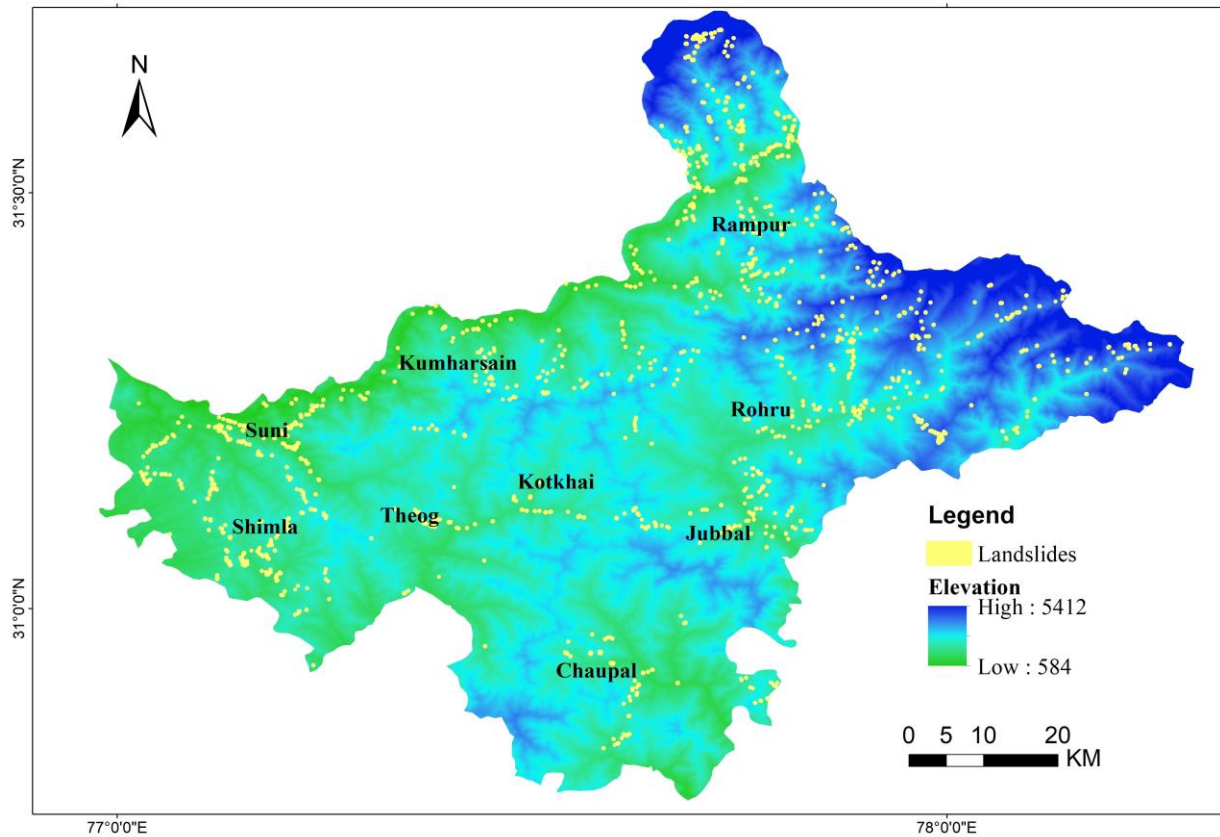


Figure 3.3. Landslide Inventory

3.4. Accuracy Assessment of Digital Elevation Model

The digital elevation model is used to extract the various causative factors like slope, aspect, relative relief etc. The DEM can be validated for vertical and horizontal accuracy. The possible errors in the digital elevation model for Shimla district are checked [128]. The study was conducted to validate the digital elevation model (DEM) in Shimla and Dehradun districts by comparing the ground control points with the observations in the digital elevation model. Three ground control points (GCPs) are established at different reliefs and the errors are measured in vertical and horizontal directions. Table 3.2 provides the details of the errors in the digital elevation model in Shimla district.

Table 3.2. DEM error analysis for Shimla district [128]

Station No.	Residuals (m)		
	Easting (m)	Northing (m)	Elevation (m)
1	3.9	-3.3	0.655
2	-3.3	2.4	6.045
3	-1.2	0.3	1.98
RMSE (m)	3.02	2.36	3.69

3.5. Mathematical Modelling

The factors which are responsible for the occurrence of the landslide events are identified. The relative importance of the causative factors and their contribution toward the occurrence of landslides is modelled using mathematical models like analytic hierarchy process (AHP), frequency ratio (FR) and Shannon's entropy.

The contribution of each factor and sub-factor towards landslide is observed and weightage for each factor is obtained. A chapter dealing with mathematical modelling is also discussed separately.

3.6. Processing of the Data

The digital elevation model (DEM) is imported into ArcGIS software. The DEM is used to extract the DEM-based factors like slope, aspect, relative relief etc. The spatial analyst tool is used to obtain these causative factors. The topo-sheets and map-based causative factors like faults and roads are imported as scanned maps in the GIS environment. The required features from these maps are digitized so that the parameters can be used as causative factors. All the inputs are

converted into raster format. The causative factors are reclassified and the weightage of each causative factor and sub-factors are assigned. The layers of causative factors are overlaid to obtain the landslide susceptibility maps which are further validated for their accuracy. The input data in the case of landslide studies are the causative factors. The layers of the causative factors are converted into raster format which divides the whole study area into pixels or grids. The qualitative and quantitative models are used to calculate the contribution of each causative factor and sub-factor towards the occurrence of landslides in the form of a numerical value. These numerical values are assigned to each grid as weightage. The process of overlaying the layers creates the output map which represents the cumulative impact of causative factors in the form of a numerical index. This numerical index is the landslide susceptibility index in the case of landslide susceptibility studies. The landslide susceptibility maps can be divided into three or four classifications based on this index.

3.7. Concluding Remarks

A framework to achieve the objectives is prepared in this chapter. The digital elevation model (DEM) is obtained from the Survey of India website. The DEM-based factors are extracted using geographic information system (GIS). The landslide inventory is prepared from the Survey of India practical sheets, field surveys and Bhukosh portal. The non-DEM data is converted into digital form from the maps of Survey of India. The reliability of the data is checked by the error analysis. After proposing this framework, there is a need to understand the causative factors of landslides in detail.

Causative Factors of Landslides

4.1. Introduction

According to the conceptual framework discussed in the previous chapter, the identification of causative factors is needed for microzonation of landslide susceptibility. The purpose of this Chapter is to understand the different causative factors of landslides from existing literature and further explore through, expert opinion and field conditions. The occurrence of landslides depends upon the various causative factors that should be identified carefully. The causative factors selected in this study are based on the field conditions, previous literature and the opinion of experts. The causative factors of the landslides can be categorized into digital elevation model (DEM) based and non-DEM based factors. The causative factors in this study are classified into five categories:

- Topographic factors
- Geological factors
- Hydrological factors
- Land-use / land-cover factors
- Anthropogenic factors

4.2. Topographic Causative Factors

The topography of the study area has a significant impact on the occurrence of landslides. Shallow landslides are highly impacted by the topography of the region. The topographic factors considered in this study are slope gradient, slope aspect, relative relief and Topographic Wetness Index (TWI).

4.2.1. Slope Gradient

Slope gradient is considered a very important causative factor of landslides. A slope gradient may be defined as the rate of change of the elevation with respect to the horizontal axis [119]. The slope gradient represents the impact of gravity, erosion, sunlight and it also impacts the drainage pattern. The shear stress in the mass increases as the slope angle increases. The slope gradient is extracted from the digital elevation model (DEM) of the area using the spatial analyst tool. Slope angle is divided into five categories in this study. Figure 4.1 shows the slope map of the study area.

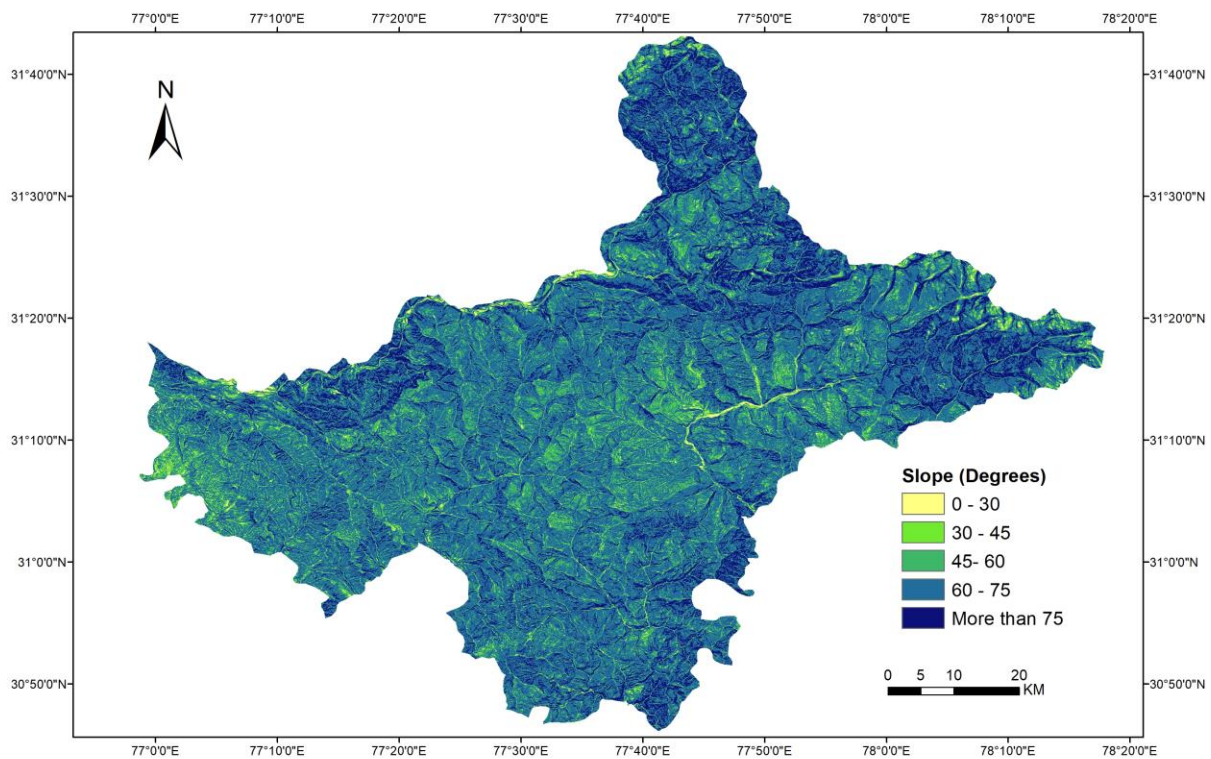


Figure 4.1 Slope in Degrees

The major proportion (around 60%) of the study area is covered with slopes with a gradient from 60 degrees to 75 degrees. Only 15% of the total study area is covered with the slope gradient from

45 degrees to 60 degrees. It is observed that a very small proportion of the study area lies under a gentle slope (less than 30 degrees).

4.2.2. Slope Aspect

The slope aspect may be defined as the direction of the maximum slope with respect to the magnetic north [119-120]. The direction of the slope shows the impact of winds and sunlight on the slope. Aspect is measured as clockwise faces of the landslide between 0 degrees to 360 degrees. The slope aspect has an indirect impact on the occurrence of landslides. Figure 4.2 shows the aspect in the study area.

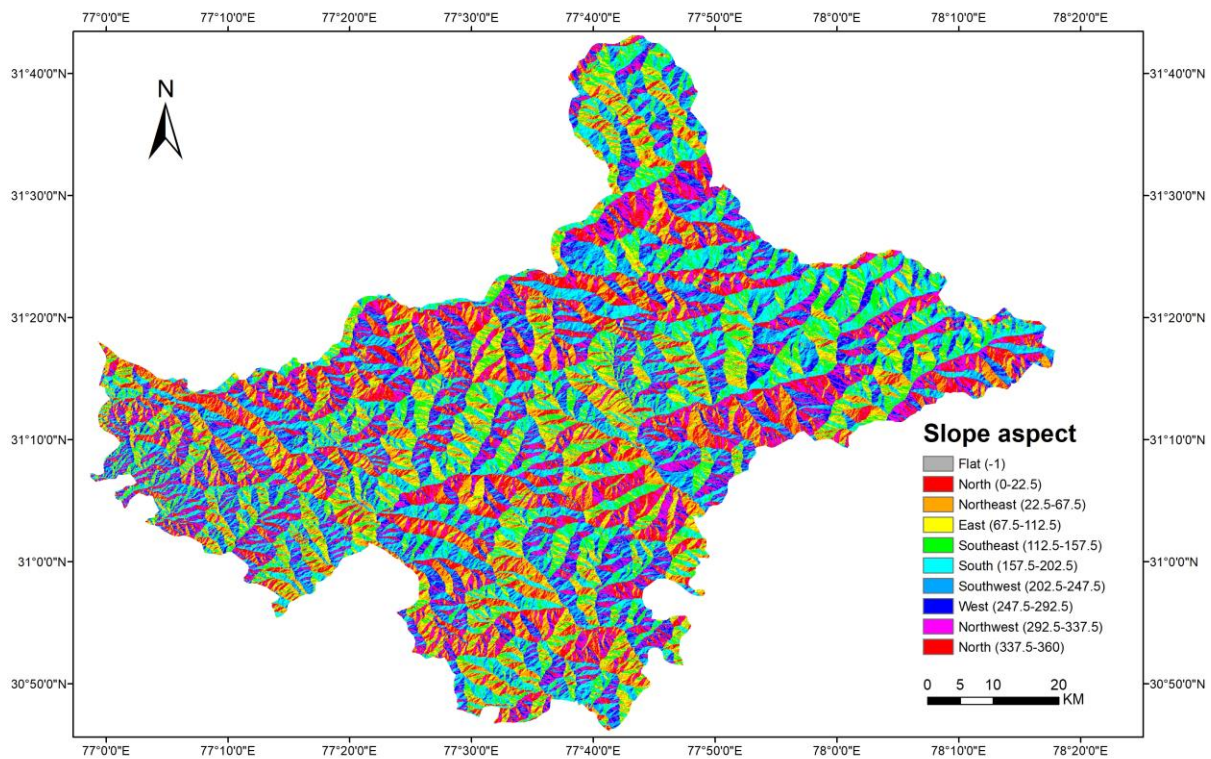


Figure 4.2 Slope Aspect

The direction of the slope has an impact on erosion due to wind. The wind action is more in some aspects. Similarly, sunlight has also a varied impact on the different aspects. Some researchers also considered that the slope aspect also represents the impact of the rainfall. The aspect which receives more rainfall is more prone to the occurrence of landslides. The snow retaining capacity also varies according to the slope direction. The aspect which faces the freezing and thawing action for a longer time is more prone to failure. As discussed earlier, sunlight has a varied impact on the slope aspects. The slope which faces more sunlight has more tendency of drying up. The moisture content in the sunlight-facing aspect is lesser as compared to the other directions. The variation of moisture content affects the vegetation characteristics of the slope. It is found that the particular aspect directions may have less vegetation.

The slope aspect is extracted from the digital elevation model (DEM). The aspect is divided into nine categories i.e. flat, north, northeast, east, southeast, south, southwest, west and northwest. The percentage of flat aspects is negligible in the region. 14.56% of the total study area consists of the north aspect while 14.31 % of the study area is covered by the south aspect. Northeast, southeast, southwest and northwest aspects cover a significant region of the study area i.e. 12.58%, 12.77%, 12.86% and 12.73% of the total study area. Similarly, east and west aspects cover around 20% of the total study area.

4.2.3. Relative Relief

Relative relief is the difference between the maximum and minimum elevation in an area [50]. It shows the change in the elevation of the region. As the relative relief changes the vegetation characteristics of the study area also change. The relative relief is the primary derivative of the

digital elevation model (DEM). There is not a clear relationship between the relief and occurrence of landslides however relief plays an important role in the occurrence of landslides. Relative relief in this study varies from 0 m to 254 m. Figure 4.3 shows the relative relief of the region.

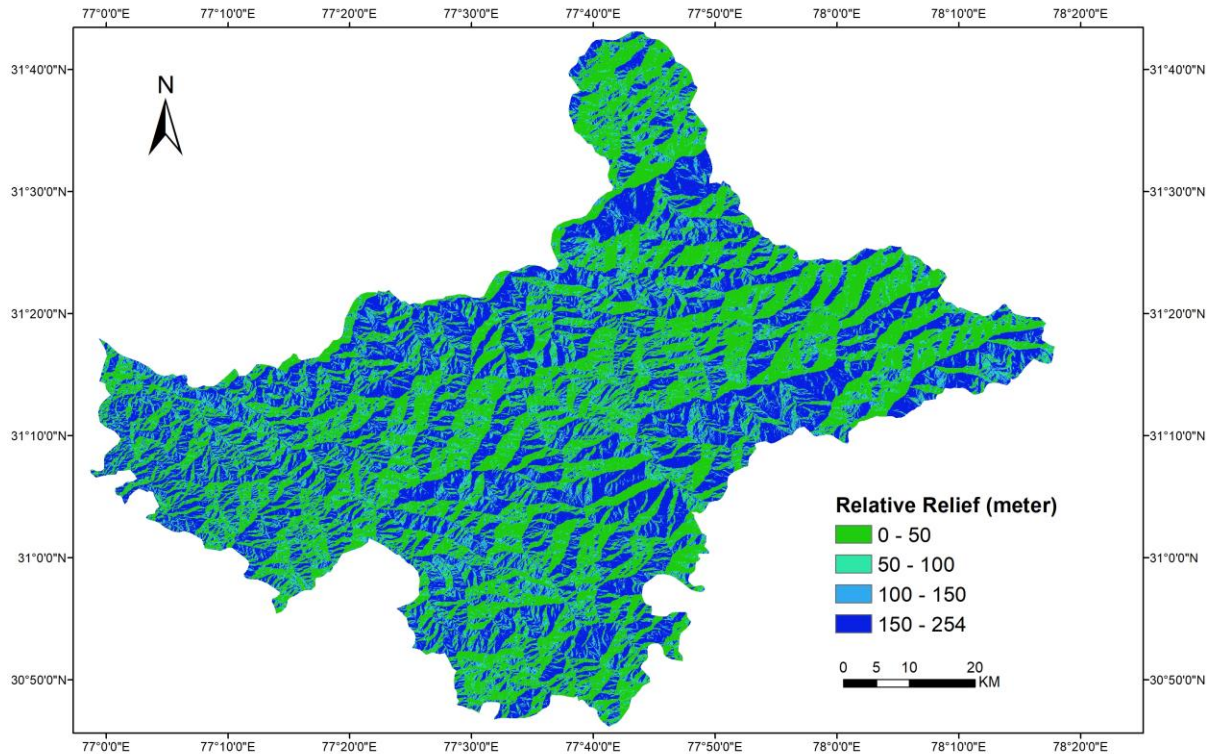


Figure 4.3 Relative Relief

It is divided into four categories i.e. 0 m to 50 m, 50 m to 100 m, 100 m to 150 m and more than 150m. It can be observed that around 40% of the region lies under low relief (0-50m). Around 36% of the total study area is covered with a relative relief of more than 150 m. The intermediate reliefs cover the remaining area in the study region.

4.2.4. Topographic Wetness Index (TWI)

The topographic wetness index (TWI) is also known as compound topographic index (CTI). TWI controls the hydrology of the soil or rock mass. It represents the moisture-retaining capacity of the soil. Figure 4.4 shows the topographic wetness index (TWI) of the region.

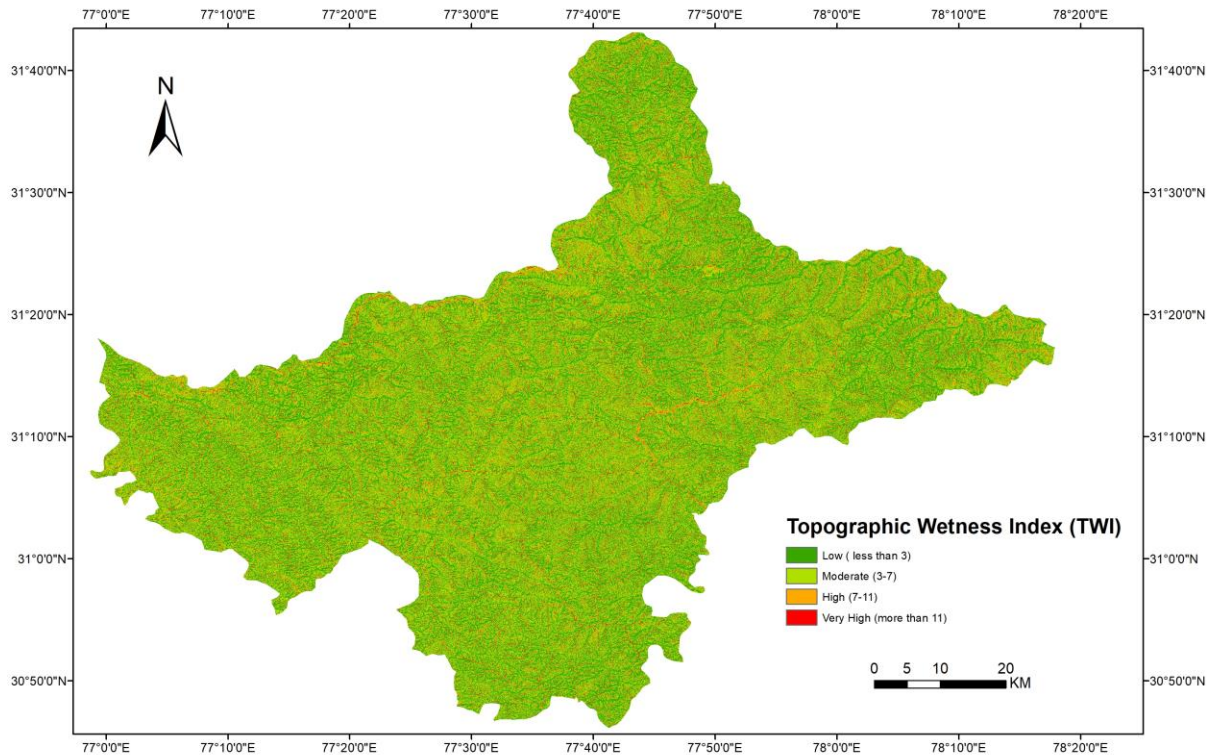


Figure 4.4. Topographic Wetness Index (TWI)

TWI establishes a relationship between specific catchment area (SCA) and slope angle. The topographic wetness index (TWI) is calculated using the following equation:

$$TWI = \ln\left(\frac{SCA}{\tan \varphi}\right) \quad 4.1$$

Here, SCA is specific catchment area and ϕ is the angle of slope. TWI acts on the principle of the mass balance equation. Specific catchment area (SCA) represents the tendency of receiving the water while slope angle shows the tendency of draining out of the water. Lower TWI values are more prone to the occurrence of landslides.

TWI is divided into four categories i.e. low (less than 3), moderate (3 to 7), high (7 to 11) and very high (more than 11). Around 45% of the total area is covered with TWI less than 3. High (7 to 11) and very high (More than 11) values of topographic wetness index (TWI) cover only around 15% of the total study area. The remaining area is covered with a moderate topographic wetness index (TWI) with values from 3 to 7.

4.3. Geological Causative Factors

The geology of the study area has a significant impact on the occurrence of landslides in the study area. There are varying characteristics of the materials found in the study area. The geological settings vary in moisture-holding capacity, permeability, porosity and shear strength. There are two geological causative factors considered in this study:

- Lithology of the region
- Faults in the region

4.3.1. Lithology

The lithological characteristics of the study area are heterogeneous. Different rock formation categories are found in the study area. The lithological deposits are divided into six categories according to their age. Table 4.1 gives the details about the lithology of the region. The study area

consists of shale, siltstone, sandstones and conglomerates of neoproterozoic age. These deposits belong to Sanjauli formation of the Simla group. Around 22% of the study area is covered with such deposits. Around 48% of the total study area is covered with phyllite, quartzite, schist and quartzite deposits of the proterozoic age.

Table 4.1. Lithology of the study area [125]

Age	Group Name	Geological Formation	Lithology
Mesoproterozoic	Shali	Tatapani	Pink and grey dolomite, phyllite, shale
Neoproterozoic	Shali	Sorgharwari	Pink and grey limestone, sporadic shale
Palaeocene-Eocene	Sirmur Dharmshala Group	Subathu	Green carbonaceous shale, limestone, quartzite
Palaeoproterozoic	Kullu	Khokhan	Schist and quartzite
Paleozoic	-----	-----	Medium to coarse biotite granite
Proterozoic (Undiff)	Jutogh	Manal, chor, pabar	White grey quartzite, schist, carbonaceous dolomite, granite, gneiss

These deposits belong to Taradevi formation of the Jutogh group. Around 22% of the region is covered with the Manikaran formation of the Rampur narnaul group which is of paleo-proterozoic age. Lithological deposits of Paleozoic, Eocene-Miocene and Meghalayan ages are also found in the study area but they cover less than 0.5% of the total area. So, their contribution to the study area is negligible. Figure 4.5 shows the lithology of the study area

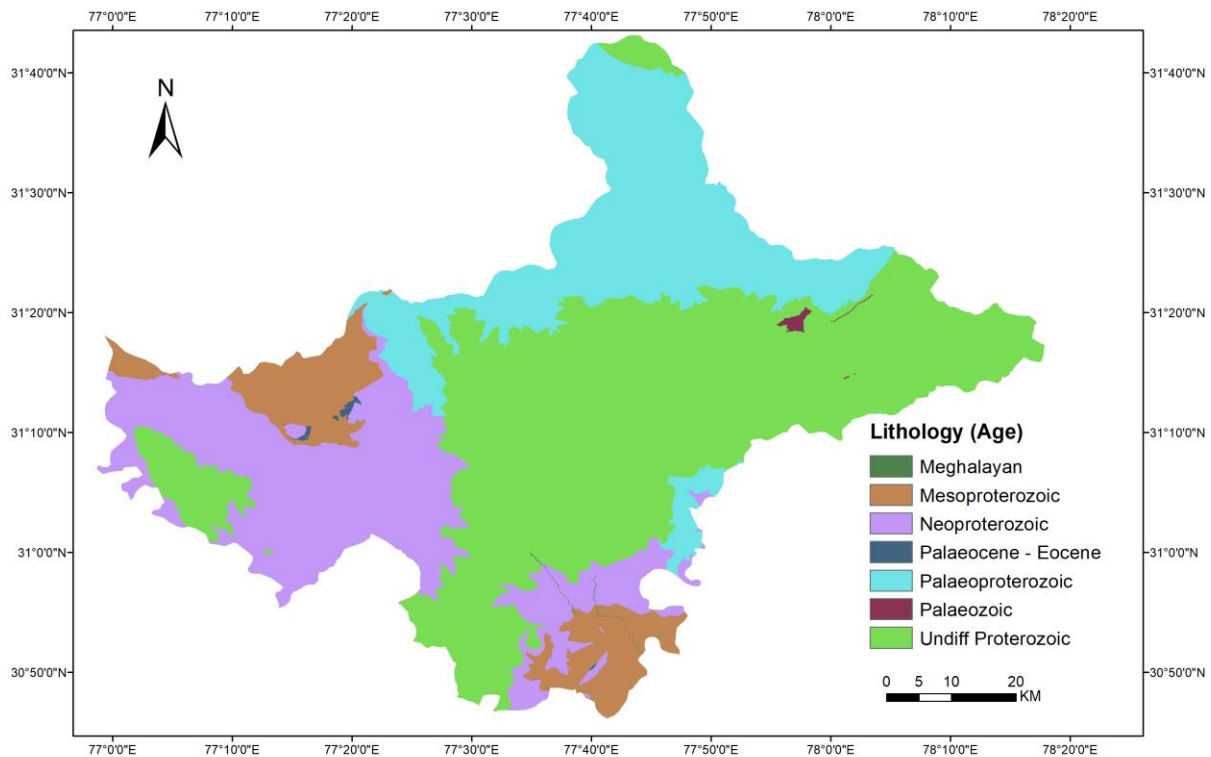


Figure 4.5 Lithology of the Study Area

4.3.2. Distance from Faults

The occurrence of landslide events can also be correlated with the proximity to faults, fissures and lineament too. The faults in the rocks and soil mass increase the pore water pressure and also forms weak planes. So, the distance from faults becomes an important causative factor. Faults are digitized from the groundwater prospects map.

Euclidean distance is measured from the faults using spatial analyst and the distance from the fault parameter is divided into three categories i.e. low (0 to 1.5 Km), moderate (1.5Km to 3 Km) and high (More than 3 Km). It can be observed that 44% of the study area shows a low distance from

faults while around 58% of the study area lies at a moderate distance from the faults. The remaining study area lies at a high distance from the faults. Figure 4.6 shows the distance from faults.

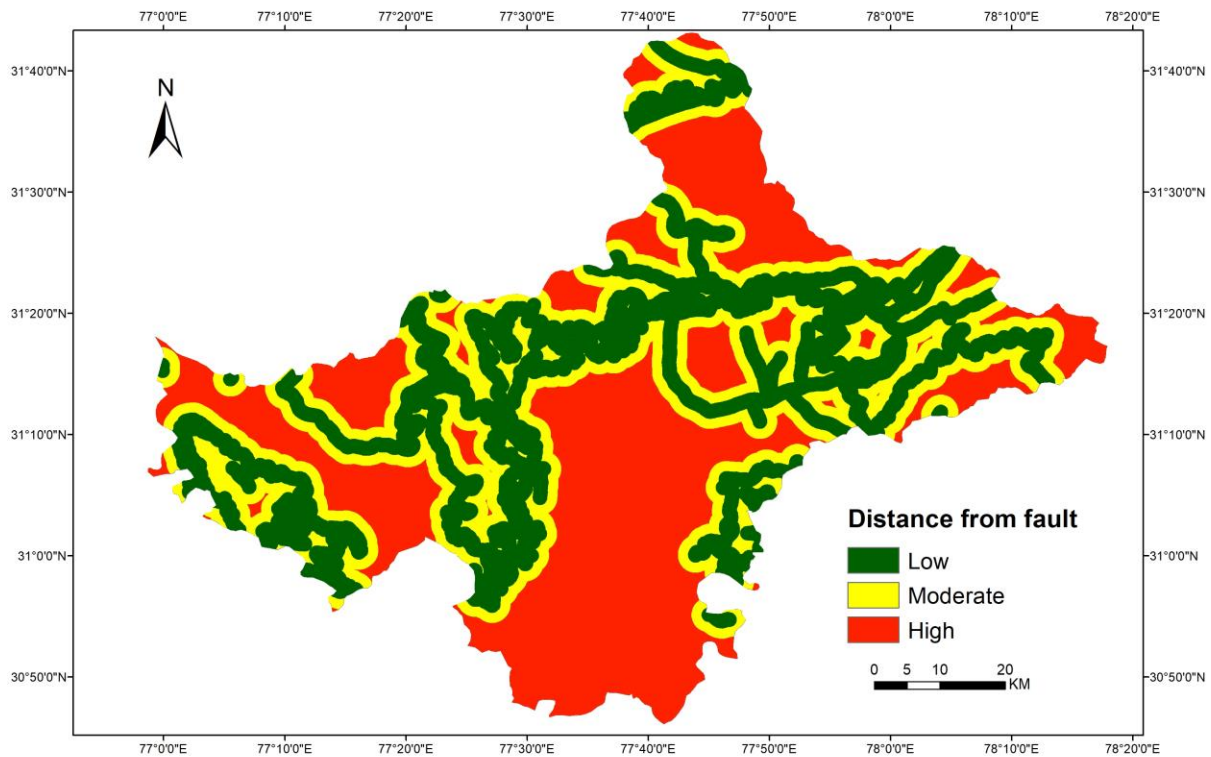


Figure 4.6 Distance from Faults

4.4. Hydrological Causative Factors

The hydrology of the study area has also its impact on the occurrence of the landslides. The impact of water is already considered in combination with the topography as explained in the topographic wetness index (TWI). Streamflow increases the erosion at their edges which results in the cutting of the toe of the slopes. The excessive erosion along the streams reduces the stability of slopes along the toe and results in the failure of slopes.

The saturation of the soil near the streams is also more prone to the occurrence of landslides. So, drainage density is also considered a hydrological causative factor of landslides. Figure 4.7 shows the drainage density of the study area.

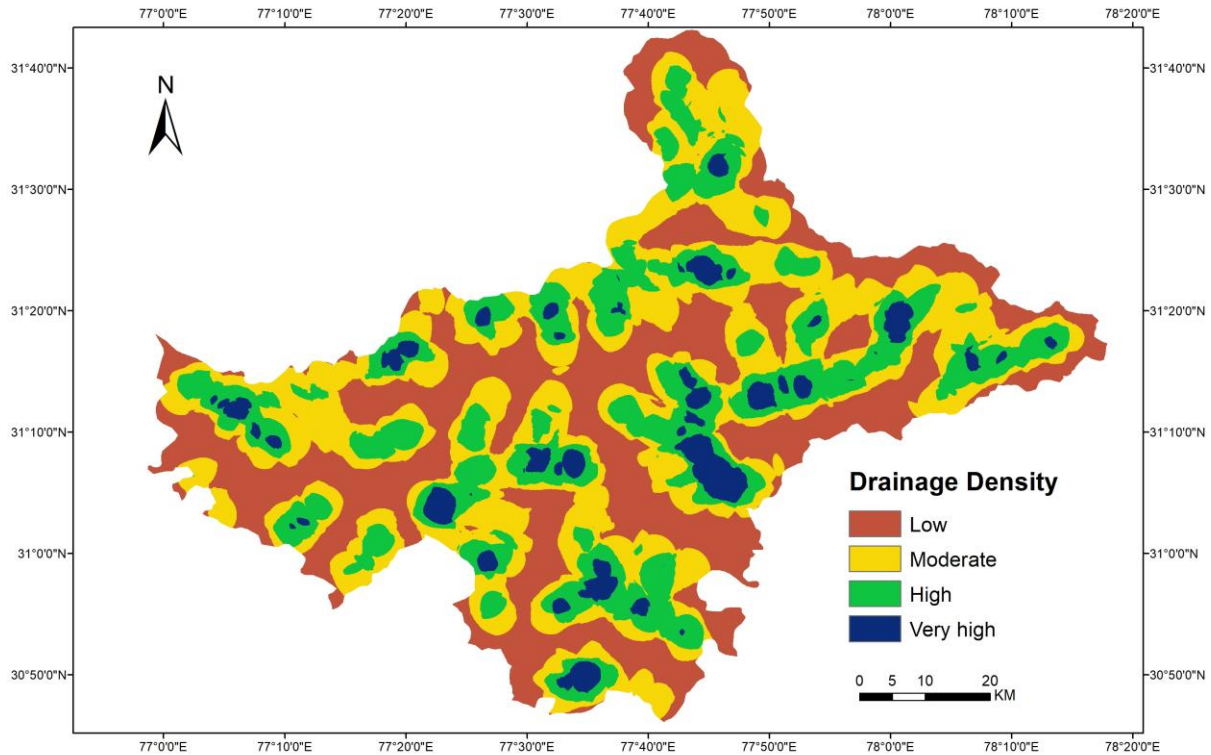


Figure 4.7 Drainage Density

The drainage density may be defined as the ratio of the length of streams per unit area. Drainage density is divided into four categories i.e. low, moderate, high and very high. Around 37% of the study area is covered with low (0-15) drainage density while 34% of the study area is covered with moderate (15-30) drainage density. 23% of the study area lies under a high (30-45) drainage density parameter and a small region lies under a very high (more than 45) drainage density.

4.5. Anthropogenic Causative Factor

The study area is developing in road infrastructure rapidly. The anthropogenic activities can disturb the natural slopes and make the slopes unstable. The slopes disturbed due to the engineering and construction activities are more prone to failure [50]. Distance from the road is taken as a causative factor that represents the impact of anthropogenic activities on the occurrence of the landslides. Road construction and widening activities are very frequent in the study area. Figure 4.8 shows the distance from the road.

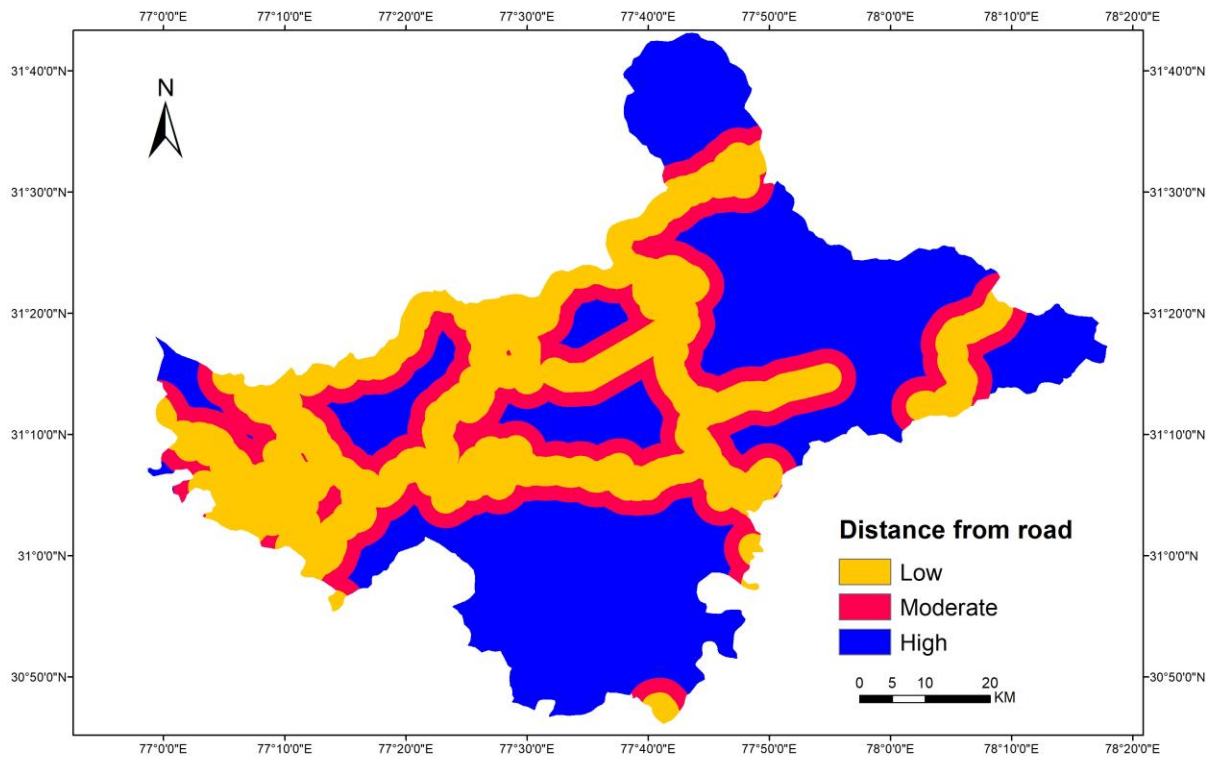


Figure 4.8 Distance from the Roads

During the widening or construction of roads the slopes are cut from the bottom. The toe portion of the slopes becomes weaker during this process. The weight of the upper portion of the slope

dominates in this case and slope failure takes place. Even vehicular vibrations may also trigger landslide activities. So, distance from the road is also considered as a causative factor in this study. Euclidian distance from the roads is measured and distance from the roads is divided into three categories i.e. low (less than 1.5 Km), moderate (1.5 Km-3.0 Km) and high (More than 3 Km). Around 27% of the region lies very near to roads while around 38% of the study area lies away from the road network. The remaining study area is in moderate proximity to roads.

4.6. Land-use/ Land-cover

Land-use/land-cover has a significant impact on the occurrence of landslides in the study area.

Figure 4.9 shows the land-use map of the study area.

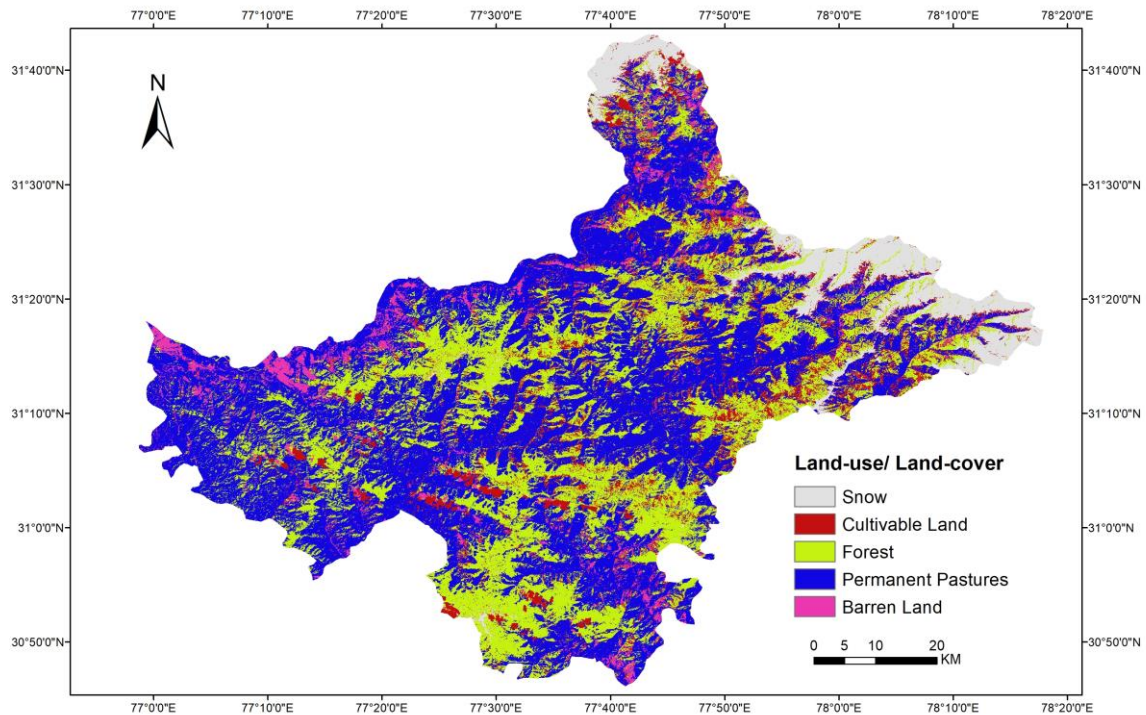


Figure 4.9 Land-use/ Land-cover

The land-use characteristics of the study area vary with the change in the elevation. The land-use map is prepared from the Landsat 8 data downloaded from the USGS website. A supervised learning technique is used to identify the land use of the study area. The study area is majorly covered with grassland and permanent pastures. Around 50% of the study area is covered with permanent pastures. Around 25% of the study area is covered by forests. Around 5% of the land lies under the barren land category. The upper elevation regions are covered with snow cover. Around 9% of the study area is covered with snow cover.

4.7. Discussion on Causative Factors

The identification of the causative factors for landslide susceptibility mapping is a crucial task. If the actual causative factors of the landslides are identified, the accuracy of the landslide susceptibility maps can be enhanced significantly. The DEM-based factors are extracted from the digital elevation model (DEM) while the non-DEM based factors are digitized from the scanned maps. The impact of the different causative factors is discussed in detail but still, the occurrence of landslides depends on the complex interaction of these factors. However, the historical landslide data can give a better picture of the contribution of the causative factors in landslides.

4.8. Concluding Remarks

As discussed in the objectives, the role of different causative factors in the occurrence of landslides is identified in this chapter. The causative factors are derived according to the conceptual framework of this study. The resolution of the thematic layers of the causative factors is kept the same. The digitized data is converted into the raster format. The contribution of causative factors is discussed in general terms in this Chapter. However, the previously occurred landslide size and

location may help in deciding the contribution of the causative factors. In the next step to achieve the objectives, the role of individual causative factors and their sub-categories needed to be modelled mathematically or semi-qualitatively. A deep understanding of the statistical models and semi-qualitative models is required for the preparation of landslide susceptibility maps.

Mathematical Modelling

5.1. Introduction

As discussed in the conceptual framework, the weightage is assigned to the grids of the raster data after the extraction of the causative factors. The role of the sub-factors and causative factors is calculated in the form of weightage. The weightage can be calculated using the different models as discussed in the literature review. A landslide susceptibility map shows the cumulative contribution of different causative factors to the occurrence of landslides. If the contribution of the causative factors is modelled properly, the researchers can predict the landslide susceptibility of the study area accurately. One semi-qualitative model and two quantitative models are applied in this study.

Analytic hierarchy process (AHP), frequency ratio (FR) and Shannon's entropy (SE) models are used to calculate the weightage of different causative and sub-factors. A new model is also proposed which is a combination of Shannon's Entropy and Analytic Hierarchy Process. These models are explained in detail. The main purpose of this chapter is to calculate the weightage of the sub-factors and causative factors using different models i.e. AHP, FR, SE, and AHP-SE models. This weightage will be further used for understanding the contribution of landslide causative factors on the occurrence of the landslides. The calculation of weightage will also be used for the preparation of landslide susceptibility maps too.

5.2. Analytic Hierarchy Process (AHP)

The analytic hierarchy process (AHP) is developed by Thomas L. Saaty [96-97]. AHP helps in breaking the complex problems into parts and sub-parts. AHP also helps in reducing errors and keeps the results consistent. The analytic hierarchy process works in three steps i.e. decomposition of the problem, comparative judgment and synthesis of relative importance or rankings [96].

Table 5.1. Saaty's scale of pairwise comparison [96]

Degree of Preference [92-93]	Definition	Explanation
1	Equally Important	Both criteria are equally important or both the factors have the same effect on the occurrence of landslides
3	Moderately Important	One factor is more effective compared to the other factor
5	Highly Important	One factor affects highly compared to the other factor
7	Very Highly Important	A factor is highly dominated over other
9	Extremely Important	A factor has the highest possibility of affecting the occurrence of a landslide over another factor
2,4,6,8	Intermediate Values	If a compromise between two factors is required, intermediate values can be used

In the first step, the problem is decomposed into simpler criteria and these criteria are further broken into sub-criteria. It is easier to make decisions with respect to the sub-criteria and criteria instead of a complex problem like landslides. The criteria for landslide susceptibility are the causative factors which are further divided into sub-factors. These sub-factors and factors are compared to each other. The process of comparison of causative factors and sub-factors is known as pair-wise comparison. In pairwise comparison, it is easy to choose the priority or contribution of causative factors in the occurrence of landslide events. A nine-point scale is used for assigning the weights during the pairwise comparison of the criteria.

If two criteria or factors have the same contribution towards the occurrence of the landslides, the weightage given is 1. If criteria A is moderately important as compared to criteria B, the weightage of 3 is assigned to criteria A [92-93]. Table 5.1 shows Saaty's scale of pairwise comparison. The inverse values can also be assigned. The intermediate values like 2, 4, 6 and 8 are also possible according to the suitability of the user. The pairwise comparison matrix can be formed by using expert weights. The Eigenvalue is calculated after the normalization of the pairwise comparison matrix. If n is the number of criteria and λ_{max} is the maximum Eigenvalue, Consistency Index (C.I) is calculated using the following formula:

$$Consistency\ Index\ (CI) = \frac{\lambda_{max} - n}{n - 1} \quad (5.1)$$

The Consistency Index (CI) is used to calculate the Consistency Ratio (CR). The Consistency Ratio (CR) is the ratio of the consistency index to the randomness index (RI).

$$\text{Consistency Ratio (CR)} = \frac{\text{Consistency Index (CI)}}{\text{Randomness Index (RI)}} \quad (5.2)$$

Randomness index (RI) is calculated by Saaty based on numerous experiments. Table 5.2 shows the values of the randomness index with respect to number of criteria (n).

Table 5.2. Randomness index [92]

n	1	2	3	4	5	6	7	8	9	10	11	12	13	14	15
R.I.	0.0	0.0	0.58	0.9	1.12	1.24	1.32	1.41	1.45	1.49	1.51	1.48	1.56	1.57	1.58

Consistency ratio (CR) is used to check the consistency of the assigned weight during the pairwise comparison. If the consistency ratio lies below 10%, the input is considered consistent while if the CR value exceeds 10%, the input is considered inconsistent. The user will have to change the weightage given in the pairwise comparison matrix. It is mandatory to keep the inputs consistent so that we can reach a consistent solution. So, by changing the input weightage and checking them by consistency ratio (CR) criteria, the rankings of each causative factor and sub-factor are calculated. The causative factors of landslides considered in this study are explained in the previous chapter. The ranking or weightage of these causative factors shows their contribution to the occurrence of landslides. Table 5.3 shows the pairwise comparison matrix of the causative factors and their weightage is calculated using AHP. The consistency ratio (CR) is also shown which is maintained below 10%. The causative factors such as slope, aspect and curvature are classified into sub-factors further and the pairwise comparison matrix is formed for the sub-factor's level too. Table 5.4 shows the pairwise comparison matrix, rankings and consistency ratio for the sub-factors also. The consistency ratio for sub-factors is also maintained below 10%.

5.3. Frequency Ratio (FR)

The frequency ratio (FR) technique for landslide susceptibility mapping is a statistical technique in which a statistical relationship is established between the occurrence of the landslides and the causative factors of the landslides [113, 118]. The landslide inventory of the study area is used to establish the relationship between causative factors and landslide distribution. The frequency ratio is the ratio between the percent areas where landslides occurred in a class to the percent area of the influencing class relative to the whole study area [118]. It is expressed as the following formula:

$$\text{Frequency Ratio (FR)} = \frac{Loi}{Pit} \quad 5.3$$

Here Loi is the percentage of landslides that occurred relative to the area covered by the influencing factor. Pit is the area of influencing factor relative to the total area. The frequency ratio for each influencing factor of landslide is calculated. The frequency ratio can be further elaborated using the following formula:

$$\text{Frequency Ratio (Fr)} = \frac{\left(\frac{Mi}{M}\right)}{\left(\frac{Ni}{N}\right)} \quad 5.4$$

Here, Mi= Number of pixels containing landslides in a class

M= Total number of pixels in a class

Ni= Total number of pixels containing landslides

N= Total number of pixels in the study area

Table 5.3. Pairwise Comparison of Causative Factors

Causative Factors	1	2	3	4	5	6	7	8	9	Weightage
Slope	1									0.105
Aspect	0.14	1								0.016
Relative relief	0.33	4	1							0.036
TWI	2	5	3	1						0.081
Lithology	0.33	6	3	3	1					0.096
Drainage density	3	7	5	3	3	1				0.205
Distance from Road	2	9	7	5	3	3	1			0.28
Distance from Faults	3	8	6	4	2	0.33	0.33	1		0.161
Landuse	0.14	2	0.33	0.14	0.14	0.14	0.14	0.17	1	0.02
CR= 0.09										

Table 5.4. AHP Pairwise Comparison Matrix

Conditioning Factor	Classes	1	2	3	4	5	6	7	8	9	Weightage (Wi)
Slope											0.04
	>30	1									0.054
	30-45	2	1								0.102
	45-60	3	3	1							0.209
	60-75	5	5	3	1						0.596
	More than 75	9	8	7	5	1					
		CR= 0.059									
Aspect											
	Flat	1									0.023
	North	2	1								0.047
	Northeast	7	4	1							0.204
	East	4	2	0.33	1						0.082
	South East	9	8	3	4	1					0.362
	South	5	3	0.5	2	0.25	1				0.125
	South West	4	2	0.25	1	0.2	0.5	1			0.078
	West	3	0.5	0.25	0.5	0.14	0.33	0.5	1		0.046
	North West	2	1	0.14	0.33	0.12	0.25	0.33	0.5	1	0.033
		CR= 0.025									
Relative Relief											
	0-50	1									0.581
	50-100	0.33	1								0.255
	100-150	0.2	0.33	1							0.114
	More than 150	0.11	0.2	0.33	1						0.05

		CR= 0.028									
TWI											
	Low	1									0.565
	Moderate	0.33	1								0.262
	High	0.2	0.33	1							0.118
	Very High	0.14	0.2	0.33	1						0.055
		CR=0.043									
Lithology											
	Neoproterozoic	1									0.194
	Proterozoic (Undiff)	0.33	1								0.098
	Mesoproterozoic	0.5	4	1							0.168
	Palaeoproterozoic	5	7	3	1						0.43
	Palaeozoic	0.2	0.33	0.33	0.2	1					0.053
	Palaeocene- Eocene	0.17	0.2	0.2	0.14	0.5	1				0.033
	Meghalayan	0.2	0.14	0.14	0.11	0.33	0.5	1			0.024
		CR= 0.085									
Drainage Density											
	Low	1									0.046
	Moderate	3	1								0.094
	High	5	5	1							0.203
	Very High	9	7	5	1						0.657
		CR= 0.063									

Distance from road											
	Low	1									0.751
	Moderate	0.2	1								0.178
	High	0.11	0.33	1							0.07
		CR=0.03									
Distance from Faults											
	Low	1									0.751
	Moderate	0.2	1								0.178
	High	0.11	0.33	1							0.07
		CR=0.03									
Landuse/Landcover											
	Snow	1									0.5
	Cultivable Area	0.14	1								0.046
	Permanent Pastures	0.11	0.5	1							0.034
	Forest	0.2	5	5	1						0.137
	Barren Land	0.33	9	7	3	1					0.284
		CR=0.072									

The landslide susceptibility index (LSI) is calculated by the combination of the frequency ratio of the different causative factors [83]. Landslide susceptibility index (LSI) using frequency ratio can be presented as the following equation:

$$\text{Landslide susceptibility index (LSI)} = Fr_1 + Fr_2 + Fr_3 \dots \dots \dots 5.5$$

Fr₁, Fr₂, Fr₃ etc. are the frequency ratio for the different causative factors of the landslides. If the frequency ratio value is more than 1, it shows a high correlation between the causative factor towards landslides while if the FR values are less than 1, there is a poor correlation between the causative factor and the occurrence of the landslide.

It is easy to implement the frequency ratio models in GIS environment. The inputs can be calculated in the pixels. The landslide inventory can be prepared in GIS environment which shows the areas covered by landslide events. The number of pixels covered by the influencing factor and the landslide event on the influencing factor can be observed from thematic layers and the input can be calculated in pixels on the map [118]. Table 5.5 shows the frequency ratio (FR) calculated using equation 5.4 for the causative sub-factors.

5.4. Shannon's Entropy

The frequency ratio (FR) technique calculates the weightage for the sub-factors only. The weightage of causative factors is not calculated in frequency ratio [15, 23, 29, 63, 72, 87, 118]. So, an improvement over the frequency ratio method is proposed in Shannon's entropy technique [130-132].

Table 5.5. Calculation of Weightage using Frequency Ratio and Shannon's Entropy

Causative Factor	Classes	No. of Pixels in class	%age in Class (a)	No. of landslides pixel in class	%age of landslides pixel (b)	FR (b/a)	Pij	Eij	Hij= 1-Eij	Wj
Slope										
	<30	107718	1.71	13	0.8	0.468	0.115	-0.108	0.442	0.12
	30-45	246772	3.9	13	0.8	0.205	0.05	-0.065		
	45-60	1001205	15.91	91	5.95	0.374	0.092	-0.095		
	60-75	3779957	60.05	803	52.51	0.874	0.214	-0.143		
	More than 75	1158974	18.41	609	39.83	2.163	0.53	-0.146		
	Total	6294626		1529		4.085		-0.558		
Aspect										
	Flat	105	0.002	0	0	0	0	0	0.124	0.033
	North	916307	14.56	210	13.73	0.943	0.116	-0.108		
	Northeast	792179	12.59	156	10.2	0.81	0.1	-0.1		
	East	627294	9.97	255	16.68	1.673	0.206	-0.141		
	South East	804073	12.77	290	18.97	1.486	0.183	-0.135		
	South	900237	14.31	230	15.04	1.051	0.129	-0.115		
	South West	809177	12.86	135	8.83	0.687	0.084	-0.091		
	West	643538	10.22	150	9.81	0.96	0.118	-0.109		
	North West	801716	12.73	103	6.74	0.529	0.065	-0.077		
	Total	6294626		1529	100	8.139		-0.876		
Relative Relief										
	0-50	2612642	41.66	804	52.58	1.262	0.323	-0.159	0.408	0.11
	50-100	691263	11.023	145	9.48	0.86	0.22	-0.145		
	100-150	710948	11.337	186	12.16	1.073	0.274	-0.154		

	More than 150	2256417	35.98	394	25.77	0.716	0.183	-0.135		
		6271270		1529		3.911		-0.592		
TWI										
	Low	2810725	44.65	712	46.56	1.043	0.34	-0.159	0.5	0.135
	Moderate	2473126	39.29	596	38.98	0.992	0.323	-0.159		
	High	855581	13.59	207	13.54	0.996	0.325	-0.159		
	Very High	155194	24.65	14	0.91	0.037	0.012	-0.023		
	Total	6294626		1529		3.068		-0.5		
Lithology										
	Neoproterozoic	1364515	21.68	415	27.15	1.252	0.408	-0.159	0.401	0.109
	Proterozoic (Undiff)	3023399	48.03	415	27.14	0.565	0.184	-0.135		
	Mesoproterozoic	502058	7.97	143	9.35	1.173	0.382	-0.16		
	Palaeoproterozoic	1384339	22	556	36.36	1.653	0.539	-0.145		
	Palaeozoic	10282	0.16	0	0	0	0			
	Palaeocene - Eocene	7564	0.13	0	0	0	0			
	Meghalayan	2469	0.03	0	0	0	0			
	Total	6294626		1529		4.643		-0.599		
Drainage Density										
	0-15	2309122	36.68	320	20.93	0.571	0.186	-0.136	0.403	0.109
	15-30	2194591	34.86	628	41.07	1.178	0.384	-0.16		
	30-45	1441690	22.9	438	28.64	1.251	0.408	-0.159		
	More than 45 (upto 66)	349223	5.55	143	9.35	1.685	0.549	-0.143		
	Total	6294626		1529				-0.597		
Distance from road										

	0-1.5 KM	1743800	27.7	531	34.72	1.253	0.409	-0.159	0.547	0.148
	1.5-5.5 km	2114630	33.59	286	18.7	0.557	0.181	-0.134		
	More than 5.5	2436196	38.7	712	46.56	1.203	0.392	-0.159		
	Total	6294626		1529				-0.453		
Distance from Faults										
	0-1.5KM	2790363	44.33	674	44.08	0.994	0.324	-0.159	0.587	0.159
	1.5km-3.0 km	1295638	58.66	298	19.49	0.332	0.108	-0.105		
	more than 3 km	2208625	35.09	557	26.42	0.753	0.245	-0.15		
	Total	6294626		1529				-0.413		
Landuse/ Landcover										
	Snow	374936	0.069917	220	14.39	2.059	0.671	-0.116	0.287	0.078
	Cultivable Area	514825	0.096003	104	6.8	0.708	0.231	-0.147		
	Permanent Pasture	2681924	0.500117	246	16.08	0.562	0.183	-0.135		
	Forest	1534207	0.286094	855	55.91	1.118	0.364	-0.16		
	Barren Land	256697	0.047868	104	6.8	1.42	0.463	-0.155		
	Total	5362589		1529				-0.713		

Entropy shows the uncertainty of an event. The frequency ratio values of sub-factors are used to calculate Shannon's entropy weightage of the causative factors. In landslide susceptibility mapping, Shannon's entropy measures the uncertainty of the occurrence of the landslides depending upon the cumulative impact of the causative factors [130-132].

The weightage of the causative factors is calculated using the following series of the equations:

$$P_{ij} = FR / \sum_{i=1}^m FR \quad (5.6)$$

$$\sum_{i=1}^m E_{ij} = \sum_{i=1}^m (P_{ij}) \times (\ln P_{ij}) \quad (5.7)$$

$$H_{ij} = 1 + \sum_{i=1}^m E_{ij} \quad (5.8)$$

$$W_j = H_{ij} / \sum_{i=1}^n H_{ij} \quad (5.9)$$

P_{ij} is the probability density and FR is the frequency ratio of sub-factors. W_j is the weightage of causative factors obtained from Shannon's entropy technique. Probability density shows the average frequency ratio of a parameter. Now, these values can be used for assigning weight to causative factors while frequency ratio values are used for sub-factors. Table 5.5 shows Shannon's entropy values for the causative factors.

5.4. Hybridization of Expert Opinion with Statistical Models

The analytic hierarchy process (AHP) works on the concept of the expert-based weightage and the inputs can be biased due to the perception of an expert. In this section, we proposed hybrid techniques by hybridization of the AHP and Shannon's entropy (SE) technique. In the AHP-SE

technique, the weightage of sub-factors is taken from the AHP approach while the weightage of causative factors is taken from SE technique. In this technique, the weightage of causative factors is restricted by the SE values which are data driven. The weightage of sub-factors is used from the Table 5.4 while the weightage of causative factor are the Shannon's Entropy values in Table 5.5.

5.5. Concluding Remarks

The contribution of different causative factors and sub-factors is calculated using different models in this Chapter. The relative importance of the causative factors and sub-factors can be analyzed from the Tables prepared by different models. The weightage calculated by the different models is to be assigned to the thematic layers as discussed in Chapter 3. The cumulative impact of these sub-factors and factors will give the landslide potential in the study area.

Results and Discussion

6.1. Introduction

The causative factors are extracted from the different data sources. The DEM-based causative factors and land use of the study area are already in the raster format while the factors digitized from the data sources like SOI maps are in vector format. The data which is in vector format is converted into raster format. All the layers are reclassified and weightage to each causative factor is assigned. The weightage calculated using different models in the previous chapter is assigned to the sub-factors and causative factors. The calculations are done in map algebra and the final output is produced in the form of landslide susceptibility maps. The results are validated using the receiver operation characteristics curve.

In this Chapter, the results are obtained by processing the data obtained in the previous chapters. The landslide potential obtained by the different models is discussed. The role of different causative factors and sub-factors according to the different models is also discussed. The landslide susceptibility maps obtained in this Chapter are validated using the Receiver's Operation Characteristics (ROC) curve and the performance of the models is compared.

6.2. Analysis of Landslide Susceptibility by Analytic Hierarchy Process

A landslide susceptibility map showing the impact of causative factors according to the analytic hierarchy process (AHP) approach is prepared. The weightage of causative factors and sub-factors

is shown the Table 5.3 and Table 5.4. The impact of causative factors on the occurrence of landslide susceptibility can be observed using these tables according to the AHP approach.

6.2.1. Analysis of Sub-factors of landslide

Table 5.4 shows the details of the contribution of sub-factors toward landslide events. Slope gradients less than 45° show poor contribution towards the occurrence of landslides. The AHP weightage for slope gradients less than 30° and 30°-45° are 0.04 and 0.054 respectively. The slope gradient which has an angle between 45° to 60° moderately affects the occurrence of landslides with an AHP weightage of 0.102. Slopes with gradients 60°- 75° have an AHP weightage of 0.209 which shows the high landslide susceptibility of such slopes. The slope angles more than 75° are extremely susceptible to the occurrence of landslides with an AHP weightage of 0.596.

Aspect is divided into nine categories. It can be observed that the southeast and northeast directions have maximum weightage in AHP calculations which are 0.362 and 0.204 respectively. The south direction is also significantly susceptible to landslides with 0.204 AHP weightage. The rest of the directions show less contribution towards the occurrence of landslides. East and Southwest aspect has the AHP weightage of 0.082 and 0.078 respectively while the rest directions have an AHP weightage of less than 0.05.

Relative relief is divided into four categories. It can be observed that lower relative relief values have more AHP weightage showing their more contribution to the occurrence of landslides. The relative relief from 0-50m shows the AHP weightage of 0.581 which is the highest as compared to the higher relative relief values. 50 m to 100 m relative relief category got a weightage of 0.255

while the region with very high relative relief (more than 150 m) got the least AHP weightage i.e. 0.05. The relative relief with 100 m to 150 m shows an AHP weightage of 0.114 which shows its moderate impact on the occurrence of landslides. As the TWI increases, the AHP weightage decreases.

The topographic wetness index (TWI) is divided into four categories. Lower values of the topographic wetness index (TWI) are more susceptible to the occurrence of landslides according to the analytic hierarchy process (AHP) weightage. The low and moderate TWI have the AHP weightage of 0.565 and 0.262 respectively while very high TWI has the least AHP weightage of 0.055.

As the study area is covered with varying lithology, the lithology of the study area plays an important role in the landslide susceptibility. The Paleoproterozoic deposits show the maximum susceptibility toward the occurrence of landslides with a weightage of 0.430 and the Neoproterozoic deposits have the AHP weightage of 0.194. Meghalayan deposits cover very less area in the region and are hence rarely responsible for the occurrence of landslides in the study area. Meghalayan, Eocene-Miocene and Palaeoproterozoic deposits have the AHP weightage 0.024, 0.033 and 0.043 which shows their insignificant contribution to the occurrence of landslides according to the AHP approach. Drainage density is also an important causative factor of landslides according to the AHP approach. The regions with higher drainage density are more susceptible to landslides. A very high drainage density region got a weightage of 0.657 while a region with high drainage density has a weightage of 0.203. The high values of AHP weightage show the prominence of higher values of drainage density. The regions in proximity to faults and

roads have high AHP weightage while the regions which are away from faults and roads have lesser weightage. Snow and barren land are found to be more susceptible to landslides with AHP weightage of 0.5 and 0.284 respectively. Forests cover a significant area in the region and have an AHP weightage of 0.137. Permanent pastures have the least AHP weightage which is 0.034.

6.2.2. Analysis of Causative Factors of Landslides

The contribution of the causative factors in the occurrence of landslides can be observed in table 5.3. It can be seen that the contribution of the distance from the road causative factor is the highest among all the factors. The AHP weightage of distance from the roads is found to be 0.280. The landslides that occurred due to the cut slopes along the roads represent this impact. AHP weightage of the drainage density and distance from faults are 0.205 and 0.161 respectively which show their high correlation toward the occurrence of landslides. Slope angle has also a significant contributing factor in landslide susceptibility of the region with an AHP weightage of 0.105. Lithology and topographic wetness index (TWI) show the AHP weightage of 0.096 and 0.081 respectively. Aspect has the least impact on the occurrence of landslides as per the AHP approach. The weightage of aspect is 0.016 and the weightage of land use is 0.02 which are the lowest as compared to the other causative factors.

6.2.3. Landslide Susceptibility Map using Analytic Hierarchy Process (AHP)

The causative factors of the landslides can be linked to the landslide susceptibility index. The landslide susceptibility index (LSI) in the analytic hierarchy process (AHP) approach can be calculated using equation 6.1. The susceptibility map is divided using natural breaks into five

categories i.e. very low, low, moderate, high and very high. Figure 6.1 shows the landslide susceptibility map by the analytic hierarchy process (AHP) approach.

Landslide Susceptibility Index (LSI)

$$\begin{aligned}
 &= 0.12 \times \textit{Slope} + 0.033 \times \textit{Aspect} + 0.11 \times \textit{Relative Relief} + 0.081 \times \textit{TWI} \\
 &+ 0.096 \times \textit{Lithology} + 0.205 \times \textit{Draiage Density} + 0.280 \\
 &\times \textit{Distance from Roads} + 0.168 \times \textit{Distance from Faults} + 0.020 \\
 &\times \textit{Land use}
 \end{aligned} \tag{6.1}$$

The landslide susceptibility index (LSI) by the AHP approach varies from 0.061 to 0.648. It can be observed from the landslide susceptibility map that the region has very low and low landslide susceptibility is around 46% of the total study area and only 38% of the total landslide area lies in this zone. 21.61% of the total study area is under the moderate landslide susceptibility zone and around 25% of the total landslide lies in this category.

Around 32% of the total region lies under high and very high susceptibility to landslides while more than 35% of the total landslide area lies in this region. According to AHP, only 8% of the total study area lies under a very high landslide susceptibility zone while 9.24% of landslides occur in this area.

6.3. Analysis of Landslide Susceptibility by Frequency Ratio

A statistical relationship between the causative factors and the occurrence of landslides is established using the frequency ratio (FR) approach. The weightage of the sub-factors of landslides is assigned from the landslide inventory. The frequency ratio approach weightage is purely based on the landslide inventory and the area of sub-factors of landslides. So, the weightage in frequency ratio (FR) is more reliable as compared to the analytic hierarchy process (AHP).

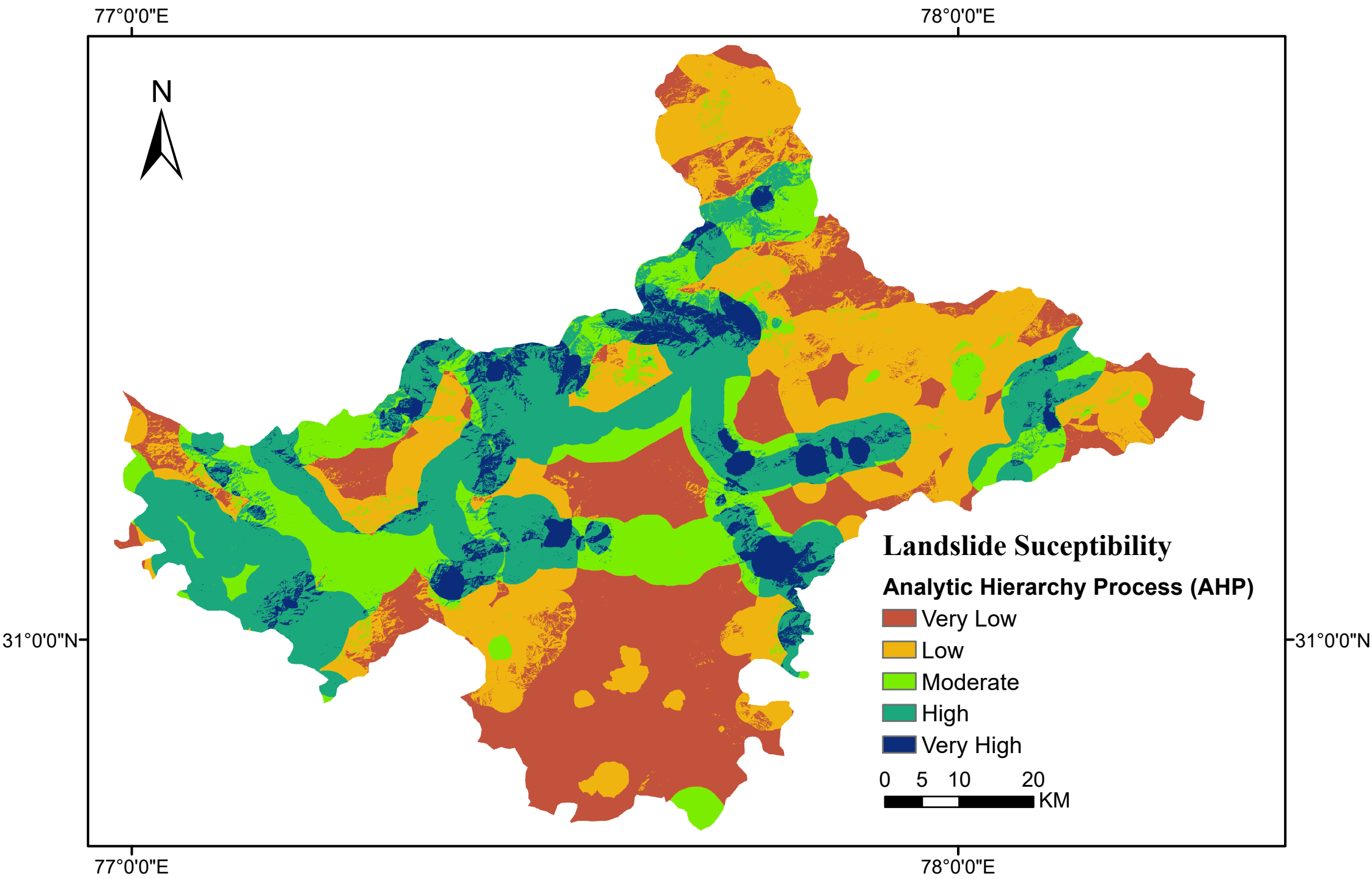


Figure 6.1. Landslide Susceptibility Map using AHP

6.3.1. Analysis of Sub-factors of Landslides

The percentage of the classes of the study area and the area covered by landslides is evaluated in the pixels. The study area is covered with steep slopes majorly. The slopes with an angle less than 45° cover only around 6% of the total area but only 1.6% of the total landslide area is found in this region. The landslide occurrence increases as the slope gradient increases. Slopes with gradients from 45° to 60° cover around 16% of the total study area and 5.95% of the landslide area lie in such zones. Most of the study area (more than 60%) is covered with slopes with gradients from 60° to 75° and more than 52% of the total landslide area lies on such slopes. The slope gradients with more than 75° angle are extremely susceptible to the occurrence of landslides. Such slopes cover only 18% of the total study area but are responsible for the occurrence of around 40% of the total landslides.

The frequency ratio (FR) values of the lower slope angles in less and increases as the slope gradient increases. For slopes, the FR weightage varies from 0.205 to 2.163. Slopes with a gradient of more than 75° show the highest FR value i.e. 2.163 while the slopes with a gradient between 60° to 75° show the FR value of 0.874. The rest of the slope categories have an FR value of less than 0.5 which shows a lesser correlation with the occurrence of landslides.

The flat aspect covers very less area and has an insignificant contribution to the occurrence of landslides. The frequency ratio (FR) for the flat aspect is zero. The east aspect shows the highest correlation with the occurrence of landslides and has a frequency ratio of 1.673. The east aspect covers 9.97% of the total study area while around 17% of the total landslides occur in the region of the east aspect. The Southeast and South aspect also shows a significant impact on the

occurrence of landslides according to frequency ratios of 1.486 and 1.051 respectively. Southeast and South aspects cover 12.77% and 14.31% of the total study area respectively and are covered by 18.97% and 15.04% of the total landslide area. The rest of the aspects show poor correlation with landslides having a frequency ratio of less than 1%. West, North, Northeast, and Southwest have frequency ratio values of 0.96, 0.943, 0.81 and 0.687 respectively showing their relatively lesser correlation with the occurrence of landslides.

Landslide susceptibility of the study area varies with the relative relief but the variation is not linear. The regions with low relative relief (0m-50m) have a frequency ratio of 1.262. The low relief area covers 41.66% of the total study area and more than 52% of the landslide area lies in such regions. The moderate relative relief (50m-100m) covers around 11% of the total study area but around 9% of the landslide area lies in this region.

The moderate relative relief has a frequency ratio of 0.86. The study area with relative relief from 100m to 150 m shows a high correlation with the occurrence of landslides with a frequency ratio of 1.073. More than 11% of the study area is covered by such a region and more than 12% of the total landslides occur in this area. The regions with very high relative relief (more than 150m) cover around 36% of the study area while only 25% of the total landslides occur in this region which shows their relatively lesser contribution to landslides. The very high relative relief category has a frequency ratio of 0.716.

The topographic wetness index (TWI) shows the inverse relationship with the occurrence of landslides. As the TWI increases the frequency ratio decreases. The low TWI covers around 45%

of the study area and 47% of the total landslide area lies in this category approximately. The frequency ratio of the low TWI category is the highest i.e. 1.043. Moderate and high TWI shows almost equal contribution toward landslides with frequency ratios of 0.992 and 0.996 respectively. The very high TWI category has the least contribution towards the occurrence of landslides with a frequency ratio of 0.037.

Paleozoic, Eocene-Miocene and Meghalayan deposits cover less than 0.5% of the total study area in total. So, the contribution of these deposits towards the occurrence of landslides is negligible and has a frequency ratio of zero. Lithological deposit of the Proterozoic age group covers 48% of the total study area but only 27% of the landslide area lies in such deposits. Proterozoic deposits have a frequency ratio of 0.565 which shows their low susceptibility toward landslides. Paleoproterozoic deposits show high susceptibility towards landslides with a frequency ratio of 1.653. Palaeoproterozoic deposits cover 22% of the study area but these are responsible for more than 36% of the total landslides in the study area. Mesoproterozoic deposits with a frequency ratio of 1.173 covers around 7% of the study area but more than 9% of the landslide area lies in these deposits. The rest of the study area (around 21%) is covered with Neoproterozoic aged deposits which faced 27.15% of the total landslide area. They have a frequency ratio of 1.252 which shows their significant contribution to the occurrence of landslides in the study area.

As the drainage density in the study area increases, the frequency ratio increases. The region of low drainage density (less than 15) with a frequency ratio of 0.571 covers around 37% of the study area but only 20.93% of the total landslide area lies in this region. The region with moderate

drainage density (15-30) covers around 35% of the study area while more than 41% of the landslide area lies in this category.

The moderate drainage density (15-30) and high drainage density (30-45) score the frequency ratio weightage 1.178 and 1.251 respectively. Only 5.55% of the study area is covered with very high (more than 45) drainage density which is responsible for 9.35% of the landslide area. The frequency ratio for such regions is 1.685 which shows the highest correlation with the occurrence of landslides.

The distance from the road represents the contribution of anthropogenic activities toward the occurrence of landslides. The region is very close proximity to roads covering 27% of the study area but around 35% of the landslide area lies in this zone. The frequency ratio of the low distance from the road is 1.253. The regions which are more than 5.5 km away from the roads have a frequency ratio of 1.203. The regions which are very close to the faults cover 44% of the study area and are also responsible for the occurrence of 44% of the total landslides. The frequency ratio of the low distance from fault is 0.994 and the frequency ratio for the region with a high distance from faults is 0.753.

Around 50% of the study area is covered with permanent pastures while these are responsible for only 16% of the total landslide area. The frequency ratio for permanent pastures is 0.321 which shows its lesser contribution to the occurrence of landslides. Forest covers around 28% of the study area and 55.91% of the total landslide area lies in this zone. The frequency ratio of forest land use is 1.95.

Around 5% of the study area is barren land and 7% of the total landslide area lies in this category. The frequency ratio of barren land is 1.42. The region with snow cover forms 7% of the total study area which is responsible for the occurrence of 14% of the total landslides. The frequency ratio of the snow-covered region is 2.05 which shows its high correlation with landslide susceptibility. A small percentage of the study area (less than 10%) comes under the category of the cultivable area which is responsible for 7% of the total landslide area. Such regions have relatively lesser frequency ratio values i.e. 0.708.

6.3.2. Landslide Susceptibility Map using Frequency Ratio

The contribution of causative factors is modelled using the frequency ratio technique based on the landslide inventory. A landslide susceptibility map is prepared by overlaying the layers of causative factors in the GIS environment. The landslide susceptibility map is based on the landslide susceptibility index (LSI). If Fr represents the frequency ratio, the equation of landslide susceptibility index (LSI) can be given as follows:

$$Landslide\ Susceptibility\ Index\ (LSI) = Fr_1 + Fr_2 + Fr_3 + Fr_4 \dots \dots \dots + Fr_n \quad (6.2)$$

The landslide susceptibility map using the frequency ratio approach is shown in the figure 6.2. The frequency ratio based landslide susceptibility index (LSI) varies from 3.173 to 13.297. It is divided into five categories using natural breaks i.e. very low, low, moderate, high and very high susceptibility.

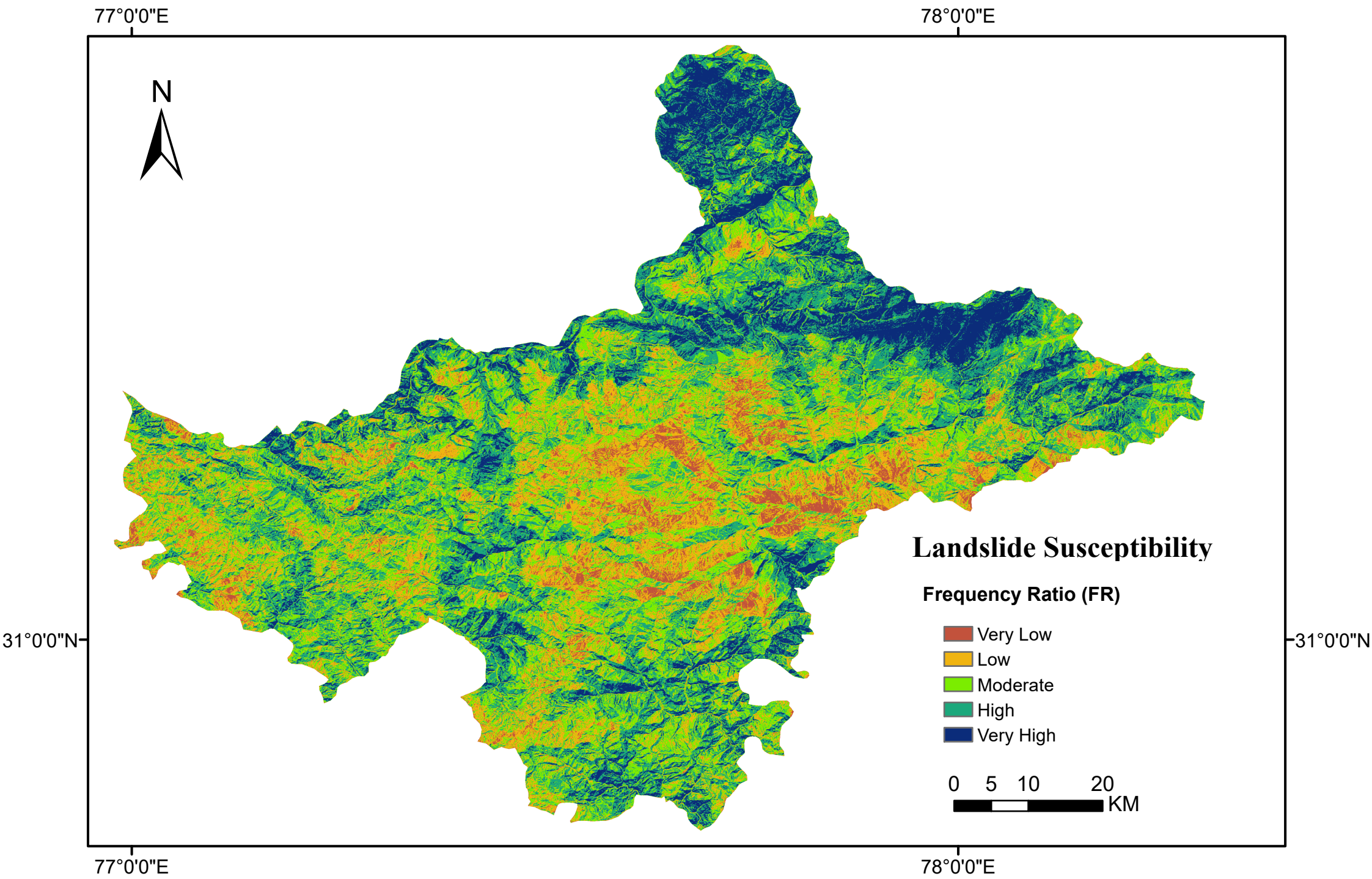


Figure 6.2. Landslide Susceptibility Map using Frequency Ratio

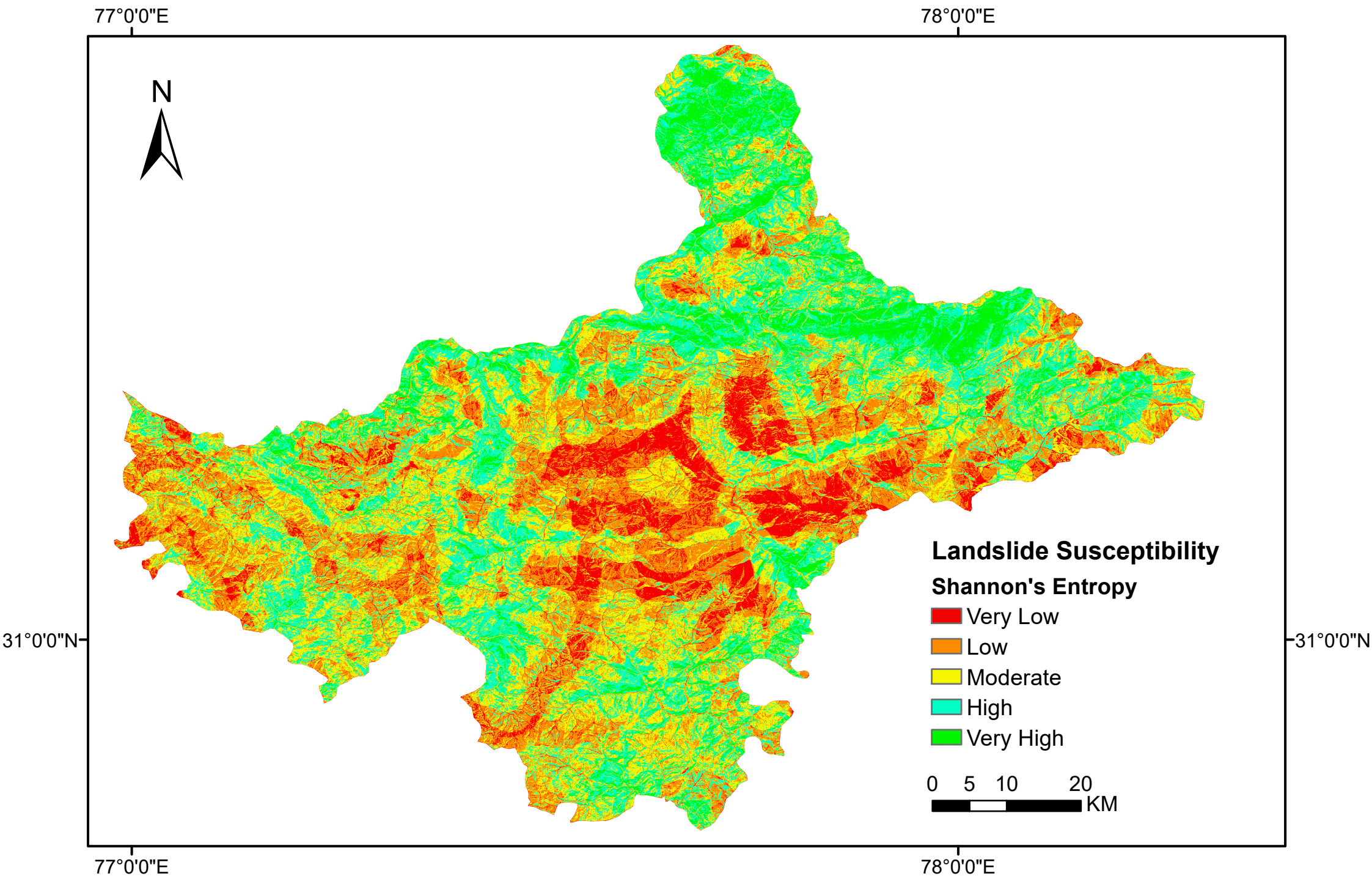


Figure 6.3. Landslide Susceptibility Map using Shannon's Entropy

The region which shows very low susceptibility towards landslides covers 5.7% of the total study area and less than 1% of landslide area lies in this region. 20.7% of the total study area lies under low landslide susceptibility and 10% of the total landslide area lies in this zone approximately. The region which is moderately susceptible to landslides covers 28.66% of the total study area and around 18% landslide area lies in this region. The rest of the study area lies in the high and very high landslide susceptibility zone which is around 44% of the total study area and more than 70% of the landslide area lies in these zones. The zone which shows very high landslide susceptibility covers only around 16% of the total study area but is responsible for more than 40% of the total landslide area.

6.4. Analysis of Landslide Susceptibility using Shannon's Entropy

The frequency ratio (FR) model only calculates the weightage for the sub-factors and FR can't be calculated for the causative factors. Shannon's entropy is an approach in which the weightage of causative factors is calculated from the frequency ratio of the different sub-factors. Shannon's entropy shows the uncertainty of landslide conditioning factors. The weightage of causative factors is calculated using the following procedure:

$$P_{ij} = FR / \sum_{i=1}^m FR \quad (6.3)$$

$$\sum_{i=1}^m E_{ij} = \sum_{i=1}^m (P_{ij}) \times (\ln P_{ij}) \quad (6.4)$$

$$H_{ij} = 1 + \sum_{i=1}^m E_{ij} \quad (6.5)$$

$$W_j = H_{ij} / \sum_{i=1}^n H_{ij} \quad (6.6)$$

The equation for landslide susceptibility index (LSI) using Shannon's Entropy (SE) can be given as follows:

Landslide Susceptibility Index (LSI)

$$\begin{aligned} &= 0.105 \times \textit{Slope} + 0.016 \times \textit{Aspect} + 0.036 \times \textit{Relative Relief} + 0.135 \\ &\times \textit{TWI} + 0.109 \times \textit{Lithology} + 0.109 \times \textit{Drainage Density} + 0.148 \\ &\times \textit{Distance from Roads} + 0.159 \times \textit{Distance from Faults} + 0.078 \\ &\times \textit{Land use} \end{aligned} \quad (6.7)$$

P_{ij} is the probability density and FR is the frequency ratio of sub-factors. W_j is the weightage of causative factors obtained from Shannon's entropy technique. Now, these values can be used for assigning weight to causative factors while frequency ratio values are used for sub-factors.

Distance from the faults is considered the most important causative factor of landslides according to Shannon's Entropy approach with a weightage of 0.159. The proximity to the roads is the second most influential causative factor of landslides. Distance from the road has a weightage of 0.148. ‘

The topographic wetness index (TWI) showed a significant impact on the occurrence of landslides as per the SE approach. TWI has the third-highest weightage among the causative factors i.e. 0.135. Lithology and drainage density show the same impact on the occurrence of landslides with a weightage of 0.109 each. It can be observed that the impact of aspect and land use is the least

among all the causative factors. The weightage of land use is 0.078 and the aspect has an SE weightage of 0.016 which shows its least impact on the occurrence of landslides.

6.4.1. Landslide Susceptibility Map using Shannon's Entropy

The landslide susceptibility map by Shannon's Entropy is based on equation 6.7. The landslide susceptibility index (LSI) varies from 0.402 to 1.412. The landslide susceptibility map is divided using the natural breaks. Figure 6.3 shows the landslide susceptibility map by Shannon's Entropy approach.

The results from Shannon's Entropy approach show that around 35% of the total study area comes under very low and low landslide susceptibility and less than 16% of landslide area lies in such regions. 12.06% under very high susceptibility which contains 31.93% landslide area of the region. 23.66% area lies under high susceptibility which contains 34.45% landslide area. The rest of the study area is moderately susceptible to the occurrence of landslides and around 18% of the total landslide area lies in this zone. The landslide susceptibility has been changed slightly as compared to the frequency ratio (FR) method.

6.5. Hybrid Map by SE-AHP Technique

The biasness of expert is reduced by using the Shannon's Entropy-based approach for assigning weightage to causative factors while AHP is used for assigning the weightage to sub-factors of landslides. In this way, a hybrid map by mixing both the approaches is prepared. The SE-AHP approach improved the results significantly as compared to AHP approach.

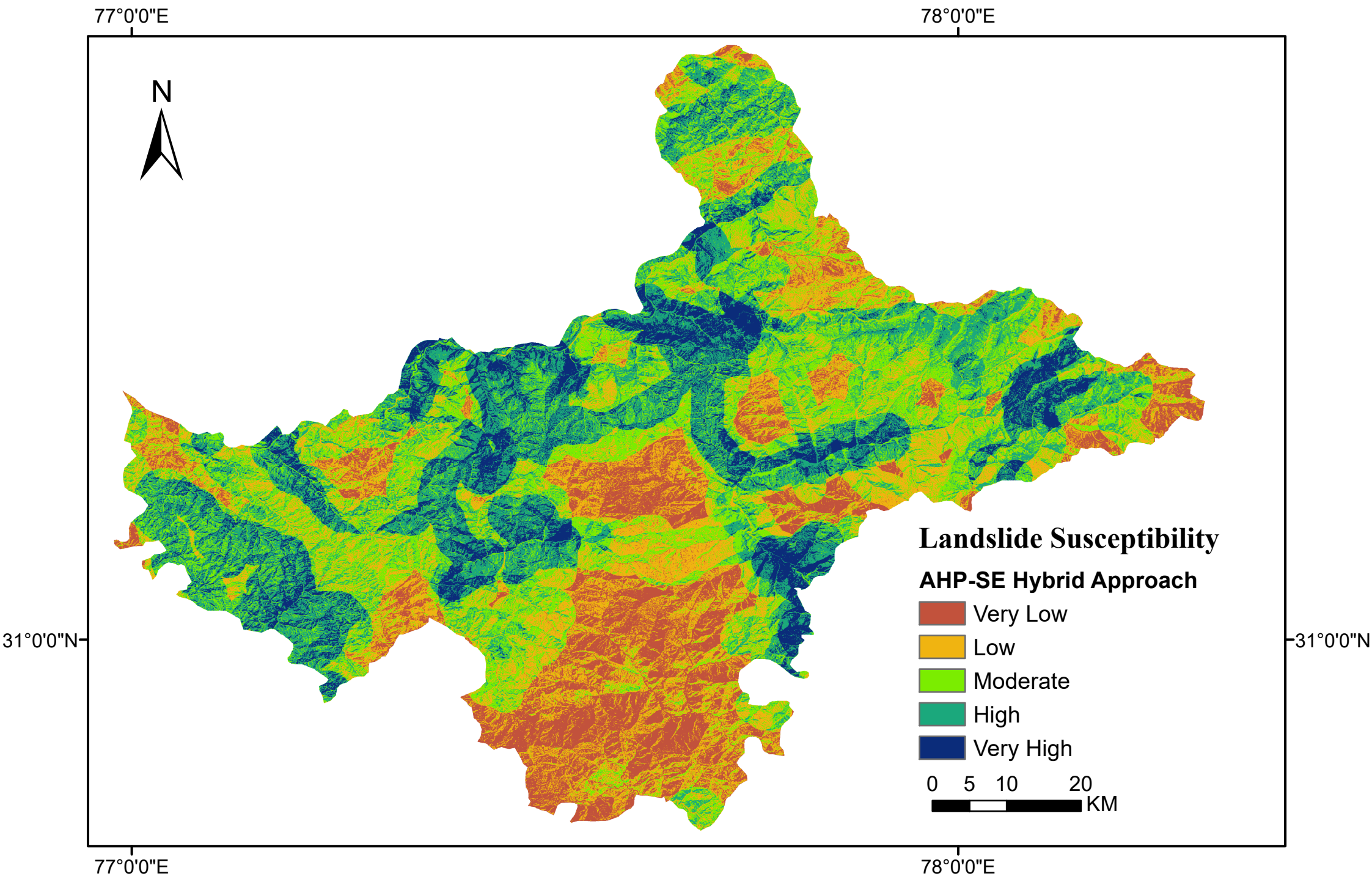


Figure 6.4. Landslide Susceptibility Map using AHP-SE Hybrid approach

According to the SE-AHP approach 14.71% of the study area lies under very low landslide susceptibility zone however only 6.89% of the total landslide area lies in this zone. The moderately susceptible area accounts for around 27% of the total study area and more than 28% of the landslide area lies in this region. Around 24% of the total study area lies under high landslide susceptibility while it is responsible for around 31% of the total landslide area. It can be observed that around 11% of the study area lies under very high susceptibility towards landslides and around 20% of the landslide area lies in this region.

6.6. Discussion, Comparisons and Validation of Results

The landslide susceptibility maps of Shimla region using the statistical models and analytic hierarchy process (AHP) are prepared. These maps can be validated using the receiver operation characteristics (ROC) curve. The landslide inventory is divided into two parts. 30% of the total landslide area is used for training purposes and 70% of the landslide area is used for testing purposes.

The receiver operation characteristics (ROC) curve is prepared between the cumulative area of landslide susceptibility zones and the cumulative area of landslides. Figure 6.4 shows the ROC curve for all three techniques. The graph is plotted between sensitivity and 1- specificity. ROC shows the accuracy of the model in dividing the different landslide zones. It is constructed by plotting the true positive rate and false-positive rate. The true positive rate is the ratio between the correctly predicted positive observations out of all the positive observations that are predicted. Similarly, the true negative rate is the ratio between correctly predicted negative observations to all the predicted negative observations.

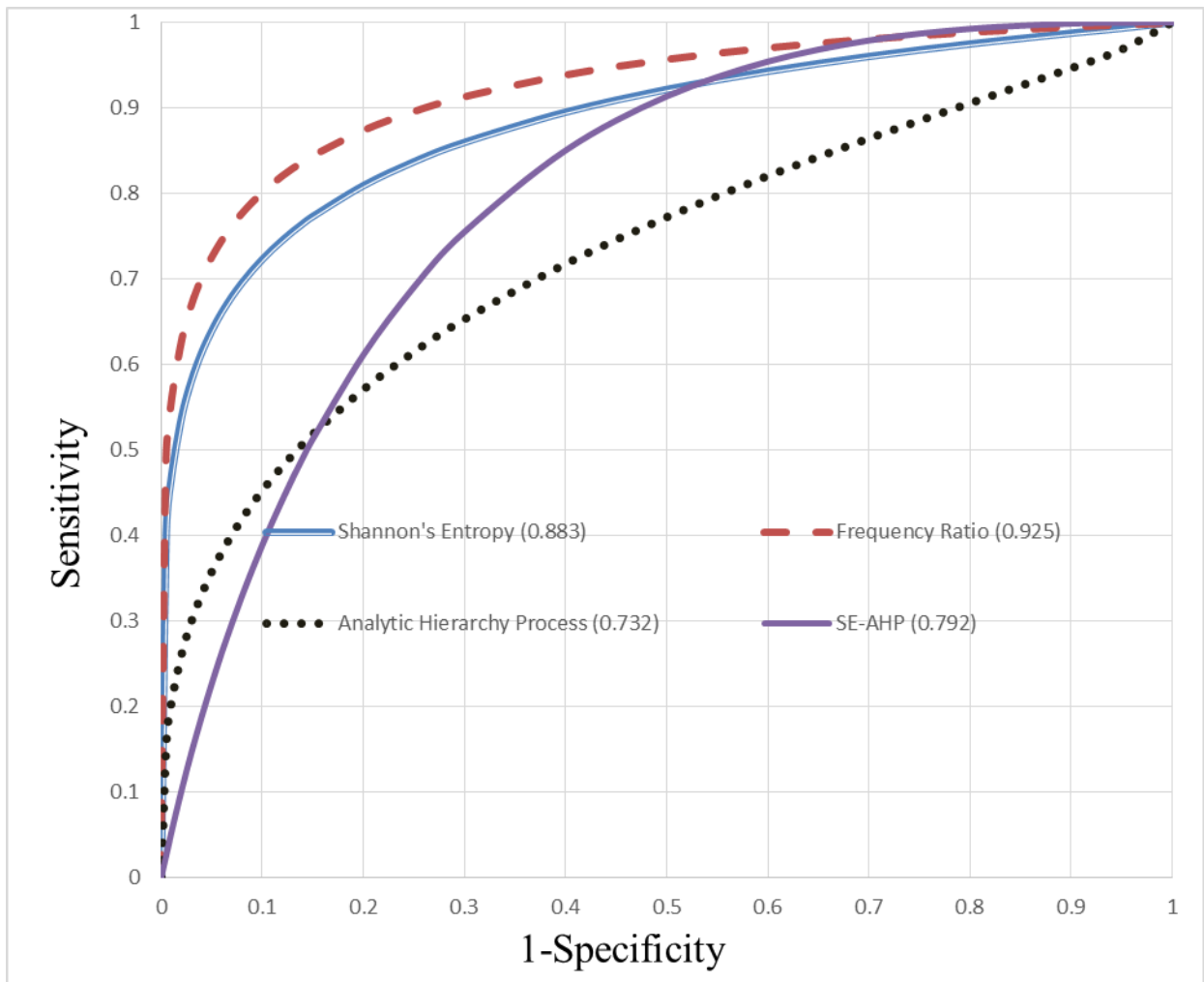


Figure 6.4. Receiver operation characteristics curve

The accuracy of the predicted results can be calculated using the area under the curve (AUC). It can be observed from ROC that the frequency ratio technique shows the maximum accuracy with a prediction rate of 0.925. The higher accuracy of the frequency ratio technique is due to the well-distributed landslide inventory prepared in the study. The prediction rate for Shannon's Entropy technique is reduced to 0.883. The newly proposed hybrid model i.e. SE-AHP approach has

improved the accuracy as compared to the analytic hierarchy process (AHP). The prediction rate of the SE-AHP approach is 0.792. It can be observed that the weightage calculated by the SE technique for causative factors has reduced the accuracy a little but still the results are highly accurate. The analytic hierarchy process (AHP) shows the least prediction rate i.e. 0.732. The results by AHP show the biasness in the weightage by experts.

6.7. Concluding Remarks

The landslide susceptibility maps are prepared using the Analytic Hierarchy Process (AHP), Frequency Ratio (FR), Shannon's Entropy, and AHP-SE hybrid approach. These maps are validated using the ROC curve technique with the help of 30% of landslide data from the landslide inventory. It is found that the frequency ratio is the most suitable technique for studying the landslide susceptibility in this region. However, the newly proposed hybrid technique enhanced the accuracy significantly.

Conclusions and Recommendations

7.1. Conclusions

Shimla is an important region from a tourism and economic point of view. Landslides have remained a very crucial problem in this region. In this study, landslide susceptibility maps for Shimla districts are prepared in GIS environment and the statistical methods and semi-quantitative techniques are compared. The Analytic hierarchy process (AHP), frequency ratio (FR), Shannon's entropy (SE) and Shannon's entropy-analytic hierarchy process (SE-AHP) hybrid models are used to prepare landslide susceptibility maps of the study area. The following conclusions can be drawn from this study:

1. A landslide inventory containing more than 1300 landslide events is prepared from the GSI factsheets and Bhukosh portal. Out of 1300 landslide data, 70% of the landslide data is used for the preparation of landslide susceptibility maps while 30% of the data is used for validation of the maps.
2. Nine causative factors based on the topography, geology, drainage characteristics, anthropogenic characteristics and land use of the region are selected. The relative importance and contribution of causative factors in the occurrence of landslides are identified using three models i.e. frequency ratio, Shannon's entropy, and analytic hierarchy process.

3. The landslide susceptibility maps for the region are prepared using frequency ratio, Shannon's entropy, analytic hierarchy process and SE-AHP hybrid approach. The results are validated using the receiver operation characteristics (ROC) curve.
4. For Shimla region, the accuracy on the ROC curve is found to be maximum for frequency ratio i.e. 0.925 while the least for the AHP technique i.e. 0.732. The prediction rate for Shannon's entropy curve is found to be 0.883.
5. A new hybrid technique i.e. SE-AHP method is proposed by hybridization of Shannon's entropy and analytic hierarchy process. The main purpose of developing the hybrid technique is to reduce the subjectivity in the AHP technique.
6. The results of the SE-AHP technique are better as compared to AHP in terms of accuracy but the accuracy for the SE-AHP technique is lesser as compared to Shannon's entropy and frequency ratio. The prediction rate for the SE-AHP approach is found to be 0.792.
7. The results of the study can be used in the study area by policymakers and risk managers for landslide mitigation and management.

7.2. Recommendations based on the Landslide Potential of the Study Area

It can be observed from the results that a significant area in the region lies under threat of landslides and slope failures. The following recommendations are proposed based on the landslide susceptibility maps:

1. The anthropogenic activities and unplanned construction in the study area have increased the region's slope instability. The number of landslides during the monsoon region is significantly increased in the study area. The extensive rainfall can trigger the landslide movement.
2. The landslides along highways are also a matter of concern. The weak toes of slopes along the highway are highly prone to landslides. So, there is a need for proper planning of infrastructure in the study area.
3. The construction activities must be planned carefully in the regions of high landslide susceptibility. The measures can be taken to stabilization of slopes along the highways and near important infrastructure.
4. The up-gradation of highways and proposal of new highways must be planned according to the landslide susceptibility of regions.
5. The regions which are highly sensitive to landslides can be identified from the landslide susceptibility maps and the slopes which are highly susceptible to failure can be treated and stabilized.

7.3. Recommendations for Preparation of Landslide Susceptibility Maps

The landslide susceptibility maps are prepared worldwide but there is no standard procedure for the preparation of landslide susceptibility maps. The methods for landslide susceptibility mapping

can be selected based on the suitability and available data. Few suggestions based on the results of the study for the preparation of landslide susceptibility maps are given.

7.3.1. Selection of Causative Factors

Identification and selection of causative factors of landslides play an important role in achieving the desired output. The causative factors can be selected based on the experience of the researchers, available literature and available data. Few suggestions for the selection and processing of causative factors of landslides are given as follows:

1. Accurate data should be available for the causative factors. The data can be extracted from the digital elevation model (DEM) and available maps. The maps should be properly updated and accurate. The DEMs can be resampled for accuracy.
2. The previous literature, site visits and opinion of experts can help in the selection of realistic causative factors of landslides.
3. The multiple impacts of a single parameter should be avoided. Some studies considered the effect of a single factor multiple times. Drainage density and distance from stream both are considered in some studies. The drainage effect may be overrated in such studies. Similarly, rainfall and curvature both show the effect of rainfall. So, the multiple effects of a single factor can be removed for better results.
4. The causative factors should be independent of each other. It means that there should not be overlapping of the impact of causative factors on landslide susceptibility.

5. The resolution of the causative factor layers must be kept the same. If the available data has not the same resolution, the grid sizes can be changed.

7.3.2. Selection of Method for Landslide Susceptibility Mapping

The landslide susceptibility maps are prepared using numerous techniques including qualitative approach, quantitative approach and semi-qualitative approaches. The following recommendations are proposed for the selection of the suitable method of landslide susceptibility mapping:

1. The selection of the method for landslide susceptibility mapping should be chosen based on the availability of data, field conditions and suitability of the technique. The required accuracy is also an important parameter in choosing the technique for landslide susceptibility mapping in a particular region.
2. If the site visits are not possible for the preparation of landslide inventory and there is no historical landslide data available, expert-based techniques are the only way to prepare landslide susceptibility maps. However, the problem of subjectivity and less accuracy will remain in such cases. The recommendations of Indian Standard Code IS 14496: 1998 can be considered for the preparation of landslide susceptibility maps.
3. The expert-based technique is relatively simple to use. If the landslide inventory is available for the region, the experts can use the inventory to understand the impact of causative factors on landslides.

4. The quality of landslide susceptibility maps depends on the input data. So, the input data must be accurate for achieving a better output. The weightage of the causative factors can be varied for obtaining a better output. The variation of weightage of factors is possible only in the case of expert weightage and analytic hierarchy process (AHP).
5. Semi-qualitative techniques like the analytic hierarchy process (AHP) are preferred as compared to the purely expert-based techniques. It helps in reducing the subjectivity of the opinion of experts. In the absence of landslide inventory, this technique is highly recommended.
6. Human perception is included in the analytic hierarchy process and subjectivity is restricted by the consistency ratio. The pair-wise comparison of the causative factors depends upon the perception of the researcher. It is simple to use in a spatial environment and the tools required for AHP calculations are easily available. The analytic hierarchy process (AHP) can be performed even using an excel sheet or SPSS (statistical package of social science).
7. The statistical techniques are highly accurate. If an accurate and well-distributed landslide inventory is available, statistical techniques can be used. The statistical techniques will require mathematical modelling and will be time-consuming as compared to expert-based techniques.
8. Frequency ratio (FR) is found to be the simplest among statistical techniques and still has very high accuracy. The other methods like the information value (Info-value) technique

and other probabilistic methods yield almost the same accuracy and can be used based on the suitability of the user.

9. Artificial intelligence and machine learning algorithms are relatively new techniques in the field of landslide susceptibility mapping. Further research is required for landslide susceptibility mapping using these techniques.

7.4. Future Scope

The future scope of the study is described as follows:

1. The study can be extended to predict landslide hazards and landslides risk assessment of the study area.
2. The seasonal variation in causative factors such as rainfall, land-use variation and vegetation cover variation can be studied and their impact on the occurrence of landslides can be observed.
3. Further, the neural network and machine learning models can be applied for landslide susceptibility mapping of the region.
4. The mitigation measure for landslide hazards can be planned considering the results of the study.
5. The relationships between landslides and climate change can be studied for better prediction of landslides in the future.

REFERENCES

1. Kumar, A., & Pushplata. (2015). Building regulations for hill towns of India. *HBRC Journal*, 11(2), 275–284. <https://doi.org/10.1016/j.hbrcj.2014.06.006>
2. Cruden, D. M. (1991). A simple definition of a landslide. *Bulletin of the International Association of Engineering Geology*, 43(1), 27–29. <https://doi.org/10.1007/BF02590167>
3. Highland, L. M., Bobrowsky, P. (2008). *The Landslide Handbook – A Guide to Understanding Landslides* (1st ed., Vol. 1). U.S. Geological Survey, Reston, Virginia. https://pubs.usgs.gov/circ/1325/pdf/C1325_508.pdf
4. Lehmann, P., Ruetter, J., & Or, D. (2019). Deforestation Effects on Rainfall-Induced Shallow Landslides: Remote Sensing and Physically-Based Modelling. *Water Resources Research*, 55(11), 9962–9976. <https://doi.org/10.1029/2019WR025233>
5. Punjab Government. (1910). “Punjab District Gazetteers, Vol. VIII, Gazetteer of the Simla Hill State.” *Government Printing, Punjab, Lahore 1910, Indus Publishing Company, New Delhi*, (Reprinted in 1995).
6. Kahlon, S., Chandel, V.B.S., Brar, K. K. (2014). Landslides in Himalayan mountains: a study of Himachal Pradesh, India. *International Journal of IT, Engineering and Applied Sciences Research*, 3 (9), 28-34.
7. Cruden, D.M., Varnes D. J. (1996). Landslide types and processes. *Landslides: Investigation and Mitigation, Transportation Research Board Special Report*, 247, 36-75, <https://onlinepubs.trb.org/Onlinepubs/sr/sr247/sr247-003.pdf>

8. Varnes, D. J. (1978). Slope movement types and processes. In: Schuster RL, Krizek RJ (eds) Landslides, Analysis and Control, Transportation Research Board Special Report 176, 11–33. <https://onlinepubs.trb.org/Onlinepubs/sr/sr176/176-002.pdf>
9. Yatini, Y., & Suyanto, I. (2018). Identification of slip surface based on geoelectrical dipole-dipole in the landslides hazardous area of Gedangsari District, Gunungkidul Regency, Province of Daerah Istimewa Yogyakarta, Indonesia. *IOP Conference Series: Earth and Environmental Science*, 212, 012013. <https://doi.org/10.1088/1755-1315/212/1/012013>
10. Knowledge Network. *Figure 1.1 b*. Retrieved January 01, 2021, from www.knowledgenetwork.ca/slide
11. Hungr, O., Leroueil, S., & Picarelli, L. (2014). The Varnes classification of landslide types, an update. *Landslides*, 11(2), 167–194. <https://doi.org/10.1007/s10346-013-0436-y>
12. Yang, R., Xiao, P., & Qi, S. (2019). Analysis of Slope Stability in Unsaturated Expansive Soil: A Case Study. *Frontiers in Earth Science*, 7. <https://doi.org/10.3389/feart.2019.00292>
13. Dinesh, S., Savitha, C., & Moghal, A. A. B. (2022). *Prediction of Stability of an Infinite Slope Using Geospatial Techniques*, Lecture Notes in Civil Engineering, 185, 1–9. https://doi.org/10.1007/978-981-16-5601-9_1
14. Gariano, S. L., & Guzzetti, F. (2016). Landslides in a changing climate. *Earth-Science Reviews*, 162, 227–252. <https://doi.org/10.1016/j.earscirev.2016.08.011>
15. Alsabhan, A. H., Singh, K., Sharma, A., Alam, S., Pandey, D. D., Rahman, S. A. S., Khurshed, A., & Munshi, F. M. (2022). Landslide susceptibility assessment in the Himalayan range based along Kasauli – Parwanoo road corridor using weight of evidence, information value, and frequency ratio. *Journal of King Saud University - Science*, 34(2), 101759. <https://doi.org/10.1016/j.jksus.2021.101759>

16. Pradhan, B., Chaudhari, A., Adinarayana, J., & Buchroithner, M. F. (2012). Soil erosion assessment and its correlation with landslide events using remote sensing data and GIS: a case study at Penang Island, Malaysia. *Environmental Monitoring and Assessment*, 184(2), 715–727. <https://doi.org/10.1007/s10661-011-1996-8>
17. Bogaard, T. A., & Greco, R. (2016). Landslide hydrology: from hydrology to pore pressure. *WIREs Water*, 3(3), 439–459. <https://doi.org/10.1002/wat2.1126>
18. Masi, E.B., Segoni, S., & Tofani, V. (2021). Root Reinforcement in Slope Stability Models: A Review. *Geosciences*, 11(5), 212. <https://doi.org/10.3390/geosciences11050212>
19. Nakamura, S., Wakai, A., Umemura, J., Sugimoto, H., & Takeshi, T. (2014). Earthquake-induced landslides: Distribution, motion and mechanisms. *Soils and Foundations*, 54(4), 544–559. <https://doi.org/10.1016/j.sandf.2014.06.001>
20. Perera, E. N. C., Jayawardana, D. T., Jayasinghe, P., Bandara, R. M. S., & Alahakoon, N. (2018). Direct impacts of landslides on socio-economic systems: a case study from Aranayake, Sri Lanka. *Geoenvironmental Disasters*, 5(1), 11. <https://doi.org/10.1186/s40677-018-0104-6>
21. Winter, M. G., Shearer, B., Palmer, D., Peeling, D., Harmer, C., & Sharpe, J. (2016). The Economic Impact of Landslides and Floods on the Road Network. *Procedia Engineering*, 143, 1425–1434. <https://doi.org/10.1016/j.proeng.2016.06.168>
22. Akgun, A., & Erkan, O. (2016). Landslide susceptibility mapping by geographical information system-based multivariate statistical and deterministic models: in an artificial reservoir area at Northern Turkey. *Arabian Journal of Geosciences*, 9(2). <https://doi.org/10.1007/s12517-015-2142-7>

23. Demir, G., Aytekin, M., & Akgun, A. (2015). Landslide susceptibility mapping by frequency ratio and logistic regression methods: an example from Niksar–Resadiye (Tokat, Turkey). *Arabian Journal of Geosciences*, 8(3). <https://doi.org/10.1007/s12517-014-1332-z>
24. Gautam, P., Kubota, T., Sapkota, L. M., & Shinohara, Y. (2021). Landslide susceptibility mapping with GIS in high mountain area of Nepal: a comparison of four methods. *Environmental Earth Sciences*, 80(9). <https://doi.org/10.1007/s12665-021-09650-2>
25. Aleotti, P., & Chowdhury, R. (1999). Landslide hazard assessment: Summary review and new perspectives. In *Bulletin of Engineering Geology and the Environment* (Vol. 58, Issue 1). <https://doi.org/10.1007/s100640050066>
26. El Jazouli, A., Barakat, A., & Khellouk, R. (2019). GIS-multicriteria evaluation using AHP for landslide susceptibility mapping in Oum Er Rbia high basin (Morocco). *Geoenvironmental Disasters*, 6(1). <https://doi.org/10.1186/s40677-019-0119-7>
27. Guzzetti, F., Mondini, A. C., Cardinali, M., Fiorucci, F., Santangelo, M., & Chang, K. T. (2012). Landslide inventory maps: New tools for an old problem. In *Earth-Science Reviews* (Vol. 112, Issues 1–2). <https://doi.org/10.1016/j.earscirev.2012.02.001>
28. Hasekioğulları, G. D., & Ercanoglu, M. (2012). A new approach to use AHP in landslide susceptibility mapping: A case study at Yenice (Karabuk, NW Turkey). *Natural Hazards*, 63(2). <https://doi.org/10.1007/s11069-012-0218-1>
29. Khan, H., Shafique, M., Khan, M. A., Bacha, M. A., Shah, S. U., & Calligaris, C. (2019). Landslide susceptibility assessment using Frequency Ratio, a case study of northern Pakistan. *Egyptian Journal of Remote Sensing and Space Science*, 22(1). <https://doi.org/10.1016/j.ejrs.2018.03.004>
30. Mersha, T., & Meten, M. (2020). GIS-based landslide susceptibility mapping and assessment using bivariate statistical methods in Simada area, northwestern Ethiopia. *Geoenvironmental Disasters*, 7(1). <https://doi.org/10.1186/s40677-020-00155-x>

31. Gökçeoglu, C., & Aksoy, H. (1996). Landslide susceptibility mapping of the slopes in the residual soils of the Mengen region (Turkey) by deterministic stability analyses and image processing techniques. *Engineering Geology*, 44(1–4). [https://doi.org/10.1016/s0013-7952\(97\)81260-4](https://doi.org/10.1016/s0013-7952(97)81260-4)
32. Gariano, S. L., & Guzzetti, F. (2016). Landslides in a changing climate. *Earth-Science Reviews*, 162, 227–252. <https://doi.org/10.1016/j.earscirev.2016.08.011>
33. Perera, E. N. C., Gunaratne, A. M. C. T., & Samarasinghe, S. B. D. (2022). Participatory Landslide Inventory (PLI): An Online Tool for the Development of a Landslide Inventory. *Complexity*, 2022, 1–10. <https://doi.org/10.1155/2022/2659203>
34. van Westen, C. J., Jaiswal, P., Ghosh, S., Martha, T. R., & Kuriakose, S. L. (2012). Landslide Inventory, Hazard and Risk Assessment in India. In *Terrigenous Mass Movements* (pp. 239–282). Springer Berlin Heidelberg. https://doi.org/10.1007/978-3-642-25495-6_9
35. Definition of landslide susceptibility on website of Geological Survey of Ireland <https://www.gsi.ie/en-ie/programmes-and-projects/geohazards/projects/Pages/Landslide-SusceptibilityMapping.aspx#:~:text=A%20landslide%20susceptibility%20map%20identifies,of%20water%20in%20an%20area> Retrieved April 15, 2022.
36. Brabb, E. E. (1984) Innovative approaches to landslide hazard mapping. Proc IV ISL, Toronto 1: 307 – 324
37. Reichenbach, P., Rossi, M., Malamud, B. D., Mihir, M., & Guzzetti, F. (2018). A review of statistically-based landslide susceptibility models. *Earth-Science Reviews*, 180, 60–91. <https://doi.org/10.1016/j.earscirev.2018.03.001>
38. Glade, T. (2001). Landslide Hazard Assessment and Historical Landslide Data — An Inseparable Couple?, *Advances in Natural and Technological Hazards*, pp. 153–168. https://doi.org/10.1007/978-94-017-3490-5_12

39. Pardeshi, S. D., Autade, S. E., & Pardeshi, S. S. (2013). Landslide hazard assessment: recent trends and techniques. *SpringerPlus*, 2(1), 523. <https://doi.org/10.1186/2193-1801-2-523>
40. Ou, P., Wu, W., Qin, Y., Zhou, X., Huangfu, W., Zhang, Y., Xie, L., Huang, X., Fu, X., Li, J., Jiang, J., Zhang, M., Liu, Y., Peng, S., Shao, C., Bai, Y., Zhang, X., Liu, X., & Liu, W. (2021). Assessment of Landslide Hazard in Jiangxi Using Geo-information Technology. *Frontiers in Earth Science*, 9. <https://doi.org/10.3389/feart.2021.648342>
41. Anbalagan, R., & Singh, B. (1996). Landslide hazard and risk assessment mapping of mountainous terrains — a case study from Kumaun Himalaya, India. *Engineering Geology*, 43(4), 237–246. [https://doi.org/10.1016/S0013-7952\(96\)00033-6](https://doi.org/10.1016/S0013-7952(96)00033-6)
42. Nguyen, B.-Q.-V., & Kim, Y.-T. (2021). Regional-scale landslide risk assessment on Mt. Umyeon using risk index estimation. *Landslides*, 18(7), 2547–2564. <https://doi.org/10.1007/s10346-021-01622-8>
43. Pan, W., Fu, L., Xiao, H., Yu, X., Li, X., Zhang, X., & Zhao, T. (2021). Risk assessment for landslide of FAST site based on GIS and fuzzy hierarchical method. *Environmental Earth Sciences*, 80(8), 320. <https://doi.org/10.1007/s12665-021-09571-0>
44. Azimi, S. R., Nikraz, H., & Yazdani-Chamzini, A. (2018). Landslide Risk Assessment by using a New Combination Model based on a Fuzzy Inference System Method. *KSCE Journal of Civil Engineering*, 22(11), 4263–4271. <https://doi.org/10.1007/s12205-018-0041-7>
45. Leal Sousa, R., Vargas, E., Chaminé, H. I., Ribeiro e Sousa, L., & Karam, K. (2021). Risk assessment on landslides focused on the role of the water: examples from model regions (Rio de Janeiro State and Hong Kong). *SN Applied Sciences*, 3(4), 423. <https://doi.org/10.1007/s42452-021-04300-5>

46. Gupta, S. K., & Shukla, D. P. (2022). Effect of scale and mapping unit on landslide susceptibility mapping of Mandakini River Basin, Uttarakhand, India. *Environmental Earth Sciences*, 81(14), 373. <https://doi.org/10.1007/s12665-022-10487-6>
47. van Westen, C. J., Castellanos, E., & Kuriakose, S. L. (2008). Spatial data for landslide susceptibility, hazard, and vulnerability assessment: An overview. *Engineering Geology*, 102(3–4), 112–131. <https://doi.org/10.1016/j.enggeo.2008.03.010>
48. Rabby, Y. W., & Li, Y. (2020). Landslide Susceptibility Mapping Using Integrated Methods: A Case Study in the Chittagong Hilly Areas, Bangladesh. *Geosciences*, 10(12), 483. <https://doi.org/10.3390/geosciences10120483>
49. Nepal, N., Chen, J., Chen, H., Wang, X., & Pangali Sharma, T. P. (2019). Assessment of landslide susceptibility along the Araniko Highway in Poiqu/Bhote Koshi/Sun Koshi Watershed, Nepal Himalaya. *Progress in Disaster Science*, 3. <https://doi.org/10.1016/j.pdisas.2019.100037>
50. Panchal, S., & Shrivastava, A. Kr. (2022). Landslide hazard assessment using analytic hierarchy process (AHP): A case study of National Highway 5 in India. *Ain Shams Engineering Journal*, 13(3), 101626. <https://doi.org/10.1016/j.asej.2021.10.021>
51. Wislocki, A. P., & Bentley, S. P. (1991). An expert system for landslide hazard and risk assessment. *Computers & Structures*, 40(1), 169–172. [https://doi.org/10.1016/0045-7949\(91\)90469-3](https://doi.org/10.1016/0045-7949(91)90469-3)
52. He, H., Hu, D., Sun, Q., Zhu, L., & Liu, Y. (2019). A Landslide Susceptibility Assessment Method Based on GIS Technology and an AHP-Weighted Information Content Method: A Case Study of Southern Anhui, China. *ISPRS International Journal of Geo-Information*, 8(6), 266. <https://doi.org/10.3390/ijgi8060266>

53. Corominas, J., van Westen, C., Frattini, P., Cascini, L., Malet, J.-P., Fotopoulou, S., Catani, F., van den Eeckhaut, M., Mavrouli, O., Agliardi, F., Pitilakis, K., Winter, M. G., Pastor, M., Ferlisi, S., Tofani, V., Hervás, J., & Smith, J. T. (2013). Recommendations for the quantitative analysis of landslide risk. *Bulletin of Engineering Geology and the Environment*. <https://doi.org/10.1007/s10064-013-0538-8>
54. Wang, Y., Wen, H., Sun, D., & Li, Y. (2021). Quantitative Assessment of Landslide Risk Based on Susceptibility Mapping Using Random Forest and GeoDetector. *Remote Sensing*, *13*(13), 2625. <https://doi.org/10.3390/rs13132625>
55. Milevski, I., Dragičević, S., & Zorn, M. (2019). Statistical and expert-based landslide susceptibility modeling on a national scale applied to North Macedonia. *Open Geosciences*, *11*(1), 750–764. <https://doi.org/10.1515/geo-2019-0059>
56. Yong, C., Jinlong, D., Fei, G., Bin, T., Tao, Z., Hao, F., Li, W., & Qinghua, Z. (2022). Review of landslide susceptibility assessment based on knowledge mapping. *Stochastic Environmental Research and Risk Assessment*. <https://doi.org/10.1007/s00477-021-02165-z>
57. Syam, M. A., Heryanto, & Balfas, M. D. (2019). Mapping of Landslide Susceptibility Using Analytical Hierarchy Process in Sukamaju Area, Tenggara Seberang, Regency of Kutai Kartanegara. *IOP Conference Series: Earth and Environmental Science*, *279*(1), 012002. <https://doi.org/10.1088/1755-1315/279/1/012002>
58. Zhou, X., Wu, W., Qin, Y., & Fu, X. (2021). Geoinformation-based landslide susceptibility mapping in subtropical area. *Scientific Reports*, *11*(1), 24325. <https://doi.org/10.1038/s41598-021-03743-5>
59. Sonker, I., Tripathi, J. N., & Singh, A. K. (2021). Landslide susceptibility zonation using geospatial technique and analytical hierarchy process in Sikkim Himalaya. *Quaternary Science Advances*, *4*, 100039. <https://doi.org/10.1016/j.qsa.2021.100039>

60. Shano, L., Raghuvanshi, T. K., & Meten, M. (2020). Landslide susceptibility evaluation and hazard zonation techniques – a review. In *Geoenvironmental Disasters* (Vol. 7, Issue 1). <https://doi.org/10.1186/s40677-020-00152-0>
61. Reichenbach, P., Busca, C., Mondini, A. C., & Rossi, M. (2014). The Influence of Land Use Change on Landslide Susceptibility Zonation: The Briga Catchment Test Site (Messina, Italy). *Environmental Management*, 54(6), 1372–1384. <https://doi.org/10.1007/s00267-014-0357-0>
62. Armaş, I., Vartolomei, F., Stroia, F., & Braşoveanu, L. (2014). Landslide susceptibility deterministic approach using geographic information systems: application to Breaza town, Romania. *Natural Hazards*, 70(2), 995–1017. <https://doi.org/10.1007/s11069-013-0857-x>
63. Park, S., Choi, C., Kim, B., & Kim, J. (2013). Landslide susceptibility mapping using frequency ratio, analytic hierarchy process, logistic regression, and artificial neural network methods at the Inje area, Korea. *Environmental Earth Sciences*, 68(5), 1443–1464. <https://doi.org/10.1007/s12665-012-1842-5>
64. Wang, H. B., Sassa, K., & Xu, W. Y. (2007). Assessment of Landslide Susceptibility Using Multivariate Logistic Regression: A Case Study in Southern Japan. *Environmental and Engineering Geoscience*, 13(2), 183–192. <https://doi.org/10.2113/gseegeosci.13.2.183>
65. Nandi, A., & Shakoor, A. (2010). A GIS-based landslide susceptibility evaluation using bivariate and multivariate statistical analyses. *Engineering Geology*, 110(1–2), 11–20. <https://doi.org/10.1016/j.enggeo.2009.10.001>
66. Shahabi, H., Ahmad, B. B., & Khezri, S. (2013). Evaluation and comparison of bivariate and multivariate statistical methods for landslide susceptibility mapping (case study: Zab basin). *Arabian Journal of Geosciences*, 6(10), 3885–3907. <https://doi.org/10.1007/s12517-012-0650-2>
67. Murillo-García, F. G., & Alcántara-Ayala, I. (2015). *Landslide Susceptibility Analysis and Mapping Using Statistical Multivariate Techniques: Pahuatlán, Puebla, Mexico* (pp. 179–194). https://doi.org/10.1007/978-3-319-11053-0_16

68. El-Fengour, M., el Motaki, H., & el Bouzidi, A. (2021). Landslides susceptibility modelling using Multivariate Logistic Regression Model in the Sahla Watershed in Northern Morocco. *Sociedade & Natureza*, 33. <https://doi.org/10.14393/SN-v33-2021-59124>
69. Zhu, L., & Huang, J. (2006). GIS-based logistic regression method for landslide susceptibility mapping in regional scale. *Journal of Zhejiang University-SCIENCE A*, 7(12), 2007–2017. <https://doi.org/10.1631/jzus.2006.A2007>
70. Mathew, J., Jha, V. K., & Rawat, G. S. (2007). Application of binary logistic regression analysis and its validation for landslide susceptibility mapping in part of Garhwal Himalaya, India. *International Journal of Remote Sensing*, 28(10), 2257–2275. <https://doi.org/10.1080/01431160600928583>
71. Talaei, R. (2014). Landslide hazard assessment in *Hashtchin area, NW-IRAN*. *Carpathian Journal of Earth and Environmental Sciences* 9(3):123-134. <http://www.cjees.ro/viewTopic.php?topicId=451>
72. Rasyid, A. R., Bhandary, N. P., & Yatabe, R. (2016). Performance of frequency ratio and logistic regression model in creating GIS based landslides susceptibility map at Lompobattang Mountain, Indonesia. *Geoenvironmental Disasters*, 3(1), 19. <https://doi.org/10.1186/s40677-016-0053-x>
73. Sun, X., Chen, J., Bao, Y., Han, X., Zhan, J., & Peng, W. (2018). Landslide Susceptibility Mapping Using Logistic Regression Analysis along the Jinsha River and Its Tributaries Close to Derong and Deqin County, Southwestern China. *ISPRS International Journal of Geo-Information*, 7(11), 438. <https://doi.org/10.3390/ijgi7110438>
74. Hemasinghe, H., Rangali, R. S. S., Deshapriya, N. L., & Samarakoon, L. (2018). Landslide susceptibility mapping using logistic regression model (a case study in Badulla District, Sri Lanka). *Procedia Engineering*, 212, 1046–1053. <https://doi.org/10.1016/j.proeng.2018.01.135>

75. Wubalem, A., & Meten, M. (2020). Landslide susceptibility mapping using information value and logistic regression models in Goncha Siso Eneses area, northwestern Ethiopia. *SN Applied Sciences*, 2(5), 807. <https://doi.org/10.1007/s42452-020-2563-0>
76. Lee, S., & Talib, J. A. (2005). Probabilistic landslide susceptibility and factor effect analysis. *Environmental Geology*, 47(7), 982–990. <https://doi.org/10.1007/s00254-005-1228-z>
77. Sujatha, E. R., Rajamanickam, G. V., & Kumaravel, P. (2012). Landslide susceptibility analysis using Probabilistic Certainty Factor Approach: A case study on Tevankarai stream watershed, India. *Journal of Earth System Science*, 121(5), 1337–1350. <https://doi.org/10.1007/s12040-012-0230-6>
78. Pandey, V. K., & Sharma, M. C. (2017). Probabilistic landslide susceptibility mapping along Tipri to Ghuttu highway corridor, Garhwal Himalaya (India). *Remote Sensing Applications: Society and Environment*, 8, 1–11. <https://doi.org/10.1016/j.rsase.2017.07.007>
79. Wubalem, A. (2021). Landslide susceptibility mapping using statistical methods in Uatzau catchment area, northwestern Ethiopia. *Geoenvironmental Disasters*, 8(1), 1. <https://doi.org/10.1186/s40677-020-00170-y>
80. Saha, A., & Saha, S. (2021). Application of statistical probabilistic methods in landslide susceptibility assessment in Kurseong and its surrounding area of Darjeeling Himalayan, India: RS-GIS approach. *Environment, Development and Sustainability*, 23(3), 4453–4483. <https://doi.org/10.1007/s10668-020-00783-1>
81. Lee, S., & Choi, J. (2004). Landslide susceptibility mapping using GIS and the weight-of-evidence model. *International Journal of Geographical Information Science*, 18(8), 789–814. <https://doi.org/10.1080/13658810410001702003>

82. Mathew, J., Jha, V. K., & Rawat, G. S. (2007). Weights of evidence modelling for landslide hazard zonation mapping in part of Bhagirathi valley, Uttarakhand. *Current Science*, 92(5), 628–638. <http://www.jstor.org/stable/24097851>
83. Kumar, R., & Anbalagan, R. (2019). Landslide susceptibility mapping of the Tehri reservoir rim area using the weights of evidence method. *Journal of Earth System Science*, 128(6), 153. <https://doi.org/10.1007/s12040-019-1159-9>
84. Getachew, N., & Meten, M. (2021). Weights of evidence modeling for landslide susceptibility mapping of Kabi-Gebro locality, Gundomeskel area, Central Ethiopia. *Geoenvironmental Disasters*, 8(1), 6. <https://doi.org/10.1186/s40677-021-00177-z>
85. Pradhan, B., Oh, H.-J., & Buchroithner, M. (2010). Weights-of-evidence model applied to landslide susceptibility mapping in a tropical hilly area. *Geomatics, Natural Hazards and Risk*, 1(3), 199–223. <https://doi.org/10.1080/19475705.2010.498151>
86. Fan, W., Wei, X., Cao, Y., & Zheng, B. (2017). Landslide susceptibility assessment using the certainty factor and analytic hierarchy process. *Journal of Mountain Science*, 14(5), 906–925. <https://doi.org/10.1007/s11629-016-4068-2>
87. Chen, Z., Liang, S., Ke, Y., Yang, Z., & Zhao, H. (2019). Landslide susceptibility assessment using evidential belief function, certainty factor and frequency ratio model at Baxie River basin, NW China. *Geocarto International*, 34(4), 348–367. <https://doi.org/10.1080/10106049.2017.1404143>
88. Wang, Q., Li, W., Chen, W., & Bai, H. (2015). GIS-based assessment of landslide susceptibility using certainty factor and index of entropy models for the Qianyang County of Baoji city, China. *Journal of Earth System Science*, 124(7), 1399–1415. <https://doi.org/10.1007/s12040-015-0624-3>
89. Devkota, K. C., Regmi, A. D., Pourghasemi, H. R., Yoshida, K., Pradhan, B., Ryu, I. C., Dhital, M. R., & Althuwaynee, O. F. (2013). Landslide susceptibility mapping using certainty factor, index of entropy and logistic regression models in GIS and their

comparison at Mugling–Narayanghat road section in Nepal Himalaya. *Natural Hazards*, 65(1), 135–165. <https://doi.org/10.1007/s11069-012-0347-6>

90. Myronidis, D., Papageorgiou, C., & Theophanous, S. (2016). Landslide susceptibility mapping based on landslide history and analytic hierarchy process (AHP). *Natural Hazards*, 81(1), 245–263. <https://doi.org/10.1007/s11069-015-2075-1>
91. Kumar, R., & Anbalagan, R. (2016). Landslide susceptibility mapping using analytical hierarchy process (AHP) in Tehri reservoir rim region, Uttarakhand. *Journal of the Geological Society of India*, 87(3), 271–286. <https://doi.org/10.1007/s12594-016-0395-8>
92. Achour, Y., Boumezbeur, A., Hadji, R., Chouabbi, A., Cavaleiro, V., & Bendaoud, E. A. (2017). Landslide susceptibility mapping using analytic hierarchy process and information value methods along a highway road section in Constantine, Algeria. *Arabian Journal of Geosciences*, 10(8), 194. <https://doi.org/10.1007/s12517-017-2980-6>
93. Panchal, S., & Shrivastava, A. K. (2020). Application of analytic hierarchy process in landslide susceptibility mapping at regional scale in GIS environment. *Journal of Statistics and Management Systems*, 23(2), 199–206. <https://doi.org/10.1080/09720510.2020.1724620>
94. Sonker, I., Tripathi, J. N., & Singh, A. K. (2021). Landslide susceptibility zonation using geospatial technique and analytical hierarchy process in Sikkim Himalaya. *Quaternary Science Advances*, 4, 100039. <https://doi.org/10.1016/j.qsa.2021.100039>
95. Senouci, R., Taibi, N.-E., Teodoro, A. C., Duarte, L., Mansour, H., & Yahia Meddah, R. (2021). GIS-Based Expert Knowledge for Landslide Susceptibility Mapping (LSM): Case of Mostaganem Coast District, West of Algeria. *Sustainability*, 13(2), 630. <https://doi.org/10.3390/su13020630>
96. Saaty, T.L. (1980). *The Analytic Hierarchy Process*. McGraw-Hill, New York.

97. Saaty, R. W. (1987). The analytic hierarchy process—what it is and how it is used. *Mathematical Modelling*, 9(3–5), 161–176. [https://doi.org/10.1016/0270-0255\(87\)90473-8](https://doi.org/10.1016/0270-0255(87)90473-8)
98. Ali, S., Biermanns, P., Haider, R., & Reicherter, K. (2019). Landslide susceptibility mapping by using a geographic information system (GIS) along the China–Pakistan Economic Corridor (Karakoram Highway), Pakistan. *Natural Hazards and Earth System Sciences*, 19(5), 999–1022. <https://doi.org/10.5194/nhess-19-999-2019>
99. Kayastha, P., Dhital, M. R., & de Smedt, F. (2013). Application of the analytical hierarchy process (AHP) for landslide susceptibility mapping: A case study from the Tinau watershed, west Nepal. *Computers & Geosciences*, 52, 398–408. <https://doi.org/10.1016/j.cageo.2012.11.003>
100. Mandal, B., & Mandal, S. (2018). Analytical hierarchy process (AHP) based landslide susceptibility mapping of Lish river basin of eastern Darjeeling Himalaya, India. *Advances in Space Research*, 62(11), 3114–3132. <https://doi.org/10.1016/j.asr.2018.08.008>
101. Devara, M., Tiwari, A., & Dwivedi, R. (2021). Landslide susceptibility mapping using MT-InSAR and AHP enabled GIS-based multi-criteria decision analysis. *Geomatics, Natural Hazards and Risk*, 12(1), 675–693. <https://doi.org/10.1080/19475705.2021.1887939>
102. Basu, T., & Pal, S. (2020). A GIS-based factor clustering and landslide susceptibility analysis using AHP for Gish River Basin, India. *Environment, Development and Sustainability*, 22(5), 4787–4819. <https://doi.org/10.1007/s10668-019-00406-4>
103. Wadadar, S., & Mukhopadhyay, B. P. (2022). GIS-based landslide susceptibility zonation and comparative analysis using analytical hierarchy process and conventional weighting-based multivariate statistical methods in the Lachung River Basin, North Sikkim. *Natural Hazards*. <https://doi.org/10.1007/s11069-022-05344-5>

104. Ilanloo, M. (2011). A comparative study of fuzzy logic approach for landslide susceptibility mapping using GIS: An experience of Karaj dam basin in Iran. *Procedia - Social and Behavioral Sciences*, 19, 668–676. <https://doi.org/10.1016/j.sbspro.2011.05.184>
105. Rostami, Z. A., Al-modaresi, S. A., Fathizad, H., & Faramarzi, M. (2016). Landslide susceptibility mapping by using fuzzy logic: a case study of Cham-gardalan catchment, Ilam, Iran. *Arabian Journal of Geosciences*, 9(17), 685. <https://doi.org/10.1007/s12517-016-2720-3>
106. Miles, S. B., & Keefer, D. K. (2009). Evaluation of CAMEL — comprehensive areal model of earthquake-induced landslides. *Engineering Geology*, 104(1–2), 1–15. <https://doi.org/10.1016/j.enggeo.2008.08.004>
107. Lee, S. (2007). Application and verification of fuzzy algebraic operators to landslide susceptibility mapping. *Environmental Geology*, 52(4). <https://doi.org/10.1007/s00254-006-0491-y>
108. Pradhan, B. (2010). Application of an advanced fuzzy logic model for landslide susceptibility analysis. *International Journal of Computational Intelligence Systems*, 3(3), 370. <https://doi.org/10.2991/ijcis.2010.3.3.12>
109. Kayastha, P., Bijukchhen, S. M., Dhital, M. R., & de Smedt, F. (2013). GIS based landslide susceptibility mapping using a fuzzy logic approach: A case study from Ghurmi-Dhad Khola area, Eastern Nepal. *Journal of the Geological Society of India*, 82(3), 249–261. <https://doi.org/10.1007/s12594-013-0147-y>
110. Zeng-wang, X. (2001). GIS and ANN model for landslide susceptibility mapping. *Journal of Geographical Sciences*, 11(3), 374–381. <https://doi.org/10.1007/BF02892323>
111. Lee, S. (2007). Landslide susceptibility mapping using an artificial neural network in the Gangneung area, Korea. *International Journal of Remote Sensing*, 28(21), 4763–4783. <https://doi.org/10.1080/01431160701264227>

112. Valencia Ortiz, J. A., & Martínez-Graña, A. M. (2018). A neural network model applied to landslide susceptibility analysis (Capitanejo, Colombia). *Geomatics, Natural Hazards and Risk*, 9(1), 1106–1128. <https://doi.org/10.1080/19475705.2018.1513083>
113. Li, B., Wang, N., & Chen, J. (2021). GIS-Based Landslide Susceptibility Mapping Using Information, Frequency Ratio, and Artificial Neural Network Methods in Qinghai Province, Northwestern China. *Advances in Civil Engineering*, 2021, 1–14. <https://doi.org/10.1155/2021/4758062>
114. Mehrabi, M., & Moayedi, H. (2021). Landslide susceptibility mapping using artificial neural network tuned by metaheuristic algorithms. *Environmental Earth Sciences*, 80(24), 804. <https://doi.org/10.1007/s12665-021-10098-7>
115. Wang, Q., Li, W., Xing, M., Wu, Y., Pei, Y., Yang, D., & Bai, H. (2016). Landslide susceptibility mapping at Gongliu county, China using artificial neural network and weight of evidence models. *Geosciences Journal*, 20(5), 705–718. <https://doi.org/10.1007/s12303-016-0003-3>
116. Mandal, S., Mondal, S. (2019). Artificial Neural Network (ANN) Model and Landslide Susceptibility. In: Statistical Approaches for Landslide Susceptibility Assessment and Prediction. Springer, Cham. https://doi.org/10.1007/978-3-319-93897-4_5
117. Pascale, S., Parisi, S., Mancini, A., Schiattarella, M., Conforti, M., Sole, A., Murgante, B., & Sdao, F. (2013). *Landslide Susceptibility Mapping Using Artificial Neural Network in the Urban Area of Senise and San Costantino Albanese (Basilicata, Southern Italy)* (pp. 473–488). https://doi.org/10.1007/978-3-642-39649-6_34
118. Shirzadi, A., Chapi, K., Shahabi, H., Solaimani, K., Kavian, A., & Ahmad, B. bin. (2017). Rock fall susceptibility assessment along a mountainous road: an evaluation of bivariate statistic, analytical hierarchy process and frequency ratio. *Environmental Earth Sciences*, 76(4), 152. <https://doi.org/10.1007/s12665-017-6471-6>

119. Yalcin, A. (2008). GIS-based landslide susceptibility mapping using analytical hierarchy process and bivariate statistics in Ardesen (Turkey): Comparisons of results and confirmations. *CATENA*, 72(1), 1–12. <https://doi.org/10.1016/j.catena.2007.01.003>
120. Mansouri Daneshvar, M. R. (2014). Landslide susceptibility zonation using analytical hierarchy process and GIS for the Bojnurd region, northeast of Iran. *Landslides*, 11(6), 1079–1091. <https://doi.org/10.1007/s10346-013-0458-5>
121. Semlali, I., Ouadif, L., & Bahi, L. (2019). Landslide Susceptibility Mapping using the Analytical Hierarchy Process and GIS. *Current Science*, 116(5), 773. <https://doi.org/10.18520/cs/v116/i5/773-779>
122. Abedini, M., & Tulabi, S. (2018). Assessing LNRF, FR, and AHP models in landslide susceptibility mapping index: a comparative study of Nojian watershed in Lorestan province, Iran. *Environmental Earth Sciences*, 77(11), 405. <https://doi.org/10.1007/s12665-018-7524-1>
123. Devkota, K. C., Regmi, A. D., Pourghasemi, H. R., Yoshida, K., Pradhan, B., Ryu, I. C., Dhital, M. R., & Althuwaynee, O. F. (2013). Landslide susceptibility mapping using certainty factor, index of entropy and logistic regression models in GIS and their comparison at Mugling–Narayanghat road section in Nepal Himalaya. *Natural Hazards*, 65(1), 135–165. <https://doi.org/10.1007/s11069-012-0347-6>
124. Wang, Q., Guo, Y., Li, W., He, J., & Wu, Z. (2019). Predictive modeling of landslide hazards in Wen County, northwestern China based on information value, weights-of-evidence, and certainty factor. *Geomatics, Natural Hazards and Risk*, 10(1), 820–835. <https://doi.org/10.1080/19475705.2018.1549111>
125. Bhukosh portal, A platform for the geoscientific data from Geological Survey of India, <https://bhukosh.gsi.gov.in/Bhukosh/MapView.aspx>
126. District Disaster Management Plan 2017, submitted to District Disaster Management Authority, Shimla accessed available on

<https://cdn.s3waas.gov.in/s3b534ba68236ba543ae44b22bd110a1d6/uploads/2018/07/2018071721.pdf>

127. Emerging Himachal. *District Survey Document Shimla*, retrieved May 03, 2021, from https://emerginghimachal.hp.gov.in/miningstone_survey_docs/shimla.pdf
128. Muralikrishnan, S., Pillai, A., Narender, B., Reddy, S., Venkataraman, V. R., & Dadhwal, V. K. (2013). Validation of Indian National DEM from Cartosat-1 Data. *Journal of the Indian Society of Remote Sensing*, 41(1), 1–13. <https://doi.org/10.1007/s12524-012-0212-9>
129. Long, N., & de Smedt, F. (2018). Analysis and Mapping of Rainfall-Induced Landslide Susceptibility in A Luoi District, Thua Thien Hue Province, Vietnam. *Water*, 11(1), 51. <https://doi.org/10.3390/w11010051>
130. Sharma, L. P., Patel, N., Ghose, M. K., & Debnath, P. (2015). Development and application of Shannon's entropy integrated information value model for landslide susceptibility assessment and zonation in Sikkim Himalayas in India. *Natural Hazards*, 75(2). <https://doi.org/10.1007/s11069-014-1378-y>
131. Roodposhti, M. S., Aryal, J., Shahabi, H., & Safarrad, T. (2016). Fuzzy Shannon entropy: A hybrid GIS-based landslide susceptibility mapping method. *Entropy*, 18(10). <https://doi.org/10.3390/e18100343>
132. Panchal, S., & Shrivastava, A. K. (2021). A Comparative Study of Frequency Ratio, Shannon's Entropy and Analytic Hierarchy Process (AHP) Models for Landslide Susceptibility Assessment. *ISPRS International Journal of Geo-Information*, 10(9). <https://doi.org/10.3390/ijgi10090603>

Publications

1. Panchal, S., & Shrivastava, A. K. (2020). Application of analytic hierarchy process in landslide susceptibility mapping at regional scale in GIS environment. *Journal of Statistics and Management Systems*, 23(2), Taylor and Francis, 199–206. <https://doi.org/10.1080/09720510.2020.1724620> (Indexed in Emerging SCI)
2. Panchal, S., & Shrivastava, A. Kr. (2022). Landslide hazard assessment using analytic hierarchy process (AHP): A case study of National Highway 5 in India. *Ain Shams Engineering Journal*, 13(3), 101626. <https://doi.org/10.1016/j.asej.2021.10.021> (Impact factor: 3.18) [Indexed in SCI Expanded, SCOPUS]
3. Panchal, S., & Shrivastava, A. K. (2021). A Comparative Study of Frequency Ratio, Shannon's Entropy and Analytic Hierarchy Process (AHP) Models for Landslide Susceptibility Assessment. *ISPRS International Journal of Geo-Information*, 10(9). <https://doi.org/10.3390/ijgi10090603> (Impact factor: 2.8) [Indexed in SCI Expanded, SCOPUS]
4. Panchal, S., & Srivastava, A. Kr. (2022). Expert based landslide susceptibility mapping for energy infrastructure planning. *Journal of Information and Optimization Sciences*, 43(3), 635–641. <https://doi.org/10.1080/02522667.2022.2054999>
5. Panchal, S., & Shrivastava, A. Kr. (2020). Landslide Susceptibility Mapping Along Highway Corridors in GIS Environment (pp. 79–89), *Lecture Notes in Civil Engineering*, https://doi.org/10.1007/978-981-15-2545-2_8 (Indexed in SCOPUS)

Conferences

1. Panchal S., Shrivastava A.K. (2021) Landslide Susceptibility Assessment using Expert Weightage, poster presented online at ICEER 2021 - The 8th International Conference on Energy and Environment Research jointly organized by School of Engineering (ISEP) of the Polytechnic of Porto (P.Porto), the Dipartimento di Ingegneria of the Università degli studi "Roma Tre", and the SCIEI on September 13-17, 2021

2. Panchal S., Shrivastava A.K. (2020) Landslide Susceptibility Assessment using Geospatial Tools, accepted for oral presentation at 36th International Geological Congress with full fee waiver (Postponed due to COVID 19 outbreak)
3. Panchal S., Shrivastava A.K. (2020) Machine Learning Applications in Geotechnical Engineering: A Review, orally presented online at International Conference on Multidisciplinary Technologies & Challenges in Industry 4.0, jointly organized by East Point College of Engineering and Technology, Bangalore in Collaboration with University of Sannio, Benevento, Italy on 18th -19th September, 2020
4. Panchal, S., & Shrivastava, A. K. (2019). Application of analytic hierarchy process in landslide susceptibility mapping at regional scale in GIS environment. *International Conference on Sustainable Computing in Science, Technology and Management*, Amity University, February 26-28, 2019

Appendix A

Table A1. Sample Landslide Inventory Data of 500 Landslides

S.No.	LU/LC	Geometry	TOPOSHEET	Material	Type of Landslide	Longitude	Latitude
1	Barren	Lowly dissected hill	53F06	Rock	Slide	77.4038	30.6026
2	Extensive cut slope	Lowly dissected hill	53F06	Rock	Slide	77.4778	30.6282
3	Barren	Lowly dissected hill	53F10	Rock		77.5153	30.6356
4	Sparse vegetation	Lowly dissected hill	53E06	Debris	Slide	77.3178	31.7157
5	Moderate vegetation	Lowly dissected hill	53E06	Debris	Slide	77.3184	31.7158
6	Barren	Lowly dissected hill	53E06	Debris	Slide	77.3142	31.7188
7	Barren	Lowly dissected hill	53E06	Debris	Slide	77.4917	31.6872
8	Barren	Lowly dissected hill	53E06	Debris	Slide	77.4837	31.6829
9	Barren	Lowly dissected hill	53E06	Debris	Slide	77.4788	31.6767
10	Sparse vegetation	Lowly dissected hill	53F06	Rock	Slide	77.2965	30.5839
11	Thick vegetation	Lowly dissected hill	53F06	Rock	Slide	77.4628	30.6239
12	Thick vegetation	Lowly dissected hill	53F06	Rock	Slide	77.4608	30.6238
13	Sparse vegetation	Lowly dissected hill	53F06	Rock	Slide	77.4576	30.6221

14	Barren	Lowly dissected hill	53F06	Rock	Slide	77.4582	30.6220
15	Barren	Talus cone	53F06	Rock	Slide	77.4359	30.6419
16	Barren	Lowly dissected hill	53F06	Rock	Slide	77.4415	30.6485
17	Barren	Lowly dissected hill	53F06	Rock	Slide	77.4279	30.6656
18	Barren	Lowly dissected hill	53F09	Debris	Slide	77.5994	30.7584
19	Barren	Lowly dissected hill	53F09	Debris	Slide	77.6034	30.7613
20	Barren	Lowly dissected hill	53F09	Debris	Slide	77.6098	30.7601
21	Barren	Lowly dissected hill	53F09	Debris	Slide	77.6328	30.7570
22	Barren	Lowly dissected hill	53F09	Debris	Slide	77.6371	30.7734
23	Sparse vegetation	Moderately dissected hill	53F09	Debris	Slide	77.4094	30.8464
24	Sparse vegetation	Lowly dissected hill	53F09	Debris	Slide	77.3214	30.9678
25	Moderate vegetation	Lowly dissected hill	53F09	Debris	Slide	77.3332	30.9875
26	Barren	Moderately dissected hill	53F10	Rock	Slide	77.6227	30.5577
27	Sparse vegetation	Lowly dissected hill	53F10	Rock	Slide	77.6231	30.5569
28	Barren	Moderately dissected hill	53F10	Rock	Slide	77.6231	30.5561
29	Barren	Moderately dissected hill	53F05	Debris	Slide	77.2957	30.7784
30	Barren	Moderately dissected hill	53F05	Debris	Slide	77.3074	30.7554

31	Barren	Moderately dissected hill	53F05	Debris	Fall	77.4430	30.7555
32	Moderate vegetation	Moderately dissected hill	53F05	Debris	Slide	77.2957	30.7773
33	Moderate vegetation	Moderately dissected hill	53F05	Debris	Slide	77.2900	30.8489
34	Cultivated land	Lowly dissected hill	53F05	Rock	Fall	77.4413	30.7548
35	Barren	Escarpment	53F05	Rock	Fall	77.4394	30.7573
36	Barren	Moderately dissected hill	53F05	Soil	Slide	77.3548	30.7903
37	Moderate vegetation	Highly dissected hill	53F05	Debris	Slide	77.2976	30.8478
38	Sparse vegetation	Escarpment	53F05	Debris	Slide	77.3451	30.8131
39	Moderate vegetation	Escarpment	53E06	Debris	Slide	77.4789	31.6763
40	Moderate vegetation	Escarpment	53E06	Debris	Slide	77.3857	31.6541
41	Barren	Highly dissected hill	53E06	Debris	Slide	77.3259	31.6977
42	Barren	Highly dissected hill	53E06	Debris	Slide	77.3264	31.6974
43	Barren	Highly dissected hill	53E06	Debris	Slide	77.3265	31.6973
44	Barren	Highly dissected hill	53E06	Debris	Slide	77.3265	31.6975
45	Barren	Moderately dissected hill	53E06	Debris	Slide	77.3254	31.6968
46	Barren	Moderately dissected hill	53E10	Debris	Slide	77.6564	31.5803
47	Barren	Highly dissected hill	53E10	Debris	Slide	77.6590	31.5004

48	Barren	Moderately dissected hill	53E15	Debris	Slide	77.8692	31.3264
49	Barren	Escarpment	53E15	Debris	Slide	77.9842	31.3412
50	Barren	Lowly dissected hill	53E14	Debris	Slide	77.9517	31.7188
51	Barren	Lowly dissected hill	53E14	Rock	Fall	77.9311	31.6406
52	Barren	Lowly dissected hill	53E15	Debris	Slide	77.8001	31.4581
53	Sparse vegetation	Lowly dissected hill	53E14	Debris	Slide	77.9600	31.6347
54	Sparse vegetation	Lowly dissected hill	53E14	Debris	Slide	77.9115	31.5182
55	Sparse vegetation	Escarpment	53E15	Rock	Fall	77.9156	31.4088
56	Barren	Moderately dissected hill	53E15	Rock	Fall	77.9119	31.4165
57	Barren	Lowly dissected hill	53E15	Debris	Slide	77.9080	31.4054
58	Barren	Moderately dissected hill	53E15	Debris	Slide	77.8877	31.3312
59	Barren	Lowly dissected hill	53E15	Debris	Slide	77.8959	31.3303
60	Barren	Lowly dissected hill	53E15	Debris	Slide	77.9145	31.3348
61	Barren	Lowly dissected hill	53E15	Debris	Flow	77.7946	31.3675
62	Barren	Moderately dissected hill	53E15	Rock	Fall	77.7740	31.3696
63	Barren	Lowly dissected hill	53E15	Rock	Slide	77.7644	31.4001
64	Barren	Escarpment	53E15	Rock	Slide	77.7536	31.4052
65	Barren	Escarpment	53F10	Rock	Slide	77.6221	30.5576
66	Barren	Escarpment	53F10	Rock	Slide	77.6212	30.5570

67	Barren	Escarpment	53F10	Rock	Slide	77.6246	30.5568
68	Sparse vegetation	Escarpment	53F10	Rock	Slide	77.6219	30.5560
69	Barren	Moderately dissected hill	53F10	Rock	Slide	77.6229	30.5551
70	Barren	Moderately dissected hill	53F10	Rock	Slide	77.6236	30.5542
71	Barren	Moderately dissected hill	53E06	Debris	Slide	77.3377	31.6726
72	Barren	Moderately dissected hill	53F05	Rock	Fall	77.2998	30.8514
73	Moderate vegetation	Moderately dissected hill	53F05	Debris	Slide	77.3018	30.8520
74	Barren	Lowly dissected hill	53F06	Rock	Slide	77.4779	30.5707
75	Barren	Lowly dissected hill	53F06	Rock	Slide	77.4939	30.5672
76	Extensive cut slope	Lowly dissected hill	53F10	Rock	Slide	77.6683	30.6900
77	Extensive cut slope	Lowly dissected hill	53F10	Rock	Slide	77.6687	30.6896
78	Extensive cut slope	Lowly dissected hill	53F10	Rock	Slide	77.6598	30.6971
79	Extensive cut slope	Lowly dissected hill	53F10	Rock	Slide	77.6551	30.7007
80	Sparse vegetation	Lowly dissected hill	53F10	Rock	Slide	77.6538	30.6986
81	Sparse vegetation	Lowly dissected hill	53F10	Rock		77.6357	30.6987
82	Extensive cut slope	Lowly dissected hill	53F06	Rock	Slide	77.2965	30.5804
83	Extensive cut slope	Lowly dissected hill	53F06	Rock	Slide	77.2955	30.5797

84	Extensive cut slope	Highly dissected hill	53F06	Rock	Slide	77.2969	30.5762
85	Cultivated land	Moderately dissected hill	53F06	Rock	Slide	77.2950	30.5742
86	Barren	Lowly dissected hill	53E10	Debris	Slide	77.6600	31.5013
87	Moderate vegetation	Lowly dissected hill	53E10	Debris	Slide	77.6508	31.5117
88	Thick vegetation	Moderately dissected hill	53E10	Debris	Slide	77.6956	31.5177
89	Extensive cut slope	Moderately dissected hill	53E10	Debris	Slide	77.6964	31.5177
90	Thick vegetation	Lowly dissected hill	53F05	Debris	Slide	77.3966	30.9424
91	Moderate vegetation	Lowly dissected hill	53F05	Debris	Slide	77.3040	30.8650
92	Extensive cut slope	Lowly dissected hill	53F05	Debris	Slide	77.3273	30.9614
93	Thick vegetation	Moderately dissected hill	53F05	Debris	Slide	77.3252	30.9639
94	Extensive cut slope	Lowly dissected hill	53F05	Debris	Slide	77.3277	30.9539
95	Extensive cut slope	Lowly dissected hill	53F05	Debris	Slide	77.4111	30.7655
96	Extensive cut slope	Lowly dissected hill	53E15	Rock	Slide	77.7554	31.4058
97	Extensive cut slope	Lowly dissected hill	53E16	Rock	Slide	77.7641	31.0901
98	Extensive cut slope	Lowly dissected hill	53E16	Debris	Slide	77.8257	31.0594
99	Extensive cut slope	Lowly dissected hill	53E16	Debris	Slide	77.8245	31.0569

100	Thick vegetation	Lowly dissected hill	53E06	Debris	Slide	77.2659	31.7193
101	Extensive cut slope	Lowly dissected hill	53E06	Debris	Slide	77.2661	31.7191
102	Extensive cut slope	Lowly dissected hill	53E06	Debris	Slide	77.2679	31.7183
103	Thick vegetation	Lowly dissected hill	53E06	Debris	Slide	77.2687	31.7181
104	Barren	Lowly dissected hill	53E06	Debris	Slide	77.2690	31.7178
105	Thick vegetation	Escarpment	53E06	Debris	Slide	77.2749	31.7187
106	Thick vegetation	Lowly dissected hill	53E06	Debris	Slide	77.2754	31.7189
107	Extensive cut slope	Lowly dissected hill	53E06	Debris	Slide	77.3278	31.6707
108	Thick vegetation	Moderately dissected hill	53E06	Debris	Slide	77.3155	31.6610
109	Sparse vegetation	Moderately dissected hill	53E06	Debris	Slide	77.3106	31.6675
110	Thick vegetation	Highly dissected hill	53E06	Debris	Slide	77.3102	31.6694
111	Thick vegetation	Moderately dissected hill	53E06	Debris	Slide	77.3067	31.6713
112	Moderate vegetation	Moderately dissected hill	53E06	Debris	Slide	77.3069	31.6712
113	Sparse vegetation	Lowly dissected hill	53F06	Rock	Slide	77.2952	30.5736
114	Moderate vegetation	Highly dissected hill	53F06	Rock	Slide	77.2945	30.5723
115	Sparse vegetation	Moderately dissected hill	53F06	Rock	Slide	77.4429	30.5786

116	Moderate vegetation	Lowly dissected hill	53F06	Rock	Slide	77.4431	30.5784
117	Sparse vegetation	Moderately dissected hill	53F06	Rock	Slide	77.4429	30.5780
118	Extensive cut slope	Moderately dissected hill	53F10	Rock	Not Available	77.5476	30.6008
119	Extensive cut slope	Moderately dissected hill	53F10	Rock	Not Available	77.5770	30.5938
120	Extensive cut slope	Lowly dissected hill	53F10	Rock	Slide	77.5766	30.5945
121	Cultivated land	Moderately dissected hill	53F10	Rock	Fall	77.5907	30.5988
122	Extensive cut slope	Lowly dissected hill	53F10	Rock	Slide	77.7306	30.5875
123	Moderate vegetation	Lowly dissected hill	53F05	Debris	Slide	77.3236	30.9715
124	Sparse vegetation	Moderately dissected hill	53F05	Debris	Slide	77.4434	30.9546
125	Sparse vegetation	Moderately dissected hill	53F05	Debris	Slide	77.3540	30.9354
126	Cultivated land	Moderately dissected hill	53F05	Debris	Slide	77.3236	30.9612
127	Moderate vegetation	Moderately dissected hill	53F05	Debris	Slide	77.3372	30.9275
128	Thick vegetation	Lowly dissected hill	53F05	Debris	Slide	77.3273	30.9539
129	Moderate vegetation	Lowly dissected hill	53F05	Rock	Slide	77.3242	30.9643
130	Thick vegetation	Lowly dissected hill	53F05	Rock	Slide	77.3234	30.9626
131	Moderate vegetation	Moderately dissected hill	53F05	Debris	Slide	77.3138	30.9726

132	Extensive cut slope	Highly dissected hill	53F05	Debris	Slide	77.3171	30.9750
133	Extensive cut slope	Highly dissected hill	53E06	Debris	Slide	77.2759	31.7192
134	Extensive cut slope	Highly dissected hill	53E06	Debris	Slide	77.2767	31.7193
135	Extensive cut slope	Highly dissected hill	53E06	Debris	Slide	77.2777	31.7203
136	Barren	Highly dissected hill	53F09	Debris	Slide	77.6034	30.7613
137	Barren	Moderately dissected hill	53F09	Debris	Slide	77.6098	30.7601
138	Barren	Lowly dissected hill	53F09	Debris	Slide	77.6850	30.9831
139	Extensive cut slope	Lowly dissected hill	53F09	Debris	Slide	77.6846	30.9820
140	Barren	Lowly dissected hill	53F09	Debris	Slide	77.6833	30.9820
141	Barren	Lowly dissected hill	53F09	Debris	Slide	77.6757	30.9104
142	Barren	Lowly dissected hill	53F09	Debris	Slide	77.5973	30.9339
143	Barren	Denudational hill slope	53E10	Debris	Slide	77.7021	31.5530
144	Sparse vegetation	Transportational mid slope	53E10	Debris	Slide	77.7021	31.5524
145	Cultivated land	Lowly dissected hill	53E14	Debris	Slide	77.7524	31.5526
146	Moderate vegetation	Moderately dissected hill	53E14	Debris	Slide	77.7521	31.5528
147	Extensive cut slope	Highly dissected hill	53E14	Debris	Slide	77.7706	31.5432
148	Barren	Moderately dissected hill	53E14	Debris	Slide	77.7552	31.6364

149	Barren	Highly dissected hill	53E14	Debris	Slide	77.7552	31.6362
150	Barren	Highly dissected hill	53E14	Debris	Slide	77.7617	31.6272
151	Barren	Lowly dissected hill	53F10	Rock	Slide	77.6516	30.7021
152	Barren	Highly dissected hill	53F10	Rock		77.5940	30.6024
153	Barren	Escarpment	53E06	Debris	Slide	77.2775	31.7032
154	Barren	Lowly dissected hill	53E06	Debris	Slide	77.2776	31.7032
155	Thick vegetation	Lowly dissected hill	53E06	Debris	Slide	77.2788	31.7033
156	Barren	Escarpment	53E06	Debris	Slide	77.2781	31.7015
157	Barren	Lowly dissected hill	53E06	Debris	Slide	77.3249	31.7046
158	Extensive cut slope	Lowly dissected hill	53E06	Debris	Slide	77.3241	31.7043
159	Moderate vegetation	Lowly dissected hill	53E06	Debris	Slide	77.3257	31.7043
160	Sparse vegetation	Lowly dissected hill	53F05	Debris	Slide	77.3041	30.9529
161	Sparse vegetation	Lowly dissected hill	53F05	Debris	Slide	77.2983	30.7797
162	Barren	Lowly dissected hill	53F05	Debris	Slide	77.3147	30.7560
163	Barren	Lowly dissected hill	53F05	Debris	Slide	77.3406	30.7741
164	Sparse vegetation	Lowly dissected hill	53F05	Debris	Slide	77.2802	30.8811
165	Thick vegetation	Lowly dissected hill	53F05	Debris	Slide	77.2658	30.8908
166	Extensive cut slope	Lowly dissected hill	53E06	Debris	Slide	77.3857	31.6538

167	Extensive cut slope	Lowly dissected hill	53E06	Debris	Slide	77.3919	31.6421
168	Extensive cut slope	Lowly dissected hill	53F09	Debris	Slide	77.5957	30.9339
169	Extensive cut slope	Lowly dissected hill	53F09	Debris	Slide	77.5424	30.9461
170	Plantation	Lowly dissected hill	53F09	Debris	Slide	77.5436	30.9600
171	Extensive cut slope	Lowly dissected hill	53F09	Debris	Slide	77.5399	30.9472
172	Extensive cut slope	Lowly dissected hill	53F09	Debris	Slide	77.5417	30.9466
173	Barren	Escarpment	53F09	Debris	Slide	77.5419	30.9458
174	Plantation	Moderately dissected hill	53F06	Rock	Fall	77.4785	30.6909
175	Moderate vegetation	Escarpment	53F06	Rock	Fall	77.4805	30.6907
176	Extensive cut slope	Escarpment	53F06	Rock	Slide	77.4711	30.6837
177	Extensive cut slope	Lowly dissected hill	53F10	Rock	Slide	77.6346	30.5717
178	Barren	Escarpment	53F10	Rock	Slide	77.6826	30.6117
179	Extensive cut slope	Escarpment	53F10	Rock	Slide	77.6831	30.5969
180	Sparse vegetation	Lowly dissected hill	53F10	Rock	Slide	77.6093	30.5545
181	Extensive cut slope	Moderately dissected hill	53F10	Rock	Slide	77.6075	30.5542
182	Cultivated land	Escarpment	53F06	Rock	Slide	77.4342	30.6018
183	Extensive cut slope	Lowly dissected hill	53F06	Rock	Slide	77.4579	30.5953
184	Extensive cut slope	Escarpment	53F10	Rock		77.5152	30.5990

185	Plantation	Lowly dissected hill	53E06	Debris	Slide	77.2849	31.7082
186	Extensive cut slope	Escarpment	53E06	Debris	Slide	77.3193	31.7021
187	Extensive cut slope	Escarpment	53E06	Debris	Slide	77.2871	31.7061
188	Extensive cut slope	Escarpment	53E14	Debris	Slide	77.8390	31.5671
189	Moderate vegetation	Lowly dissected hill	53E14	Debris	Slide	77.8388	31.5675
190	Barren	Escarpment	53F13	Rock	Slide	77.7571	30.8306
191	Extensive cut slope	Escarpment	53F13	Debris	Slide	77.7552	30.8340
192	Extensive cut slope	Escarpment	53F13	Rock	Slide	77.7567	30.8316
193	Thick vegetation	Colluvial foot slope	53F05	Debris	Slide	77.3749	30.8752
194	Extensive cut slope	Lowly dissected hill	53F05	Debris	Slide	77.3399	30.9287
195	Extensive cut slope	Escarpment	53F05	Debris	Slide	77.3312	30.8947
196	Moderate vegetation	Lowly dissected hill	53F05	Debris	Slide	77.4596	30.8088
197	Barren	Moderately dissected hill	53F05	Debris	Slide	77.4226	30.8154
198	Moderate vegetation	Moderately dissected hill	53E06	Debris	Slide	77.3767	31.6801
199	Extensive cut slope	Moderately dissected hill	53E06	Debris	Slide	77.3784	31.6806
200	Extensive cut slope	Moderately dissected hill	53E06	Debris	Slide	77.3503	31.7056
201	Sparse vegetation	Moderately dissected hill	53E06	Debris	Slide	77.3501	31.7059

202	Moderate vegetation	Moderately dissected hill	53E06	Debris	Slide	77.3499	31.7062
203	Cultivated land	Moderately dissected hill	53E06	Debris	Slide	77.3488	31.7070
204	Moderate vegetation	Moderately dissected hill	53E06	Debris	Slide	77.3489	31.7089
205	Extensive cut slope	Colluvial foot slope	53E10	Debris	Slide	77.7366	31.6144
206	Extensive cut slope	Colluvial foot slope	53E10	Debris	Slide	77.7350	31.6152
207	Cultivated land	Lowly dissected hill	53F05	Rock	Slide	77.3234	30.9626
208	Barren	Lowly dissected hill	53F05	Debris	Slide	77.3138	30.9726
209	Barren	Lowly dissected hill	53F05	Debris	Slide	77.2618	30.8928
210	Extensive cut slope	Escarpment	53F05	Debris	Slide	77.3175	30.7573
211	Extensive cut slope	Escarpment	53F05	Debris	Slide	77.2735	30.8753
212	Extensive cut slope	Lowly dissected hill	53F05	Debris	Slide	77.2701	30.8760
213	Thick vegetation	Lowly dissected hill	53F05	Debris	Slide	77.2676	30.8763
214	Thick vegetation	Moderately dissected hill	53F05	Debris	Slide	77.2664	30.8767
215	Extensive cut slope	Lowly dissected hill	53F09	Debris	Slide	77.5709	30.9462
216	Sparse vegetation	Colluvial foot slope	53F09	Debris	Slide	77.5823	30.9470
217	Moderate vegetation	Highly dissected hill	53F09	Debris	Slide	77.5882	30.9633

218	Thick vegetation	Lowly dissected hill	53E06	Debris	Slide	77.2843	31.7085
219	Cultivated land	Lowly dissected hill	53E06	Debris	Slide	77.2816	31.7099
220	Thick vegetation	Highly dissected hill	53E06	Debris	Slide	77.3098	31.6973
221	Cultivated land	Lowly dissected hill	53E06	Debris	Slide	77.3072	31.6979
222	Sparse vegetation	Lowly dissected hill	53E06	Debris	Slide	77.3124	31.6943
223	Moderate vegetation	Moderately dissected hill	53E06	Debris	Slide	77.3136	31.6686
224	Extensive cut slope	Highly dissected hill	53E14	Debris	Slide	77.7672	31.5424
225	Thick vegetation	Moderately dissected hill	53E10	Debris	Slide	77.7446	31.5345
226	Moderate vegetation	Highly dissected hill	53F05	Debris	Slide	77.2615	30.8020
227	Sparse vegetation	Moderately dissected hill	53F10	Rock		77.5135	30.5943
228	Sparse vegetation	Moderately dissected hill	53F06	Rock	Slide	77.4810	30.6083
229	Moderate vegetation	Moderately dissected hill	53F07	Debris	Slide	77.3780	30.4539
230	Thick vegetation	Highly dissected hill	53F07	Debris	Slide	77.3746	30.4546
231	Barren	Moderately dissected hill	53F07	Debris	Slide	77.3741	30.4543
232	Barren	Moderately dissected hill	53F07	Debris	Slide	77.3797	30.4487
233	Barren	Lowly dissected hill	53E15	Debris	Slide	77.8495	31.4997

234	Extensive cut slope	Moderately dissected hill	53E15	Debris	Slide	77.8408	31.4985
235	Extensive cut slope	Moderately dissected hill	53E15	Debris	Slide	77.8629	31.4919
236	Extensive cut slope	Lowly dissected hill	53E15	Rock	Fall	77.8681	31.4894
237	Extensive cut slope	Lowly dissected hill	53E15	Rock	Fall	77.8677	31.4921
238	Extensive cut slope	Escarpment	53E15	Rock	Fall	77.8678	31.4921
239	Extensive cut slope	Moderately dissected hill	53E15	Debris	Slide	77.8726	31.4973
240	Sparse vegetation	Lowly dissected hill	53E15	Debris	Slide	77.8717	31.4974
241	Barren	Escarpment	53E15	Debris	Slide	77.8772	31.4887
242	Extensive cut slope	Escarpment	53E15	Debris	Slide	77.8837	31.4669
243	Barren	Moderately dissected hill	53E15	Debris	Slide	77.8843	31.4679
244	Extensive cut slope	Lowly dissected hill	53E15	Debris	Slide	77.8801	31.4582
245	Sparse vegetation	Lowly dissected hill	53E15	Debris	Slide	77.8635	31.4633
246	Barren	Lowly dissected hill	53E15	Debris	Slide	77.8821	31.4524
247	Barren	Lowly dissected hill	53E15	Debris	Slide	77.8741	31.4555
248	Barren	Lowly dissected hill	53E15	Rock	Fall	77.9189	31.4153
249	Extensive cut slope	Lowly dissected hill	53E15	Rock	Fall	77.9049	31.3939
250	Extensive cut slope	Lowly dissected hill	53F09	Debris	Slide	77.5725	30.9687

251	Extensive cut slope	Lowly dissected hill	53F09	Debris	Slide	77.5967	30.9640
252	Barren	Lowly dissected hill	53F09	Debris	Slide	77.5920	30.9652
253	Barren	Lowly dissected hill	53F09	Debris	Slide	77.5937	30.9653
254	Extensive cut slope	Moderately dissected hill	53F09	Debris	Slide	77.5969	30.9637
255	Extensive cut slope	Moderately dissected hill	53E06	Debris	Slide	77.3455	31.7002
256	Extensive cut slope	Moderately dissected hill	53E06	Debris	Slide	77.3454	31.6998
257	Extensive cut slope	Lowly dissected hill	53E06	Debris	Slide	77.3454	31.6995
258	Thick vegetation	Moderately dissected hill	53E06	Debris	Slide	77.3453	31.6990
259	Sparse vegetation	Lowly dissected hill	53F01	Rock	Slide	77.2097	30.8745
260	Barren	Lowly dissected hill	53F01	Rock	Slide	77.2109	30.8751
261	Barren	Moderately dissected hill	53B13	Rock	Slide	77.2123	30.8782
262	Barren	Moderately dissected hill	53B13	Rock	Slide	77.2108	30.8799
263	Extensive cut slope	Moderately dissected hill	53B13	Rock	Slide	77.2093	30.8813
264	Extensive cut slope	Moderately dissected hill	53F10	Rock	Slide	77.6629	30.7148
265	Extensive cut slope	Lowly dissected hill	53F10	Rock	Slide	77.6723	30.7122
266	Extensive cut slope	Lowly dissected hill	53F10	Rock	Slide	77.6725	30.7137

267	Extensive cut slope	Moderately dissected hill	53F10	Rock	Slide	77.6683	30.7152
268	Extensive cut slope	Moderately dissected hill	53F10	Rock	Slide	77.6649	30.7126
269	Barren	Escarpment	53F10	Rock	Slide	77.6644	30.7051
270	Sparse vegetation	Highly dissected hill	53F06	Rock	Fall	77.2751	30.7443
271	Extensive cut slope	Highly dissected hill	53F06	Rock	Slide	77.2506	30.7233
272	Extensive cut slope	Highly dissected hill	53F10	Rock	Slide	77.6796	30.6654
273	Extensive cut slope	Moderately dissected hill	53F10	Rock	Slide	77.6923	30.6728
274	Extensive cut slope	Moderately dissected hill	53F10	Rock	Slide	77.7032	30.6802
275	Thick vegetation	Lowly dissected hill	53F10	Rock	Slide	77.7037	30.6802
276	Plantation	Lowly dissected hill	53F01	Rock	Fall	77.2470	30.8374
277	Thick vegetation	Lowly dissected hill	53F01	Rock	Fall	77.2323	30.8491
278	Sparse vegetation	Lowly dissected hill	53F01	Rock	Fall	77.1586	30.8452
279	Thick vegetation	Lowly dissected hill	53F01	Rock	Fall	77.1589	30.8448
280	Barren	Escarpment	53B13	Rock	Fall	77.2173	30.4774
281	Barren	Lowly dissected hill	53B13	Debris	Slide	77.2496	30.4968
282	Thick vegetation	Lowly dissected hill	53B13	Debris	Slide	77.2480	30.4966
283	Moderate vegetation	Highly dissected hill	53B13	Debris	Slide	77.2476	30.4965

284	Extensive cut slope	Highly dissected hill	53F02	Rock	Slide	77.2394	30.5823
285	Extensive cut slope	Highly dissected hill	53F02	Rock	Slide	77.2397	30.5817
286	Extensive cut slope	Moderately dissected hill	53F02	Rock	Fall	77.0514	30.9135
287	Extensive cut slope	Moderately dissected hill	53F02	Rock	Fall	77.0507	30.9138
288	Extensive cut slope	Moderately dissected hill	53F07	Rock		77.2921	30.4591
289	Barren	Escarpment	53F07	Rock	Slide	77.2920	30.4622
290	Barren	Escarpment	53F10	Debris	Slide	77.6980	30.6066
291	Extensive cut slope	Escarpment	53F06	Rock	Slide	77.3736	30.6082
292	Extensive cut slope	Escarpment	53F06	Rock	Slide	77.3749	30.6109
293	Extensive cut slope	Moderately dissected hill	53F06	Rock	Slide	77.3883	30.5956
294	Extensive cut slope	Moderately dissected hill	53F10	Debris	Subsidence	77.6928	30.6050
295	Extensive cut slope	Moderately dissected hill	53F10	Rock	Slide	77.6681	30.6927
296	Extensive cut slope	Lowly dissected hill	53F10	Rock	Slide	77.6611	30.7008
297	Extensive cut slope	Lowly dissected hill	53F10	Rock	Slide	77.6615	30.7009
298	Plantation	Lowly dissected hill	53F10	Rock	Slide	77.6603	30.7013
299	Extensive cut slope	Lowly dissected hill	53F10	Rock	Slide	77.6625	30.6978
300	Extensive cut slope	Lowly dissected hill	53F10	Rock	Slide	77.6659	30.6985

301	Extensive cut slope	Moderately dissected hill	53F10	Rock	Slide	77.6669	30.6974
302	Extensive cut slope	Lowly dissected hill	53F10	Rock	Slide	77.6685	30.6878
303	Extensive cut slope	Escarpment	53B13	Debris	Slide	77.2489	30.4887
304	Extensive cut slope	Escarpment	53F10	Rock	Slide	77.5022	30.5708
305	Extensive cut slope	Moderately dissected hill	53F10	Rock	Slide	77.5060	30.5735
306	Extensive cut slope	Lowly dissected hill	53F10	Rock	Slide	77.5193	30.5686
307	Extensive cut slope	Lowly dissected hill	53F10	Debris	Slide	77.5515	30.5581
308	Extensive cut slope	Lowly dissected hill	53F10	Rock	Slide	77.5530	30.5611
309	Extensive cut slope	Lowly dissected hill	53F10	Rock	Slide	77.5462	30.5609
310	Extensive cut slope	Lowly dissected hill	53F10	Rock	Slide	77.5448	30.5616
311	Moderate vegetation	Moderately dissected hill	53F10	Rock	Slide	77.5425	30.5607
312	Extensive cut slope	Lowly dissected hill	53F10	Debris	Slide	77.5320	30.5644
313	Barren	Lowly dissected hill	53F06	Rock	Slide	77.3935	30.6163
314	Extensive cut slope	Lowly dissected hill	53F06	Rock	Slide	77.3924	30.6165
315	Extensive cut slope	Moderately dissected hill	53F06	Rock	Fall	77.3637	30.6263
316	Plantation	Lowly dissected hill	53F10	Rock	Slide	77.5038	30.5969

317	Barren	Lowly dissected hill	53F10	Rock	Slide	77.5792	30.5793
318	Moderate vegetation	Lowly dissected hill	53F10	Debris	Slide	77.6691	30.5477
319	Extensive cut slope	Moderately dissected hill	53F10	Rock		77.6861	30.5486
320	Barren	Lowly dissected hill	53F10	Rock	Slide	77.6869	30.5499
321	Barren	Lowly dissected hill	53F14	Rock	Slide	77.7672	30.6546
322	Extensive cut slope	Lowly dissected hill	53F14	Rock	Slide	77.7660	30.6550
323	Barren	Lowly dissected hill	53F14	Rock	Slide	77.7678	30.6533
324	Extensive cut slope	Lowly dissected hill	53F01	Rock	Slide	77.2012	30.9083
325	Extensive cut slope	Lowly dissected hill	53F01	Rock	Slide	77.1983	30.9096
326	Extensive cut slope	Escarpment	53B13	Debris	Slide	77.2483	30.4890
327	Extensive cut slope	Escarpment	53F01	Debris	Slide	77.2373	30.4972
328	Extensive cut slope	Transportational mid slope	53B13	Debris	Slide	77.2418	30.4852
329	Barren	Lowly dissected hill	53B13	Debris	Slide	77.2486	30.4888
330	Extensive cut slope	Lowly dissected hill	53B13	Rock	Fall	77.0502	30.9142
331	Extensive cut slope	Lowly dissected hill	53B13	Rock	Fall	77.0495	30.9148
332	Extensive cut slope	Lowly dissected hill	53B13	Rock	Fall	77.0744	30.9234
333	Extensive cut slope	Colluvial foot slope	53B13	Rock	Fall	77.0831	30.8929

334	Extensive cut slope	Colluvial foot slope	53F01	Rock	Fall	77.1092	30.8934
335	Extensive cut slope	Moderately dissected hill	53F01	Rock	Fall	77.0197	30.7466
336	Extensive cut slope	Moderately dissected hill	53F01	Rock	Fall	77.0209	30.7456
337	Extensive cut slope	Moderately dissected hill	53F01	Rock	Fall	77.1898	30.9074
338	Barren	Escarpment	53F01	Rock	Fall	77.1955	30.8999
339	Barren	Moderately dissected hill	53F01	Rock	Fall	77.2123	30.9037
340	Barren	Escarpment	53F01	Rock	Fall	77.2141	30.9068
341	Sparse vegetation	Escarpment	53F06	Rock	Slide	77.4931	30.5645
342	Barren	Escarpment	53F06	Rock	Slide	77.4947	30.5744
343	Barren	Lowly dissected hill	53F06	Rock	Slide	77.4921	30.5747
344	Sparse vegetation	Escarpment	53F06	Rock	Slide	77.4951	30.5777
345	Barren	Colluvial foot slope	53F06	Rock	Slide	77.4890	30.5779
346	Barren	Lowly dissected hill	53F06	Rock	Slide	77.4889	30.5790
347	Barren	Escarpment	53F14	Rock	Slide	77.7669	30.6151
348	Barren	Denudational hill slope	53F14	Rock	Slide	77.7705	30.6178
349	Barren	Moderately dissected hill	53F06	Rock	Slide	77.4382	30.6063
350	Barren	Escarpment	53F06	Rock	Slide	77.4413	30.6152
351	Barren	Denudational hill slope	53F06	Rock	Fall	77.4418	30.6076
352	Barren	Denudational hill slope	53F06	Debris	Slide	77.4576	30.6084

353	Barren	Denudational hill slope	53F10	Rock	Slide	77.5326	30.5646
354	Barren	Denudational hill slope	53F10	Debris	Slide	77.6463	30.5533
355	Barren	Denudational hill slope	53F10	Rock	Slide	77.6856	30.5487
356	Barren	Denudational hill slope	53F10	Rock	Slide	77.6999	30.6084
357	Extensive cut slope	Escarpment	53F10	Rock	Slide	77.7004	30.6080
358	Extensive cut slope	Lowly dissected hill	53F06	Rock	Slide	77.3747	30.7007
359	Cultivated land	Moderately dissected hill	53F06	Rock	Slide	77.3755	30.6992
360	Cultivated land	Escarpment	53F01	Rock	Slide	77.2055	30.9094
361	Extensive cut slope	Lowly dissected hill	53F01	Rock	Slide	77.2130	30.9155
362	Moderate vegetation	Lowly dissected hill	53B13	Rock	Slide	77.2127	30.9220
363	Barren	Escarpment	53F01	Rock	Slide	77.2364	30.9316
364	Barren	Denudational hill slope	53F01	Rock	Slide	77.2094	30.9150
365	Barren	Denudational hill slope	53F01	Rock	Slide	77.2279	30.9266
366	Barren	Denudational hill slope	53B13	Rock	Slide	77.2089	30.6856
367	Barren	Denudational hill slope	53B13	Rock	Slide	77.2461	30.6721
368	Barren	Denudational hill slope	53F01	Rock	Slide	77.2488	30.6823
369	Sparse vegetation	Moderately dissected hill	53F01	Rock	Slide	77.2452	30.6717
370	Barren	Escarpment	53F01	Rock	Slide	77.2373	30.6728

371	Sparse vegetation	Lowly dissected hill	53F01	Rock	Slide	77.0659	30.8791
372	Sparse vegetation	Lowly dissected hill	53F01	Rock	Slide	77.0676	30.8730
373	Barren	Denudational hill slope	53F01	Rock	Slide	77.0792	30.8560
374	Barren	Denudational hill slope	53F01	Rock	Slide	77.0751	30.8323
375	Barren	Denudational hill slope	53F01	Rock	Fall	77.2190	30.9084
376	Barren	Denudational hill slope	53B13	Debris	Slide	77.2464	30.4989
377	Barren	Denudational hill slope	53F01	Debris	Slide	77.2443	30.4988
378	Extensive cut slope	Lowly dissected hill	53F10	Rock	Slide	77.7441	30.5852
379	Cultivated land	Escarpment	53F10	Rock	Slide	77.7363	30.5788
380	Extensive cut slope	Lowly dissected hill	53F10	Rock	Slide	77.7360	30.5793
381	Thick vegetation	Moderately dissected hill	53F10	Rock	Slide	77.7354	30.5795
382	Extensive cut slope	Escarpment	53F10	Rock	Slide	77.7336	30.5801
383	Thick vegetation	Colluvial foot slope	53F10	Rock	Slide	77.7338	30.5805
384	Extensive cut slope	Escarpment	53F10	Rock	Slide	77.7303	30.5780
385	Extensive cut slope	Moderately dissected hill	53F10	Rock	Slide	77.7321	30.5751
386	Extensive cut slope	Lowly dissected hill	53F10	Rock	Slide	77.7317	30.5757
387	Extensive cut slope	Escarpment	53F06	Debris	Slide	77.4673	30.6056

388	Extensive cut slope	Escarpment	53F06	Rock	Slide	77.4677	30.6087
389	Moderate vegetation	Lowly dissected hill	53F06	Rock	Slide	77.4718	30.6093
390	Sparse vegetation	Moderately dissected hill	53F06	Rock	Slide	77.4721	30.6092
391	Sparse vegetation	Colluvial fan	53F06	Rock	Slide	77.4824	30.6035
392	Thick vegetation	Moderately dissected hill	53F06	Rock	Slide	77.4805	30.6053
393	Extensive cut slope	Highly dissected hill	53F06	Rock	Slide	77.4776	30.5987
394	Extensive cut slope	Highly dissected hill	53F06	Rock	Slide	77.4808	30.6048
395	Barren	Lowly dissected hill	53F06	Debris	Slide	77.4779	30.5980
396	Barren	Moderately dissected hill	53F06	Debris	Slide	77.4768	30.5983
397	Barren	Escarpment	53F06	Rock	Slide	77.4957	30.5935
398	Sparse vegetation	Lowly dissected hill	53F06	Rock	Slide	77.4746	30.5940
399	Extensive cut slope	Lowly dissected hill	53F06	Rock	Slide	77.4872	30.5889
400	Plantation	Lowly dissected hill	53F06	Debris	Slide	77.4781	30.5827
401	Sparse vegetation	Lowly dissected hill	53F01	Rock	Slide	76.9543	30.9886
402	Barren	Escarpment	53F01	Rock	Slide	76.9086	30.9916
403	Extensive cut slope	Lowly dissected hill	53F01	Rock	Slide	76.9271	30.9842
404	Barren	Lowly dissected hill	53F06	Rock	Slide	77.3732	30.7010

405	Cultivated land	Colluvial foot slope	53F06	Rock	Slide	77.3710	30.7029
406	Barren	Lowly dissected hill	53F06	Rock	Slide	77.3715	30.7029
407	Barren	Escarpment	53F06	Rock	Slide	77.3860	30.6984
408	Barren	Moderately dissected hill	53F01	Rock	Slide	77.0023	30.8777
409	Barren	Moderately dissected hill	53F01	Rock	Slide	76.9964	30.8854
410	Barren	Lowly dissected hill	53F01	Rock	Slide	76.9958	30.8905
411	Barren	Lowly dissected hill	53F01	Rock	Slide	76.9983	30.8933
412	Barren	Lowly dissected hill	53F01	Rock	Slide	77.0339	30.8950
413	Barren	Lowly dissected hill	53F01	Rock	Slide	77.0730	30.8871
414	Barren	Escarpment	53F01	Rock	Slide	77.0741	30.8852
415	Barren	Lowly dissected hill	53F01	Rock	Slide	77.0986	30.8695
416	Sparse vegetation	Lowly dissected hill	53F01	Rock	Slide	77.0997	30.8724
417	Moderate vegetation	Lowly dissected hill	53F01	Rock	Slide	77.0977	30.8733
418	Cultivated land	Moderately dissected hill	53F01	Rock	Slide	77.0960	30.8784
419	Extensive cut slope	Moderately dissected hill	53B13	Rock	Slide	77.2278	30.8726
420	Barren	Escarpment	53F02	Rock	Slide	77.0904	30.8210
421	Thick vegetation	Lowly dissected hill	53F06	Rock	Slide	77.4629	30.6165
422	Plantation	Lowly dissected hill	53F06	Rock	Slide	77.4677	30.6300

423	Moderate vegetation	Lowly dissected hill	53F06	Rock	Slide	77.4757	30.6314
424	Extensive cut slope	Lowly dissected hill	53F06	Rock	Slide	77.2896	30.5971
425	Extensive cut slope	Escarpment	53F06	Rock	Slide	77.2886	30.5969
426	Sparse vegetation	Moderately dissected hill	53F06	Rock	Slide	77.2865	30.5964
427	Extensive cut slope	Moderately dissected hill	53F06	Debris	Slide	77.2855	30.5963
428	Cultivated land	Lowly dissected hill	53F06	Rock	Slide	77.2891	30.6084
429	Moderate vegetation	Moderately dissected hill	53F06	Debris	Slide	77.2880	30.6088
430	Barren	Lowly dissected hill	53F06	Rock	Slide	77.2855	30.6096
431	Plantation	Lowly dissected hill	53F06	Rock	Slide	77.2885	30.6118
432	Plantation	Lowly dissected hill	53F06	Rock	Slide	77.4595	30.5937
433	Moderate vegetation	Highly dissected hill	53F10	Rock	Not Available	77.5179	30.6456
434	Extensive cut slope	Highly dissected hill	53F10	Rock	Slide	77.7292	30.5830
435	Sparse vegetation	Lowly dissected hill	53F10	Rock	Slide	77.7296	30.5774
436	Extensive cut slope	Highly dissected hill	53F10	Rock	Slide	77.7262	30.5850
437	Thick vegetation	Moderately dissected hill	53F10	Rock	Slide	77.7127	30.5928
438	Thick vegetation	Moderately dissected hill	53F06	Rock	Slide	77.2779	30.5201

439	Thick vegetation	Moderately dissected hill	53F06	Rock	Slide	77.2774	30.5203
440	Thick vegetation	Moderately dissected hill	53F06	Rock	Slide	77.2776	30.5245
441	Extensive cut slope	Lowly dissected hill	53F07	Rock	Fall	77.2875	30.4863
442	Extensive cut slope	Escarpment	53F07	Rock	Slide	77.2874	30.4868
443	Extensive cut slope	Moderately dissected hill	53F01	Rock	Slide	76.9317	30.9431
444	Extensive cut slope	Moderately dissected hill	53F01	Rock	Slide	76.9812	30.9002
445	Extensive cut slope	Moderately dissected hill	53F01	Rock	Slide	77.2456	30.5358
446	Extensive cut slope	Lowly dissected hill	53F01	Rock	Slide	77.2454	30.5368
447	Extensive cut slope	Lowly dissected hill	53F01	Rock	Slide	77.2415	30.5239
448	Extensive cut slope	Moderately dissected hill	53F01	Rock	Slide	77.2429	30.5550
449	Extensive cut slope	Moderately dissected hill	53F01	Rock	Slide	77.2430	30.5553
450	Extensive cut slope	Lowly dissected hill	53F01	Rock	Slide	77.2426	30.5554
451	Extensive cut slope	Lowly dissected hill	53F01	Rock	Slide	77.2427	30.5559
452	Extensive cut slope	Denudational hill slope	53F01	Rock	Slide	77.2429	30.5570
453	Extensive cut slope	Denudational hill slope	53F01	Debris	Slide	77.2384	30.4900
454	Extensive cut slope	Denudational hill slope	53F01	Debris	Slide	77.2170	30.4799

455	Extensive cut slope	Moderately dissected hill	53F01	Debris	Slide	77.2227	30.4912
456	Cultivated land	Moderately dissected hill	53F01	Debris	Slide	77.2211	30.4940
457	Extensive cut slope	Moderately dissected hill	53B13	Debris	Slide	77.2207	30.4938
458	Sparse vegetation	Lowly dissected hill	53B13	Rock	Slide	76.9780	30.9764
459	Barren	Lowly dissected hill	53B13	Rock	Slide	76.9785	30.9753
460	Extensive cut slope	Moderately dissected hill	53F01	Rock	Slide	76.9829	30.8364
461	Barren	Moderately dissected hill	53F01	Rock	Slide	76.9996	30.8446
462	Extensive cut slope	Escarpment	53F01	Rock	Slide	76.9987	30.8449
463	Extensive cut slope	Lowly dissected hill	53F01	Rock	Slide	76.9948	30.8461
464	Cultivated land	Lowly dissected hill	53B13	Rock	Slide	76.9945	30.8488
465	Plantation	Lowly dissected hill	53B13	Rock	Slide	76.9943	30.8509
466	Sparse vegetation	Lowly dissected hill	53F02	Rock	Slide	77.0000	30.8535
467	Extensive cut slope	Moderately dissected hill	53B13	Rock	Slide	76.9968	30.8512
468	Barren	Lowly dissected hill	53F01	Rock	Slide	76.9932	30.9969
469	Barren	Moderately dissected hill	53F01	Rock	Slide	76.9801	30.9957
470	Barren	Escarpment	53F01	Rock	Slide	77.1486	30.8387
471	Barren	Moderately dissected hill	53F01	Rock	Slide	77.1448	30.8404

472	Barren	Escarpment	53F01	Rock	Slide	77.0771	30.8247
473	Barren	Moderately dissected hill	53F02	Rock	Slide	77.2474	30.5265
474	Barren	Moderately dissected hill	53F14	Rock	Slide	77.7658	30.5674
475	Barren	Lowly dissected hill	53F14	Rock	Slide	77.7550	30.5831
476	Barren	Lowly dissected hill	53F14	Rock	Slide	77.7550	30.5831
477	Barren	Moderately dissected hill	53F14	Rock	Slide	77.7591	30.5759
478	Barren	Moderately dissected hill	53F06	Rock	Slide	77.4709	30.5259
479	Barren	Lowly dissected hill	53F06	Rock	Slide	77.4759	30.5257
480	Thick vegetation	Moderately dissected hill	53F06	Rock	Slide	77.4750	30.5257
481	Thick vegetation	Moderately dissected hill	53F06	Rock	Slide	77.4704	30.5261
482	Extensive cut slope	Moderately dissected hill	53F06	Rock	Slide	77.2831	30.5323
483	Extensive cut slope	Moderately dissected hill	53F06	Rock	Slide	77.2823	30.5317
484	Extensive cut slope	Moderately dissected hill	53F06	Rock	Slide	77.2824	30.5314
485	Cultivated land	Lowly dissected hill	53F07	Rock		77.3289	30.4627
486	Extensive cut slope	Highly dissected hill	53F10	Rock	Slide	77.7027	30.5441
487	Extensive cut slope	Lowly dissected hill	53F10	Rock	Slide	77.7039	30.5416
488	Extensive cut slope	Lowly dissected hill	53F10	Rock	Slide	77.7022	30.5479

489	Extensive cut slope	Escarpment	53F10	Rock	Slide	77.6339	30.6994
490	Extensive cut slope	Escarpment	53F06	Rock	Slide	77.2952	30.5979
491	Extensive cut slope	Escarpment	53F06	Rock	Slide	77.2966	30.5984
492	Extensive cut slope	Lowly dissected hill	53F06	Rock	Slide	77.2963	30.5942
493	Extensive cut slope	Escarpment	53F06	Rock	Slide	77.2968	30.5940
494	Extensive cut slope	Escarpment	53F06	Rock	Slide	77.2981	30.5929
495	Extensive cut slope	Lowly dissected hill	53F06	Rock	Slide	77.2974	30.5922
496	Extensive cut slope	Lowly dissected hill	53F06	Rock	Slide	77.3652	30.5663
497	Sparse vegetation	Highly dissected hill	53F06	Rock	Slide	77.3990	30.5667
498	Extensive cut slope	Lowly dissected hill	53F06	Rock	Slide	77.3878	30.5681
499	Extensive cut slope	Lowly dissected hill	53F06	Rock	Slide	77.4962	30.5883
500	Barren	Escarpment	53F06	Rock	Slide	77.4913	30.5865



Figure A1: Some Photographs of Landslides from the Study Area